DEFORMATION AND DAMAGE PROCESSES IN WOOD

T.A.C.M. VAN DER PUT

DEFORMATION AND DAMAGE PROCESSES IN WOOD

DEFORMATION AND DAMAGE PROCESSES IN WOOD

PROEFSCHRIFT ter verkrijging van de graad van doctor aan de Technische Universiteit Delft, op gezag van de Rector Magnificus, prof.drs. P.A. Schenck, in het openbaar te verdedigen ten overstaan van een commissie aangewezen door het College van Dekanen op donderdag 15 juni 1989 te 16.00 uur door THOMAS ADRIAAN CORNELIS MARIA VAN DER PUT geboren te Bandung, civiel ingenieur.

Delft University Press 1989

Dit proefschrift is goedgekeurd door de promotor
prof.dr.ir. Y.M. de Haan

CIP-GEGEVENS KONINKLIJKE BIBLIOTHEEK, DEN HAAG

ISBN 90-6275-548-8
NUGI 841

PREFACE

This work was part of an international rheology program, sponsored by the EC, and done by the Timber group of the Faculty of Civil Engineering of the Delft University of Technology.
One of the objectives of the Dutch projects was to develop a general creep and damage model based on deformation kinetics. The derivation of this general theory, together with the mathematical verification that this theory may explain the phenomonological laws of the time dependent behaviour of wood, is the subject of this thesis.

The results of this work were published earlier in reports, magazines and proceedings, often in a different form and are here extended and brought together into one coherent account.

CONTENTS

1 INTRODUCTION

As for other materials, the time dependent behaviour of wood is non-linear and has to be described by the theory of deformation kinetics.
The basic concept of this theory is to regard plastic flow as a matter of molecular bond breaking and bond reformation, what is the same as to state that flow is the result of a chemical reaction like isomerization.
Until now, the theory was mainly applied phenomenologicaly and in this work this is extended to a general theory that may predict the time dependent behaviour of materials and may explain the phenomenological laws in this field. Further, possible simplifications are derived, in order to find the main determining molecular processes.
The mathematical derivation of this general rheological model is solely based on the reaction equations of the bondbreaking and bondreformation processes at the deformation sites (i.e. spaces where the molecules may move into) due to the local stresses in the elastic material around these sites. The model doesn't contain other suppositions and will show the consequences of the stated starting point.
In the original theory, the plastic strain rate was arbitrarily taken to be proportinal to the rate of change of the flow unit concentration and the form of the parameters in the rate equation that determine for instance the hardening and the delay time, were also arbitrary phenomelogical expressions of the strain. This is avoided in this derivation. By expressing the concentration and work terms of the rate equation in the number and dimensions of the flow units, the expressions for the strain rate, fracture, hardening and delay time are directly derived without any assumptions.
The derivation shows that time dependent behaviour is a matter of very small structural changes and the parameters of the model are constant and/or linearly dependent on the variables according to the first, or first two, terms of the polynomial expansion of these parameters.
Because of these small changes, the structure of the dislocations and the order of the reaction is not determinable. So the reaction can be regarded to be of the first order or quasi first order and also the activation enthalpy, entropy and external work can be regarded as constant and/or linearly dependent on temperature, moisture content and stress.
The activation energy and volume will provide however information about the type of bonds that is involved and the dimensions of the flow units.
To obtain simplifications, a general creep- and damage model for small

structural changes is derived by series expansion of the potential energy curve, leading to a proof of the generalized flow theory, and showing that the hypotheses, on wich this theory was based, are consequences of the series expansion. This model is also extended for a description of larger structural changes, giving an explanation of the existing damage models and phenomenological laws of fracture.

The theory is able to explain the different power models (of the stress and of the time), giving the physical meaning of the exponents and constants. This applies for instance for the explanation of the Forintek model of the strength and the Andrade and Clouser creep-equations.

An explanation of the WLF-equation (Williams-Landel—Ferry is WLF) for the time-temperature equivalence above glass-rubber transition is also derived, showing that the change of the concentration of mobile segments, and not necessarily the change of the free volume concentration, is the cause of the transition. The theory is extended for cross-linked polymers at transient creep for the component that performs the transition. It follows from the theory that for the special case of a constant concentration of flow units, the temperature dependence is according to the Arrhenius equation. For higher values of the activation enthalpy, when not the change of entropy is dominating, the theory predicts a shift factor between the Arrhenius- and WLF-equation. The WLF- equation is further extended for the influence of the time scale of the process.

It is further shown that a single process may explain the measured, broad, nearly flat mechanical relaxation spectra of glasses and crystalline polymers and an outline of the relaxation spectrum for wood can be explained by two processes in stead of the assumed infinite number of linear processes that is regarded to be the basis of the relaxation spectrum. Also the loss-spectrum by forced vibrations and the fatigue behaviour can be explained by one process.

The solutions of the model equations are given for transient processes at different loading histories and it is shown that the model can explain the phenomenological laws as for instance the linear dependence of the stiffness on the logarithmic value of the strain rate in a constant strain rate test; the logarithmic law for creep and relaxation and the necessary breakdown of the law for longer times; the shift factor along the log-time axis due to stress and temperature and the influence on this factor of a transition to a second mechanism.

As a last application of the model, a derivation of the mechano-sorptive

effect is given and the behaviour at moisture cycling is explained. The derivation throws a new light on the mechanism, being a separated sorption effect and not an interaction of creep and moisture change or an interaction of loading on the overall shrinkage.

The aim of the experimental research was to verify the model and to get a first estimate of the order of the parameters and the dependence on temperature, moisture content and loading direction. Because data are available for perfect constant humidity conditions, it was decided to use oscillating relative air humidity conditions as may occur in practise. Quick and low relative humidity cycling may be expected to behave like constant moisture content conditions. However the behaviour of the wood polymers is very sensitive for traces of diluent, the previous history and moisture changes and this may cause a different behaviour in comparison to perfect constant moisture conditions.

2 STRUCTURE AND MECHANICAL PROPERTIES OF WOOD

2.1 Structure of softwoods

Timber can be defined as a low-density, cellular (tubular), polymeric fibre composite [1], [2]. The macro structure is cellular and due to the branches of the tree, there are knots as main disturbances of the structure. On microscopic level, most cells are aligned in the vertical axis and only 5 to 10% are aligned in the radial planes (rays). These rays are the main disturbances of the alignment of the vertical cells. In softwood two types of cells are available. The greater number are called tracheids and have a length of 2 to 4 mm with an aspect ratio of 100:1. These cells have a supporting and conducting role. Most cells of the second type are in the rays and are block-like cells of 200 x 30 um. These are called parenchyma and have a function for food storage. The tracheids are thin walled (2 µm) in the early part of the seasonal growth (earlywood) and are thick walled (up to 10 µm in latewood) in the later part of the season.
The cells are interconnected by pits (holes in the cell wall) to permit food

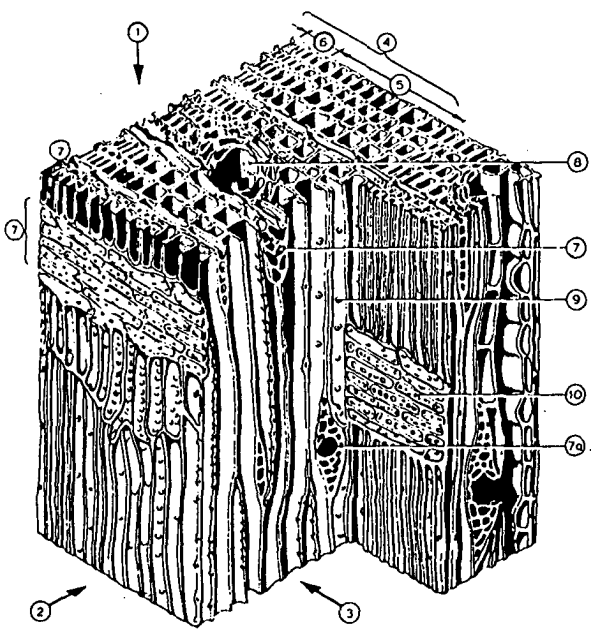

1 cross-section
2 radial plane
3 tangential plane
4 growth ring
5 earlywood
6 latewood
7 rays
7a ray with resin canal
8 resin canals
9 pits
10 pits of the rays

fig. 2.1.1 Structure of softwood

passage and these holes are the main disturbances of the structure of the cell walls.

Chemical analysis shows four constituens: cellulose, hemicellulose, lignin and extractives. The cellulose $(C_6H_{10}O_5)_n$ is formed of beta-glucose: $(C_6H_{12}O_6)$ with removal of H_2O (condensation reaction).

Cellulose chains may crystallise in many ways, but one form, cellulose I, is characteristic of natural cellulosic materials. Adjacent chains in the crystal lie in opposite directions. The unit cell (1.03 nm) of crystalline repetition is interpreted as monoclinic. The molecule is not folded and there is no evidence of primary bonding laterally between the chains. The laterally bonding between the chains is a complex mixture of fairly strong hydrogen bonds and weak van der Waals forces.

The length of the cellulosic molecules is about 5000 nm (0.005 mm). The crystalline regions are only 60 nm (length) by 5 nm (width) and 3 nm thickness. So the cellulosic molecule will pass through several of these

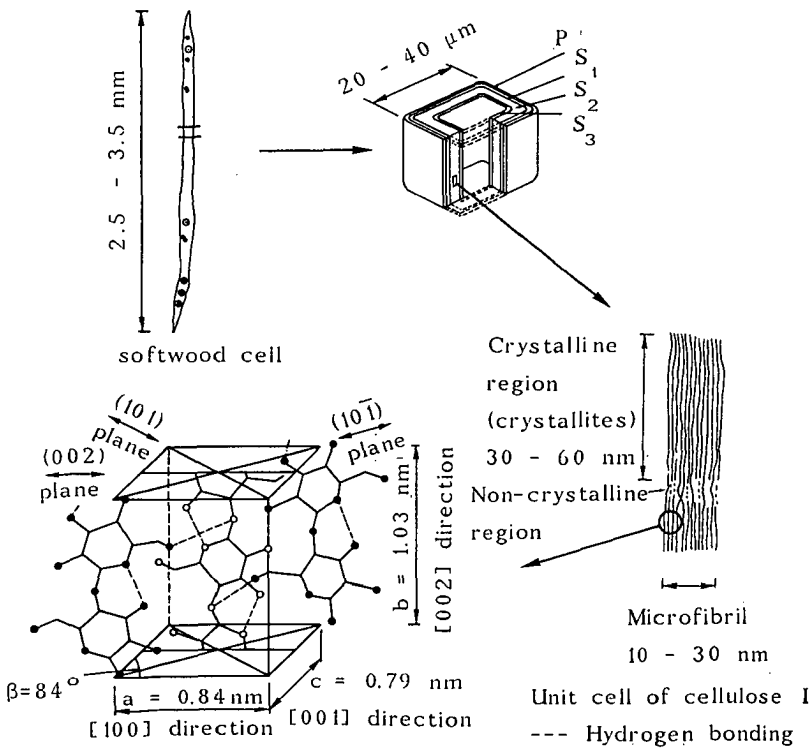

fig. 2.1.2 Structure of timber at different levels of magnitude [1]

regions of high crystallinity with intermediate noncrystalline or low-crystalline zones. The collective unit passing the crystallites is termed microfibril, having an infinite length. It is clothed with chains of sugar units (other than glucose) wich lie parallel, but are not regularly spaced making the microfibril to about 10 nm in breadth.

Hemicellulose and lignin are regarded as cementing materials. Hemicellulose is a carbohydrate like cellulose, however the degree of crystallisation and polymerisation (less than 150 units) are low. Lignin is a complex aromatic compound composed of phenyl groups and is noncrystalline; 25% is in the middle lamella (the intercellular layer composed of lignin and pectin) and 75% is within the cell wall.

So the cell wall is a fibre composite with slender microfibrils as fibres in a cementing matrix of relatively unoriented (amorphous) short-chained or branched polymers (lignin and hemicellulose) containing also tiny voids and second order pore spaces.

The cell wall is also a laminated composite because of the layered structure of the wall. To be distinguished are in succession: the middle lamella, a lignin-pectin complex without microfibrils; the primary wall with loosely packed random microfibrils and no lamellation and the secondary wall with closely packed parallel layers. The outer layer or S_1 layer of the se-

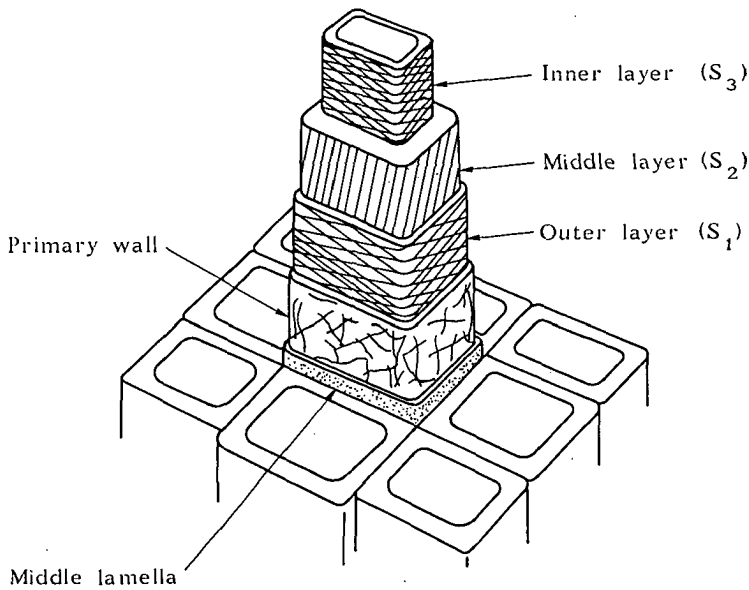

fig. 2.1.3 Wall layers with orientation of the microfibrils [1]

condary wall is thin (4 to 6 lamellae) with 2 alternating spiral microfibrils with a pitch to the longitudinal axis of about 60 degree. The middle layer or S_2 layer is thick (30 to 150 lamellae) with fibrils in a right-hand spiral with a pitch of about 20 degree and the inner layer or S_3 layer is very thin and is simular as S_1 with a pitch of about 80 deg., is however looser and contains lignin in a high proportion. Because there are 2 cell walls between the adjacent tracheids, a microfibrillar angle deviation from the longitudinal axis in a layer is compensated by the opposite angle in the equivalent layer of the second cell wall causing the orthotropic behaviour and the stiffness and strength at an angle to the grain follow the common tensor transformation laws. So the behaviour of a tracheid alone is far from orthotropic and the results of tests on separated tracheids as done for the paper industry cannot be used to predict the behaviour of wood.

2.2 Rheology of wood

2.2.1 Phenomenological approach

Because of the complex structure of wood, complete molecular models are not yet developed and the research is based on phenomenological studies. A summary of the results [3] will be given here.
Like other materials, wood can be regarded as linear elastic when stress, moisture content and temperature are sufficiently low. At higher levels of these variables the behaviour is linear viscoelastic and at still higher levels, the behaviour is nonlinear. This description applies for not too long testing times. For longer times the nonlinear behaviour is evident and can be explained by the kinetic theory. However a linear approach is possible by using spectra of relaxation times. A test of linearity is often done by applying a single step-function in stress on a specimen. Then linearity is assumed when the creep compliance is independent of the applied stress. Better is to do superposition tests. However because of the small amount of creep during short times, also nonlinear models may show a quasi linear behaviour. The creep compliance is separated into instantaneous, delayed elastic, and flow components. The instantaneous or glassy compliance is always independent of the stress. The delayed elastic and flow compliances are approximately independent of stress below certain stress

limits depending on moisture content and temperature. For tension parallel to the grain e.g. limits of 35 to 80 % are given depending on the species. Mostly the limit is taken between 40 to 50 %. Of course these limits depend on the time of testing. These limits are also regarded as the

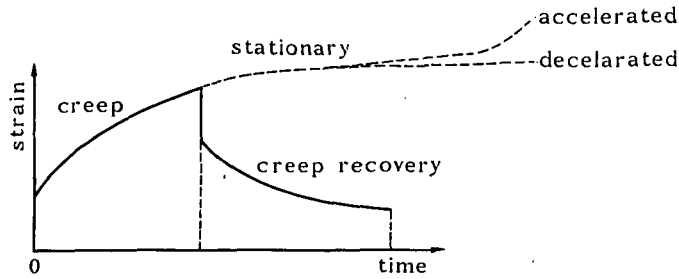

fig. 2.2 Creep and recovery

boundaries below wich there is only decelerated creep and above wich there is, after decelerated creep, stationary creep and accelerated creep (see fig. 2.2). Because wood is a cross-linked polymer, stationary creep, or creep at a constant strain rate, cannot occur. Accelerated creep is due to a structural change process, as will be shown later. Nonlinear behaviour is partly attributed to structural changes. Another part of the "irrecoverable" flow can be recovered by an increase of moisture and temperature. This indicates nonlinear behaviour providing a very stiff "dashpot" for the low internal stresses after unloading, making recovery very slow and thus showing a quasi permanent strain.

Repeated stressing may lead to stiffening shown by a decrease in hysteresis and an increase in elastic moduli (crystalization). At sufficient high stress, there may also be an increase of the glassy compliance. This stress-induced transition is also found in wet cellulose films, indicating probably the penetration of water in the (normally inaccessible) more highly ordered regions. For green wood at a constant temperature and at a given time and stress, the deflection increases exponentially with increasing temperature (between 5 and 70 °C) as can be explained by the kinetic theory as a relative increase of the stress level and with that a shift of a transition to a second (irrecoverable) creep mechanism to lower times. Between transition points, the creep compliance increases linearly with temperature. At high temperatures (100 to 180 °C) also for dry wood the exponential increase is measured due to transition to another mechanism (transition point 140 °C). The transition points depend on the moisture

content, as will be discussed later, and are close to the glass-transition points of hemicellulose and lignin. For green wood, the first transition is at about 50 to 60 °C, causing an increase in the creep rate. For dry wood this transition temperature is higher, above about 70 to 80 °C. In an investigation it was reported that in the range of 15 to 60 °C, the relaxation modulus decreased, but the rate of relaxation appeared to be hardly affected by the temperature (lower stress at the same strain and constant φ if $\omega = 0$, see later). At high initial strains there are also temperature ranges where the creep rates differ not much. For wet wood, the creep compliance may increase more than linear with temperature because of the earlier start of the second mechanism.

Simple superposition of time and moisture content is not valid because of other structural changes (shape and volume) associated with the change of moisture content.

Absorption of water by wood causes swelling up to a moisture content of about 28%. The swelling is roughly proportional to the water uptake. Although the water enters only in the amorphous zones, the strength and stiffness are reduced. The tangential shrinkage exceeds the radial shrinkage partly by the restraint of the rays. The swelling and shrinkage in longitudinal direction are very small compared with the other two directions. It is the smallest for steep micro-fibrillar helixes in the S_2 layer as can be expected in the direction of the crystalline micro-fibrills. Swelling of the secondary wall is much greater than swelling of the middle lamella. So the latter probably restrains the shrinkage of the wood causing high internal stresses. The planes, wich are the richest in hydroxyl groups, lie parallel to the microfibril surface and part of the non-crystalline material is oriented in parallel with the cellulose and this material is accessible to water. So the planes between the lamellae of the cell wall are the places for bond breaking processes due to water movement. In fact the cell wall acts as one layer for dry wood and the S_2 layer is splitted in hundreds of lamellae in the saturated stage. It is to be expected that the high restraints for swelling and shrinkage will cause "flow" in the gel-like matrix. This flow is directed if a specimen is maintained under stress during a change in moisture content. The moisture movement through the wood involves breaking of stressed hydrogen bonds and reformation of these bonds in an unstressed position causing the large creep deformation at desorption when one of two adjacent layers shrinks, while the other swells. This mechanism determines the behaviour at cycling mois-

ture content conditions. There is an increase of creep during desorption and recovery during the first, or for tension also possible in the second absorption period, depending on the initial moisture content. At large stresses and small moisture content changes there is no recovery but a reduction of the creep rate during adsorption. The deformation is usually devided in three components: overall shrinkage by moisture change; time-dependent strain by the stress history and an interaction effect between these two. The same can be said for temperature changes. There is further an interaction influence of temperature and moisture content if one of these cycles. As stated above these interaction effects are not real interactions but can be explained as consequences of the differential swelling and shrinkage of adjacent layers. This will be shown later. The sorption influence is for a single change linear with the amount of moisture change, independent on the moisture content, temperature, rate of sorption and previous creep-history at constant temperature and moisture content, indicating a flow process. The rate of the deformation is dependent on the rate of change of moisture content. It is expected that the moisture gradient is not the cause of the increased deformation (there is no influence of the size of the specimen). A stepwise increase in moisture (5% in 7 days) under loading gives a maximal deflection at the first moisture increase and this is the smallest at the last moisture jump (being above the saturation point). The sum of these deformations is probably equal to an equal one step moisture increase. Above saturation there is a little influence. The deformation at changing moisture conditions is probably independent on the loading, at least at not too low and not too high levels. There is no decrease in the modulus of elasticity.

2.2.2 Viscoelastic behaviour of the structural elements in comparison with other polymers

The cellulose molecules are very long and have very short side chains and are able to be packed close together forming crystalline areas. Hemicellulosis has different forms between the linear structure and the very strong branched structure. The linear form with not regular spaced short side chains and many polar hydroxyl groups has, as cellulosis, good fibre forming properties and the branched type has good entanglement and filler properties. Lignin is cross-linked in all directions and is able to form

strong bonds with the celluloses and has also hydroxyl groups.
The cellulose is highly crystalline (~ 70 %) and the crystallinity doesn't change much on straining or drying. Because of the physicaly side bonds (hydrogen- and vanderwaals- bonds) it is to be expected that the binding energy will be time- and temperature dependent. However the deformation of a crystallite is energy elastic (representing displacements from equilibrium positions) and time dependent behaviour is only noticeble in the amorphous regions. The modulus of elasticity is 1.1 10^5 N/mm^2 in chain direction and about 10^4 N/mm^2 perpendicular to this direction. The amorphous regions of the cellulose are highly oriented and will have many cross-links (hydrogen bonds). Because there is no "coiling" structure, an uncoiling process cannot be expected to occur.
The branched hemicellulose polymers have the function as filler of the lignin and because the strong bonds with the lignin it increases the cross-linking, acting as copolymer. The linear hemicellulose acts by hydrogen bonds as flexible bridge between the microfibrils, making movements of the fibrils possible and avoiding stress peaks between fibrils on loading.
Lignin is a random amorph cross-linked polymer that is able to form strong bonds with the polysaccharides. Real rubbery behaviour (uncoiling) is not possible.
So the polymers in wood that determine the time dependent behaviour contain densely cross-linked filled amorphous polymers as well as highly crystalline and oriented polymers. Although such polymers don't possess a zone of rubberlike behaviour, there is a transition possible to a more flexible state. Crystalline polymers with the amorphous region in the flexible state (above the transition temperature of these regions) show a quick stress relaxation loosing 25 to 50 % of the stress in a few minutes. This is followed by a slow process and the remaining stress after 17 decades (the age of the universe) is above 5 to 10 %, as follows from the time-temperature equivalence. So this stress reduction of about one order is much less drastic than that for the rubbery transition where the stress reduces 5 to 6 orders. This quick mechanism is not measured for wood, even not at high temperatures, suggesting a very high cross-linking. So the slow process is dominating in wood (at low stresses) and has the same properties as for other crystalline and cross-linked polymers. This means that the creep is recoverable; that increase of stress shortens the retardation time (crystalline materials) and that the creep rate on logarithmic time scale is not proportional to the stress but increases with a

power of the stress at higher stresses with the consequence that the creep and recovery functions have different shapes. The temperature dependence of the viscoelastic properties follows the WLF- or the Arrhenius equation. The Arrhenius form applies for cellulose. Because the crystallinity doesn't change much, there are no vertical shifts (due to change of the pseudo equilibrium modulus) of the creep lines along the log- time-axis. The creep can be described by the Andrade-equation or is a straight line on a log-time-plot. This mechanism is attributed to the mobility of the short strands in the amorphous regions, probably due to co-operative motions of groups of strands coupled through linkage points. The thermal and mechanical history is very critical for the behaviour as for glasses and also traces of diluent have an influence.

At room temperature the amorphous parts in wood are probably in the glassy state, and only the so called β-mechanism appears (the α-mechanism represents the glass-leather transition due to mobility of the backbones of the polymers). The β- or secondary mechanism is due to local readjustment of side groups in glassy amorphous polymers or in the amorphous strands of crystalline polymers. These side groups can be chemically attached groups or hydrogen bonds wich act as side group on the polymer chain and even only polar water molecules. In this last case the β-mechanism disappears on removal of the water. Dielectric measurements support this model because they reflect dipole orientation due to side group motions, showing the same temperature dependence as the viscoelastic behaviour. This temperature dependence follows the Arrhenius equation and the activation energy lies between 20 and 30 kcal/mole. The stress reduction in relaxation by the secondary mechanism is smaller than by the α-mechanism and will be smaller than a factor 0.5 to 0.8, where 0.5 is used as a rule of thumb for wood. The same as for the α-mechanism the behaviour is nonlinear for high stresses and these properties will be explained here by the kinetic model.

2.3 Strength and time dependent behaviour

2.3.1 Factors affecting the strength

The influence on the strength of the native origin of the wood, determined by the character of the soil, the climate, density of the forest, etc. is not

important, because the variability within one area is comparable with the variability of the whole population.
The main features of the macro-structure that may determine the strength are the density, moisture content, width of the growth rings and width of the latewood part of those rings. Disturbances will also have an influence. The main disturbances of the structure are the knots, deviations of the grain angle, compression wood, resin channels, growth defects and checks. Because timber is selected for structural use, larger disturbances by cracks, resin heaps, growth faults, etc. are excluded and only minor disturbances are allowed having a little influence on the strength.
Compression wood will cause twisting and splitting due to differential shrinkage by seasoning and also serious grain angle deviations may cause twisting. So by selection, this timber will not be used for structural applications and it appears that for gross wood the regression of the strength is nearly totally determined by only the knot area, the density and the moisture content (see e.g. the discussion in [4]).
Knots act similar like holes and the strength dependent on the KAR (knot area ratio) can be fully explained by the stress field around a hole [5].

An increase in moisture content in wood gives a reduction in strength by the weakening of the interchain hydrogen bonds of the cellulosic components in the amorphous regions. The moisture effects will be explained later by the chemical reaction kinetics of this water binding. At a moisture content of about 28% there is no further reduction of the strength and also no further increase in swelling of the wood.

There is a very general correlation between strength and density even when comparing different wood species. The amount of latewood is highly correlated with the density. This is not so for the total ring width so the density of earlywood varies in every ring. Because of the correlation of the strength with the density, it can be expected that mainly the latewood part determines the strength. This can be true if there is early plastic flow in the earlywood transmitting the stresses to the latewood. This also explains the higher magnitude of the tensile strength of the individual fibres compared with gross wood. In gross wood early crack formation occurs at imperfections between the layers due to stress concentrations. Because there is sufficient overlap of the adjacent fibres, these cracks have to propagate through the clear wood layers for total

fracture where the amount of latewood determines the strength.
Measurements in tension of wet early wood and late wood single fibres, indicate a 1.1 to 3 times higher ultimate strength (at about the same ultimate strain) and stiffness of the late wood fibres (from the same species) [6]. In [7] higher differences between earlywood and latewood were measured. Dry late wood was about 6 x stronger than early wood, closer to the theoretical expectation and wet late wood was about 4 x stronger, indicating more influence of plasticity for wet wood. It was also found that the ultimate strain for failure of latewood was higher than for earlywood. Preparation of single fibres test-specimens will always induce cracked surfaces with the possibility of crack propagation, diminishing the strength differences between early and late wood. Probably this explains the differences of the measurements of [6] and [7].
Elastic models of the mechanical behaviour of cell wall layers (e.g.[8]) indicate a much worser loading of springwood in comparison with summerwood. The maximum stress parallel to the microfibril is about 4 times higher and the stress perpendicular and the shear stress is about 7 times higher in springwood than in summerwood. This indicates early plastic flow in the cell wall layers of the springwood with considerable stress redistributions between the layer components because else, the relatively high experimental strength of this layer cannot be explained.
The summerwood fiber has an almost ideal stress pattern in accordance with the strengths of the different constituents and can be expected to behave elastic up to high stresses making probably a description possible by an elastic model of the cell wall strength. So whatever the mode of failure is, the strength is close to the fiber strength.
An elastic model for the tensile strength of the cell wall, [9], indicates that fracture first occurs in the S_1 layer by a shearing mechanism with a very high shear stress at failure, suggesting a strong bonding between lignin, hemicellulose and cellulose. This initial fracture of the S_1 layer follows also from the theory of maximum energy of distorsion.
The model further shows opposite signs of the shear stresses in the S_1 and S_2 layers indicating also high stresses in the interface between the S_1 and S_2 layers. Microscopic studies have confirmed this interlayer fracture by the pulling out of the S_2 and S_3 layers out of the enclosing sheet of the S_1 .
As second type of failure, helical break along the direction of the S_2 microfibrils was observed leading to the ultimate rupture of this layer.

2.3.2 Mode of fracture

The failure of wood is dependent on the type of stress. The cleavage behaviour of wood was studied by fracture mechanics tests on notched samples (e.g.[10]). The strain-energy release rate depends on temperature and moisture content and there is a dominating stability of crack extension. The slow and stable crack propagation was mainly within the cell wall of the tracheids, either between the primary and S_1 walls, or between the middle lamella and the primary wall and was moving through the middle lamella to the adjacent cells. So the cell lumina were not in general exposed. The stable crack extension indicates the existance of discontinuities with higher fracture resistance that has to be overcome for rapid extension. In many cases rapid fracture was initiated at a minor discontinuity in the orientation of the tracheids such as the points were the ray cells cross the line of tracheids. At higher temperatures and moisture contents, wood is less brittle because there is more viscous dissipation and unstable cracks are more infrequent and short in length.

Tension tests along the grain on gross wood show mostly failure within the fibre walls rather than between fibres (p.e. along the S_2 microfibrils). The overlap of the adjacent cells where the force is transmitted by shear in the middle lamella is thus in general sufficient long. As mentioned before, failure is possible between the S_1 and S_2 layers.

Tensile failure perpendicular to the grain follows, as in cleavage tests, the radial plane as preferred plane. Both transwall failure, wich goes through the cells and the lumen, and intrawall failure, wich occurs normally within the zone of the primary wall and S_1, are possible. An increase in temperature (0 to 150 ^{o}C) resulted in a high reduction of the tensile strength perpendicular to the grain and a reduction of trans-wall failures, indicating a reduction in bond strength between adjacent cells.

In compression parallel to the fibre direction, lines of buckling appear wich make an angle on the tangential face of the specimen of about 60 degree to the axial direction, which lie in the radial direction. This is a consequence of shear failure between adjacent cells and the angle of 60 deg. in stead of 45 deg. is due to anisotropy. The failure takes place within the cell wall and only occasionally does separation occur along the middle lamella mostly in the regions adjacent to the rays. The existence of microscopic cracks is visible as loosening of the bonding between microfibrils and the implication is that the lateral cohesion between micro-

fibrils of the secondary wall is less than between cells [11]. In [12] and [13] it is mentioned that rupture occurs at the cellulose-lignine interface (because of the preferentially staining with lignin stains).
Besides bond rupture (as follows from the increased chemical reactivity with dilute acid) micellar distortion occurs. There is a sequential development in types of dislocations (being permanent crinks of the fibrils) with increasing stress. Trust lines, being local thickenings of the cell wall by small fibril deformation, develope into slip planes which grow to bands of slip planes (creases) leading to failure with considerable buckling and delamination of the cell walls. Slip planes develop at about 25% loading level and the number increases about linearly with stress level. At a level of about 50 to 65% creases (bands of more than 2 slip lines) are formed increasing parabolically with stress level. At 80 to 100% gross buckling of the cell walls occur containing about 40% of the total failure strain.
The developement of these micro-failures is related to time at a given stress level. At relatively high moisture content or when deformations develope slowly at low stress levels, the micro deformations are widely distributed through the specimen. Creep tests on wood show that after long time, depending on the stress level, the deformation may increase at a higher rate indicating the development of creases after long times.
At low moisture contents and rapid stressing at high stress levels the micro deformations are fewer in number and localized preferentially at rays.
For high compression perpendicular to the fibre direction, having a modulus of elasticity of about one-tenth of that in longitudinal direction, sideways distortion of cells occur. The whole shape of the cell changes. When failure does take place separation occurs between the layers S_1 and S_2 of the secondary wall. The greater strength in radial direction than in tangential direction is due to support from the rays.

2.3.3 Failure of the ultrastructure

Two components of the fine or chemical structure have a profound influence on the strength and stiffness. The first consists of matrix material and especially of lignin and the second is the celulosic fibre material.
To investigate the failure mechanism of the cellulose chains, Ifju [7] reported the effect of reducing the cellulose chain length by gamma irradia-

tion. The degree of polymerization of the cellulose was reduced from 5000 down to about 200 by successive higher doses of radiation. If slippage of the chains is a cause of failure it can be expected that there will be a critical chain length where below failure is caused by slippage and where above failure is by primary bond breaking of the chain itself and is independent on the chain length (or independent of the degree of polymerization). Based on an assumed very high activation energy of breaking of the -C-O-C- linkage and a very low activation energy of breaking of the lateral hydrogen bonds it was calculated that this critical length is reached at a degree of polymerization of about 70. The experiments however showed a decrease of the strength at any reduction of the degree of polymerization. The conclusion that slippage at a degree of polizerization of 5000 is between micelles or fibrils through the "losely" amorphous cellulose (with very few side bonds) seems not to be right, because this expected long range interaction would indicate an early occurrence of rubbery behaviour. The stiffness is however not proportional to the absolute temperature, as is necessary for rubbery behaviour, and also the transition with temperature is different (Arrhenius equation) and the molecular models show only a very localized slip of about a cellobiosic unit.
So the basis of the calculated critical chain length is more complicated than assumed. This can be seen by the bonding model of cellulose of Giles as e.g. discussed in chapter 4 of [8] where a special type of bonding is assumed in order to explain the high experimental stiffness of cellulose.

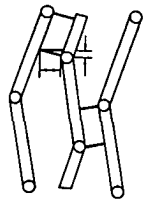

fig. 2.3 Scheme of a cellulose chain linked by hydrogen bonds

Straightening of the cellulose chain causes lateral stretching of the hydrogen bonds causing a four- to six- fold stiffness increase of the chain. So if a chain is stretched, the hydrogen bonds may fail, reducing the stiffness of the chain and so the stress on the chain. If within the crystaline

region 4 successive hydrogen bonds have failed, the maximum reduction of the force is reached. The activation energy for this will be less than 4 x 6 = 24 kcal/mol, while for primary bond breaking the activation energy will be about 60 to 80 kcal/mol. This doesn't mean that a type of dislocation propagation by cooperative bond breaking of 4 bonds is the necessary failure mechanism. Also possible is e.g. the breaking of 1 hydrogen bond with a rotation of 4 to 5 bonds of the glucose-rings (activation energy less than: 6 + 5x3.2 = 22 kcal/mol, to releave a high chain force. Also for other polymers the flipping of the ring between two isomeric chair forms, is supposed to be a deformation mechanism. There is steric possibility for this movement [14] in cellulosis. This mechanism, of breaking of one hydrogen bond, is in accordance with the measured first order reaction and the measured activation energy and volume of the bond breaking. Further the in [7] measured dependence of the strength on the logarithmic value of the degree of polymerization (being a measure of the logarithmic value of the numbers of cuts of the chain or the number of sources of dislocations) is explained by the molecular model as developed here. As shown later the flow-stress is:

$$\sigma = \frac{1}{\varphi}\ln\left(\frac{2\dot{\varepsilon}}{A}\right) = \frac{1}{\varphi}\ln\left(\frac{2\dot{\varepsilon}}{A'\rho}\right) = C_1 + \frac{1}{\varphi}\ln(D)$$

where $\dot{\varepsilon}$ is the the strain rate in a constant strain rate test, $A = A'\rho = \rho\cdot\nu\cdot\exp(-E/kT)$ is proportional to the flow unit density ρ, and D is the degree of polymerization being inversely proportional to the number of cuts, and thus inversely proportional to ρ. This leads to the expression:

$$\frac{\sigma_1}{\sigma_2} = 1 + \frac{1}{\varphi\sigma_2}\ln\left(\frac{D_1}{D_2}\right)$$

By regression analysis, it can be shown that $1/\varphi\sigma_2$ is constant, independent on temperature and moisture content and is about 0.11 for latewood and 0.17 for earlywood (coefficient of variation: 0.45). The values of this constant, $1/\varphi\sigma_2$, indicate a different failure mechanism by irradiation than occurs normaly in wood (showing values of about 0.03).

The change in molecular arrangement in the ordered, crystaline regions of the micelles by loading can be measured with the X-ray diffractometer [15]. Truly elastic behaviour is due to chain straightening, orientation of crystallites or reorganisation of the less ordered regions. Constant loading tests in tension show immediate orientation by loading and no increase in

crystallinity with time (within 24 hours). Because X-ray diffraction shows only ordered regions of molecules, these regions only show elastic behaviour. The alignment by loading gives some increase of the length of the crystallites and so of the degree of crystallinity. At unloading (independent of the loading time) some alignment remains indicating also some plasticity, increasing with increasing stress level (some of the new bonds recover at a not noticible low rate by the low internal stress after unloading). Time dependent molecular orientation activity in the amorphous regions can be observed by the infrared polarization technique. This was done in [16] for balsam fir tissues strained parallel to the fiber axis. The chosen adsorption bands in [16] contained no crystalline band with almost immidiate orientation representing the elastic behaviour. So the recorded bands gave the activity in the amorphous regions. In the chosen bands for lignin, hemicellulose and cellulose, only quick time dependent processes of orientation were recorded. The main slow stress relaxation process was not given. The explanation, given in [16], of the short periodic processes of loading and unloading as a result of the ability of the lignin network to act as an energy sink and to control the energy set up of the stressing is not probable. Obvious all components will be loaded on quick straining and because of the shorter retardation time of the lignin, the stress will be transmitted from the lignin to the cellulose chains instead of in the reversed direction. More probable is therefore that a type of dynamic crystallization occurs like in metals. Also in partly crystallized polymers this may occur if the degree of crystallinity increases during the straining. So a process of crystallization, flow and recrystallization may occur. A strong indication for this supposition is that the time of the process is dependent on the kinetics of crystalization and not on the rate of straining or the viscoelastic properties and also that the stress of the relaxation test decreases during the orientation because like in the mentioned polymers the crystallization lowers the stress on the ends of the amorphous strands. This mechanism is however of minor importance, and need not be described, because the crystallization process in wood is very small so that it results only in a small wavy form of (or around) the main stress relaxation line. It can be concluded that there is a lack of the measurement of the main slow overall relaxation by this method.

The main relaxation process of the amorphous material and the lignin is to be expected to follow the Arrhenius equation in the glassy state and the WLF-equation for the transition to the "leather" state as will be

discussed later.

2.4 Conclusions

Timber can be defined as a cellular polymeric fibre composite with slender microfibrils as fibres in a cementing matrix of relatively unoriented (amorphous) short- chained or branched polymers (lignin and hemicellulose). The cell wall is also a laminated composite because of the layered structure of the wall. These layers are: the middle lamella, an amorphous filled cross-linked polymer without microfibrils; the primary wall with loosely packed random microfibrils and no lamellation and the secondary wall with closely packed parallel layers containing spiral microfibrils with various pitches to the longitudinal axis. The microfibrils consist of parallel cellulosic molecules having regions of high crystallinity with intermediate low-crystalline zones.

So the structure is heterogeneous with disturbances of the structure at any level and many transient processes can be expected to occur at loading. This can be due to plasticity as well as due to crack propagation. Early flow has to occur in the earlywood cells and in the matrix. As around the reinforcement bar in concrete, it can be expected that stress redistribution causes mainly shear with compression in the matrix, increasing the tensile stress in the fibres. The measured negative contraction for creep in tension is an indication for this mechanism. An indication of flow of the earlywood is the correlation of the strength with the amount of latewood. Also the elastic layer models indicate early flow of the earlywood cells.

The disturbances that cause stress concentrations and thus transient processes, are for instance the knots, defects, ray-crossings, tracheid ends, pits, interlayer imperfections, voids, second order pores and previous cracks in the weak layers. If stress redistribution around these disturbances is due to crack propagation caused by mainly hydrogen-bond breaking, it is to be expected, by the heterogeneous structure, that the delay-time parameter [17] of the kinetic model will be highly random and because of the structural deviations and deviations of the alignment and of the stress states also a random value of the activation volume parameter can be expected.

The kinetic models, as usually applied, regard only one process and have

to be adapted for the possibility of description of more processes. This is done for wood in [17]. However different processes with about the same relaxation time cannot be distinguished, for instance fracture due to interlayer crack propagation shows not much preferrence for a special plane and may go through the middle lamella or through the interface with the primary wall and also between the P- and S_1 layer. This indicates the same type of bonding between these layers (the same strength) and the result is one apparent determinating process with random parameters due to the different bond densities.

An explanation can be given of the strength behaviour of cellulose chains depending on the logarithmic value of the degree of polymerization. The cuts in the chain, due to irradiation, reducing the degree of polymerization, act as flow units for a failure process.

Also a new explanation of the time dependent behaviour of the amorphous regions in the fibrils is given as a dynamic crystallization process that can be described by the kinetic model by a structural change process. However this very small influence on the creep behaviour can be neglected.

The rheologic behaviour of the wood-polymers is comparable with other high polymers and is only quasi linear. There are also specific differences as for instance the special properties of the activation volumes, as will be discussed later and for instance the special behaviour at moisture and temperature changes. These phenomena have to be explained by the kinetic model for wood.

The strength is mainly determined by the knot area, the density and the moisture content. To determine the parameters of the processes in the wood, tests have to be done on clear wood without knots because the stress redistribution processes around the knots will dominate and conceal the transient processes in the wood. As far as possible, measured properties of wood components have to be used in the model to be able to distinguish the different processes in wood.

The specimens can be taken from one plank in order to have the least influence of the variation of the structure and the density. To investigate the influence of the different modes of fracture and creep on the activation parameters, tests in shear, compression and tension, along the grain and perpendicular to the grain have to be done.

Also tests with fluctuating relative air humidity changes have to be done because the behaviour of the wood polymers is very sensitive for traces

of water, the previous history and moisture changes and this will cause a different behaviour in comparison to constant moisture conditions.

2.5 References

[1] Concrete, Timber and Metals. J.M. Dinwoodie a.o. 1979, Van Nostrand Rheinhold Company, New York.

[2] Principles of Wood Science and Technology. F.F.P. Kollmann, W.A. Cote 1968, Springer-Verlag, Berlin New york.

[3] Recent progress in the study of the rheology of wood, A.P. Schniewind, Wood Science and Techn. Vol. 2)1968) p. 188-206.

[4] Berekeningsmodel voor horizontaal gelamineerde balken. T.A.C.M. van der Put, Rapport 4-83-16 GKH 6, 1983 Stevinlaboratorium Delft.

[5] Vingerlasverbindingen in horizontaal gelamineerd hout, T.A.C.M. van der Put, Rapport 4-76-5 VL5, 1976, Stevinlaboratorium Delft.

[6] Wood fibres in tension. B.A. Jayne, Forest Prod. J., 1960, 316-322.

[7] Tensile strength behaviour as a function of cellulose in wood. G. Ifju, Forest Prod. J., 14, 1964, 366-372.

[8] Theory and Design of Wood and Fiber Composite Materials. B.A. Jayne Editor, pg. 83-95, 1972, Syracuse Wood Science Series, 3.

[9] Cell Wall Mechanics of Tracheids, R.E. Mark, 1967, Yale University Press, New Haven.

[10] Morphology and mechanics of wood fracture, G.R. Debraise, A.W. Porter, R.E. Pentoney, Mater. Res. Std., 6, 1966, 493-499.

[11] The anatomy and fine structure of wood in relation to its mechanical failure, A.B. Wardrop, F.W. Addo-Ashong, Proc. Tewksbury Symp. Melbourne, 1964, 169- 200.

[12] Failure in timber part II, The angle of shear through the cell wall during longitudinal compression stressing, J.M. Dinwoodie, Wood Science and Technology, Vol. 8, 1974, 56-67.

[13] Failure in timber part I, Microscopic changes in cell-wall structure associated with compression failure, J.M. Dinwoodie, Journal of the institute of wood science 21, 1968, 37-53.

[14] Ueber die Gestalt und die Beweglichkeit des Molekuls der Zellulose. P.H. Hermans, Kolloid Zeitsschrift, 102, Heft 2, 1943, 169-180.

[15] Cell-Wall Crystallinity as a Function of Tensile Strain. W.K. Murphy Forest Prod. J., April 1963.

[16] Molecular Rheology of Coniferous Wood Tissues, S. Chow, Transactions of the Soc. of Rheology 17:1, 1973, 109-128.

[17] Reaction kinetics of bond exchange of deformation and damage processes in wood, T.A.C.M. van der Put, Proc. IUFRO-conference Firence Italy, Sept. 1986.

3. DISCUSSION OF THE BASIC PRINCIPLES OF THE THEORY OF MOLECULAR DEFORMATION KINETICS

3.1 Introduction

For plastic flow in a material, it is necessary to have "holes" into wich the material may move, and a lowered energy potential (energy barrier) by the presence of this hole (with a bond strength of about a quarter of the bond strength in a perfect region for all materials). So the number of mobile molecules or mobile segments are determined by the number of these holes (flow units).

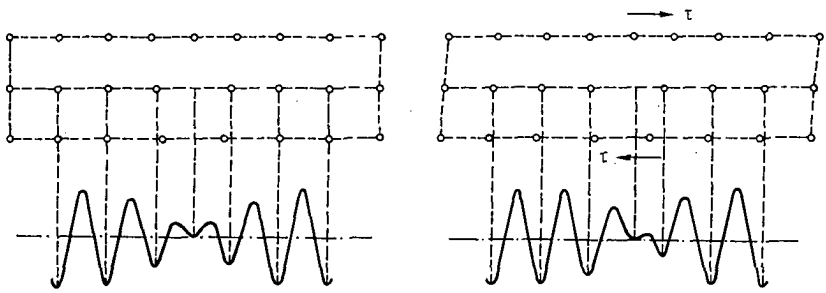

fig. 3.1 Energy surface across an edge dislocation [1]

The rate of flow is determined simularly as the chemical reaction rate of bond breaking and some aspects of this theory will be discussed (following [1]) to clarify the physical meaning of the constants of the basic equations that will be used for the derivation of a creep and damage model. The starting points on the reaction order, thermodynamics of the free energy change and parameters of the flow units are derived for use in the derivations of the next chapter.

3.2 Theory of reaction rates for plastic deformation in solids.

The basic concept of this theory is to regard plastic flow as a special form of a chemical reaction (like isomerization, where the composition

remains constant but the bond structure of the molecules changes), because flow is a matter of molecular bond breaking and bond reformation. A simple form of the reaction rate equation is:

$$\frac{d\rho_2}{dt} = -\frac{d\rho_1}{dt} = \rho_1 C_f - \rho_2 C_b, \qquad (3.2.1)$$

where ρ is the concentration of flow units, that may be kinks and holes in the polymers or vacancies and dislocation segments in the crystalline regions.

$C = \nu \cdot \exp(-E/kT)$ (where ν is a frequency) with:

E= the activation energy

k= Boltzmann's constant

T= the absolute temperature

Because there is a forward reaction into the product state and a backward reaction into the reactant state, there are two rate constants:

$$C_f = \nu \cdot \exp(-E_f/kT), \qquad (3.2.2)$$

$$C_b = \nu \cdot \exp(-E_b/kT). \qquad (3.2.3)$$

The molecules occupy equilibrium positions and are vibrating about the minimum of the free energy potential. Every position of the molecules with respect to each other determines a point of the potential energy surface. The molecules must reach an activated state on this potential surface in going from the reactant to the product state. The thermal energy is not equaly devided among the molecules and it is a matter of chance for a molecule to get high enough energy to be activated and to be able to break bonds.

The explanation of the form of the rate constants C_i above is given by Bolzmann statistics.

$C = (kT/h)\exp(-E/kT)$,

$\nu = kT/h$ can be approximated to the Debye frequency (about 10^{-13}) that may be regarded as the number of attempts per second of a particle to cross the barrier of height E. However, any attempt can succeed only if the energy of the particle exceeds E, and the probability of a jump per second is: $P = \nu \cdot \exp(-E/kT)$, where kT is the mean vibrational energy of the particles (in that direction).

Mostly not one group of reacting atoms is considered but a molal quantity. The molal free energy is then $E_m = N_m E$ and the Boltzmann constant k

is replaced by the gas constant R, where $R = N_m k$ and N_m is Avogadro's Number. So: $E/(kT) = N_m E/(N_m kT) = E_m/(RT)$.

$k = 8.616 * 10^{-5}$ eVK^{-1}
$h = 4.135 * 10^{-15}$ eVsec
$k/h = 2.084 * 10^{10}$ sec^{-1} K^{-1}
$R = 1.987$ cal K^{-1} mol^{-1}
$N_m = 6.02 * 10^{23}$
1 Joule = 1Nm = $0.618 * 10^{19}$ eV = 0.239 cal

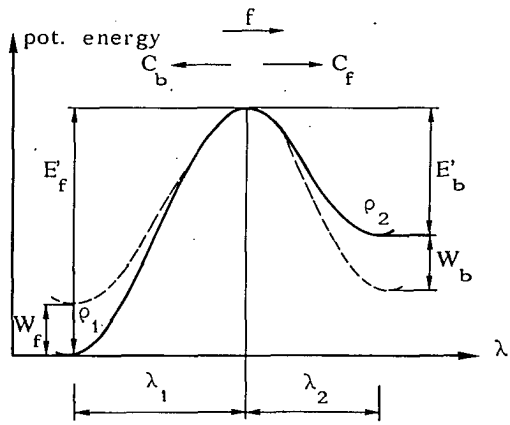

fig. 3.2 Potential energy change for an elementary reaction [1]

The free energy of the activated complex consist of an enthalpy term, an entropy term and a work term due to the applied stress (see 3.4).
When the molecules are displaced from their equilibrium positions by an applied stress, the potential energy is increased. This means that the potential energy surface is changed, making the reaction more probable, decreasing the barrier height with W_f in forward direction and increasing the barrier height with W_b in backward direction, where $W = W_f + W_b$ is the work of the external constraints. So:

$$C_f = \frac{kT}{h} \exp\left(\frac{-E'_f + W_f}{kT}\right), \qquad (3.2.4)$$

$$C_b = \frac{kT}{h} \exp\left(\frac{-E'_b - W_b}{kT}\right). \qquad (3.2.5)$$

3.3 Reaction order of deformation and fracture processes.

The theory is given for first order reactions because nearly all materials appear to follow that law. So the slowest determining bond breaking reactions are of first order or quasi first order.
A description by higher order reactions is also possible and is e.g. given in [2] where a Taylor series expansion of the rate equation is given for hydrogen bonded materials, leading to terms with increasing reaction order. The first term of the expansion will not be zero, because it gives the first order reaction that is shown to occur in processes like relaxation, first moisture regain, etc. in dry cellulosic material. The disadvantage of this approach by Taylor series is, that the rate equation for these cases reduces to a single forward reaction. This is insufficient to describe the total behaviour of relaxation and a better approach is then possible by a single first order process (with a, for equilibrium necessary, backward process) as done by Meredith [2] for the same material. An explanation why a first order theory can be used is given below and in chapter 4, where we have shown that the generalized Eyring theory can be regarded as an expansion into simple parallel processes. Deviations from the first order are due to these parallel acting processes. The same appears to be possible even for the complex reactions of decomposition of wood at high temperatures that can be given by pseudo-first order reactions, (W = weight loss; W_e = residual weight)[3]:

$$dW/dt = - \sum_i k_i \cdot (W - W_e).$$

The determining (slowest) bond breaking processes must be of first order (or quasi first order) in this case, because the overall reaction has an order close to one (at the highest rate). This follows from thermogravic experiments [4].
The possibility of a quasi first order reaction in a co-operative bond breaking process can be shown by the following higher order reaction:

$$- \frac{d\rho}{dt} = C.\rho^n. \qquad (3.3.1)$$

In the Eyring model for creep, the density of the flow units ρ is taken to be constant, as given by the last term of equation (3.3.2). This can only be true for processes that may approach the steady state. If ρ is splitted in an initial value ρ_0 and a small change $\Delta\rho$, eq.(3.3.1) becomes:

$$-\frac{d(\rho_0+\Delta\rho)}{dt} = -\frac{d\Delta\rho}{dt} = C\rho_0^n\left(1+\frac{\Delta\rho}{\rho_0}\right)^n \approx C\rho_0^n\left(1+\frac{n\Delta\rho}{\rho_0}\right) \approx C\rho_0^n. \qquad (3.3.2)$$

It appears that the last two terms of eq.(3.3.2) are sufficient for the description of flow and fracture. The last term ($C\rho_0^n$), for steady state processes, and the fore last term for severe changes in behaviour like dislocation -multiplication and -breakaway, causing yield drop in a constant strain rate test. So it appears that the theory describes small structural changes, and is linear in the variable: $1 + n\Delta\rho/\rho_0$, being a quasi first order process. To know the order, the flow unit density ρ has to be known and this cannot be found by indirect methods (by measuring creep). So we have shown, that as a first approximation, it is possible to regard only first order reactions for deformation and fracture processes.

3.4 Thermodynamics

The thermodynamic system is chosen to be a small volume around the dislocations (i.e. around the deformation- or fracture- site). This volume is surrounded by elastic material containing the effective stress (applied and internal stresses), and the temperature dependence of the elastic constants of this surrounding material has to be regarded separately.
The local internal stresses σ at the sites act as external stresses on this closed system. The first law of thermodynamics, for a closed system, can be given in the differential relation of the change of the internal energy U of a process at constant pressure P, temperature T and stress σ.

$$dU = \delta Q - PdV + \delta W, \qquad (3.4.1)$$

where δQ is the heat absorbed by the system; PdV is the work against pressure P by an increase of the total volume dV, and δW the other reversible work done by the system. $\delta Q = TdS$ is the change of entropy S by changes in volume, vibrational spectrum and segment orientation. δW can be splitted here in the work done by the constant external stress σ, by a jump $d\lambda$ of a segment at activation, shifting the volume with $Ad\lambda$ (A is the area of the cross section of the segment) and by other work terms. So: $\delta W = \sigma Ad\lambda + \delta W'$. The amount $\delta W'$ may consist of the increase of elastic energy stored in the volume, if there is any in the small volume, and a rubberlike work term by uncoiling bonds, that can be given as an entropy drop $-TdS_{el}$. Real plastic strain (i. e. the strain by a process

with a very short relaxation time), uncoiling and structural changes will be regarded as separate parallel acting processes later. In general $\delta W'$ is thus neglectable if there is no elastic material and no uncoiling in the small volume. Eq.(3.4.1) can now be written:

$$dU - TdS + PdV = \sigma A d\lambda + \delta W'. \qquad (3.4.2)$$

In this equation is $dU + PdV = dH$ called the change of enthalpy H, and $dH - TdS = dG$ is called the change of Gibbs free energy G, both under conditions of constant P and T. So eq.(3.4.2) becomes:

$$dG = \delta W, \qquad (3.4.3)$$

making it possible to calculate ΔG for an assumed mechanism. For a process in wich only work is done by pressure, or $\delta W = 0$, eq.(3.4.1) gives:

$$dH = \delta Q, \text{ or } \Delta H = Q. \qquad (3.4.4)$$

Thus for a process at constant pressure the heat exchanged between the system and the surroundings is the difference between the initial and final enthalpy of the system. A further consequence of eq.(3.4.4) is that the heat capacity at constant pressure C_p is:

$$C_p = \left(\frac{\delta Q}{\partial T}\right)_p = \left(\frac{\partial H}{\partial T}\right)_p, \qquad (3.4.5)$$

or:

$$\Delta C_p = \left(\frac{\partial \Delta H}{\partial T}\right)_p. \qquad (3.4.6)$$

Thus it is seen that the change of the heat of a reaction is directly related to the differences between the heat capacity of the products and that of the reactants (Kirchhoff's law), and depending on the sign of ΔC_p, the reaction is exo- or endo-thermic. If $\Delta C_p = 0$, the reaction is thermally neutral.

Because the energy change of a system, passing from one state to another, is independent of the particular course followed, the reaction may be splitted in different chemical steps if pressure, temperature and crystalline form are the same (Hess' law). The same can be done with other state properties e.g. volume or energy. As a consequence of this law, it is possible to expand the total potential energy curve into sinus series, as is done in the next chapter. Except for the first expanded term, this results in parallel rows of symmetrical barriers. Beause, at zero stress, the forward and backward activation energy is the same for each barrier of the row, the reaction is neutral and the enthalpy change is constant independent of the temperature for the total row and because, at constant temperature and pressure, $\Delta C_p = T(\partial \Delta S / \partial T) = 0$, is also the entropy

change ΔS constant during passage of the row. So the row acts as one process with a specivic enthalpy and entropy, (both independent of the temperature) and with a specific activation volume.
If mass is added to the, above mentioned, closed system, for instance by absorbing moisture, the energy equation (3.4.1) becomes for zero δW:

$$dU = \delta Q - PdV + \omega d\mu, \tag{3.4.7}$$

where ω is here the relative moisture content, or $\omega = 1$ at saturation of all bonds, and μ is the chemical potential or $d\mu$ is the change of the internal energy by saturation with water.
To find the potential energy change for a single process, so without structural changes and other variations of the energy, a general thermodynamic potential E can be chosen in the determining variables T, λ and ω. The pressure P doesn't perform work for flow at constant volume and can be regarded to be constant.

$$dE = d(H - TS - \sigma A\lambda - \mu\omega) = dH - TdS - SdT - \sigma Ad\lambda - A\lambda d\sigma + \\ - \mu d\omega - \omega d\mu. \tag{3.4.8}$$

At equilibrium, or when P, T, λ and ω are constant, $dE = 0$, or:

$$0 = dH - TdS - A\lambda d\sigma - \omega d\mu, \tag{3.4.9}$$

giving the first law of thermodynamics.
Substraction of eq.(3.4.9) from eq.(3.4.8) gives:

$$dE = - SdT - \sigma Ad\lambda - \mu d\omega = \frac{\partial E}{\partial T}dT + \frac{\partial E}{\partial \lambda}d\lambda + \frac{\partial E}{\partial \omega}d\omega, \tag{3.4.10}$$

being the second law.
As seen before, the enthalpy and entropy are constant with respect to T, (at zero stress), and thus $\partial E/\partial T$ is constant, and E is linear in T (by ST). From the Maxwell relations: $\partial^2 E/\partial T\partial\lambda = \partial^2 E/\partial\lambda\partial T$, and so on, it can be found that:

$$-\frac{\partial S}{\partial \lambda} = -A\cdot\frac{\partial \sigma}{\partial T}; \qquad A\cdot\frac{\partial \sigma}{\partial \omega} = \frac{\partial \mu}{\partial \lambda} \quad \text{and} \quad \frac{\partial S}{\partial \omega} = \frac{\partial \mu}{\partial T}. \tag{3.4.11}$$

If now the potential energy curve E, as function of λ (T, ω constant), is approached by a straight line, then, in the first expression of eq(3.4.11) is $\partial S/\partial\lambda$ constant, independent on λ and T. So S or E is linearly dependent on λ giving:

$$S = \lambda f_1(\omega) + f_2(\omega), \tag{3.4.12}$$

and the stress σ will be, according to this first Maxwell relation:

$$\sigma A = Tf_1(\omega) + f_3(\omega,\lambda). \tag{3.4.13}$$

Because E has the form: $E = -ST + f_4(\omega,\lambda,T)$,

$$E = -\lambda Tf_1(\omega) - Tf_2(\omega) + f_4(\omega,\lambda,T). \tag{3.4.14}$$

Also E has the form: $E = -\sigma A\lambda + f_5(\omega,\lambda,T)$ or:

$$E = -\lambda Tf_1(\omega) - \lambda f_3(\omega,\lambda) + f_5(\omega,\lambda,T). \tag{3.4.15}$$

Because eq.(3.4.14) and eq.(3.4.15) has to be identical, E has the form:

$$E = -\lambda Tf_1(\omega) - \lambda f_3(\omega\lambda) - Tf_2(\omega) + C, \tag{3.4.16}$$

where C is a constant. This equation satisfies the other Maxwell relations of eq.(3.4.11) and can be written:

$$E = C - \sigma\lambda A - Tf_2(\omega). \tag{3.4.17}$$

So E is linearly dependent on λ, σ and T. The value $\sigma\lambda$ is a function of ω and can be linearly dependent of T.

To determine the relations of ω, E can be regarded as function of the variables ω, σ and T, or:

$$dE = -SdT - \lambda Ad\sigma - \mu d\omega, \tag{3.4.18}$$

giving the Maxwell relations:

$$\frac{\partial S}{\partial \sigma} = A\cdot\frac{\partial \lambda}{\partial T}; \quad A\cdot\frac{\partial \lambda}{\partial \omega} = \frac{\partial \mu}{\partial \sigma} \quad \text{and} \quad \frac{\partial S}{\partial \omega} = \frac{\partial \mu}{\partial T}. \tag{3.4.19}$$

The expansion of wood with moisture content is linear, so $\partial\lambda/\partial\omega$ is constant and λ is linear dependent on ω. Also is λ linear dependent on T, (indicating a constant thermal expansion coefficient of λ up to activation). So $\partial\lambda/\partial T$ is linear with ω and also $\partial S/\partial\sigma$ and S. Further also μ is linear dependent on σ, ω and T, the same as S.
It is now shown that E can be assumed to be linear dependent on σ,T and ω.

$$E = a_1 + a_2\omega + a_3T + a_4\omega T + \sigma(a_5 + a_6\omega + a_7T + a_8\omega T), \tag{3.4.20}$$

and the energy change on activation has the same form:

$$\Delta E = \Delta a_1 + \Delta a_2\omega + \Delta a_4\omega T + \sigma(\Delta a_5 + \Delta a_6\omega + \Delta a_7T + \Delta a_8\omega T). \tag{3.4.21}$$

This can be given by a stress independent change of enthalpy H' and entropy S' denoted by a slash ', and a stress dependent part:

$$\Delta E = \Delta H' - \Delta S'T - \sigma V_a, \tag{3.4.22}$$

where V_a is the activation volume λA.
Leaving out the Δ-sign, because misunderstanding is not possible:

$$E = H' - S'T - \sigma V_a = E' - \sigma V_a = E' - W, \tag{3.4.23}$$

as used before. In this equation is, with the moisture content ω:

$H' = H_0 - H_1\omega/\omega_m$,

$S' = S_0 + S_1\omega/\omega_m$,

$V_a = V_0 + \omega/\omega_m(V_1T/T_m + V_2) + V_3T/T_m$,

where T_m is a scaling temperature and ω_m the moisture content of saturation.

From tests of [5], it can be deduced that $H_1 = S_1 = 0$ and V_a is constant for fracture processes with respect to T for $\omega = 0$ (see later). So $V_3 = 0$ in that case. For very quick loading however, fracture is in the lignin and follows the WLF-equation above the transition temperature [6]. Then V_a has a different form, $A'\lambda/N$, according to a structural change mechanism, changing the "constant" N, as will be discussed in chapter 6. For that case λ has to be replaced by $1/N$ in the equations above and A has to be replaced by $\lambda A'$. Because $N = N_0 + \beta(T - T_0)$, the first Maxwell relation of eq.(3.4.11), is then: $\partial S/\partial N^{-1} = -(N^2/\beta)\cdot\partial S/\partial T = A'\lambda\partial\sigma/\partial T$, or: $-S = \beta A'\lambda\sigma/N^2 + C = \beta A'\lambda\sigma_0/N + C$ (with $\sigma/N = \sigma_0$), giving the relationship for this transition (see 6).

E is often taken to be proportional to the modulus of elasticity because the height of the energy barrier must be proportional to the modulus of elasticity. This cannot be applied for wood because the elasticity is determined by the crystalline regions and the viscoelastic behaviour is in the amorphous zones between the crystalline zones. The decrease of the modulus is linear with temperature (between transition zones) indicating a decrease of the free energy or an increase of entropy with temperature (increasing disorder) for the crystalline material. Creep tests on cellulosic materials, affecting the amorphous material, show a linear increase of the free energy with temperature, so a high increase of negative entropy with temperature, although there is no rubbery behaviour. An explanation could be that movement by activation is complicated and is not very probable and thus giving rise to a high negative entropy.

3.5 Parameters of the flow units

For the derivations in the next chapter, we may express the reaction equations in the dimensions of the flow units.

If a segment is moving upwards, the hole 2λ in fig.3.5 is moving downwards. The activation volume V is 2λ times A, and the work when moving

over a barrier, on one unit is: $f.V/2 = f.A.\lambda$, where f is the stress on the unit and A is the area. This can be expressed in the stress σ in the material by: $\sigma = N.f.A$ where N is the number of elements per unit area. So the force per element, is the force per unit area divided by the number of elements per unit area. λ_1 is the length of the flow segment or the distance between flow-points. So the concentration of flow units ρ, being the number of activated volumes per unit volume, can be written: $\rho = N.2\lambda.A/\lambda_1$.

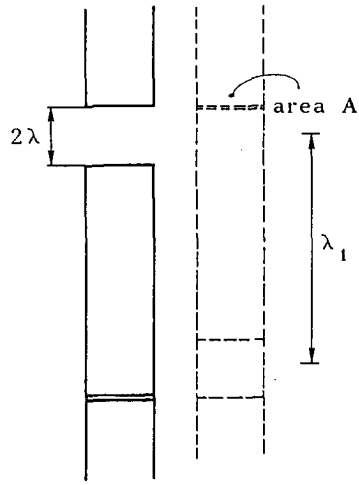

fig. 3.5 Moving space

3.6 References

[1] Deformation kinetics. A.S. Krausz, H. Eyring 1975 John Wiley & Sns.

[2] Cellulose as Viscoelastic Material. A.H. Nissan, S.S. Sternstein, Dep. of Chem. Engin. Troy, N.Y., U.S.A.

[3] Influence of Heat on Creep of Dry D.-Fir. E.L. Schaffer For. Prod. Lab. Madison , Wisconsin.

[4] Thermogravimetric Analysis of Pulps. Wood Science and Techn. V10-2 1976

[5] Ueber die Abhangigkeit der Festigk. d. Holzes v. d. Feuchte. J.M. Ivanov Holztechnologie 22 1981 1.

[6] R.J. Hoyle, M.C. Griffith, R.Y. Itany, 1985, Wood and Fiber Science, July 1985 V.17

4. DERIVATION OF A CREEP AND DAMAGE MODEL BASED ON THE THEORY OF DEFORMATION KINETICS

4.1 Introduction

In this chapter the mathematical derivation is given of a general creep- and damage- model that is solely based on the reaction equations of the bondbreaking and bondreformation processes at the deformation sites due to the local stresses in the elastic material around these sites. The model doesn't contain the hidden suppositions of the other known models and is able to explain the phenomenological laws.

4.2 Basic reaction rate equations.

In this paragraph the reaction rate equations of [1] are given with all the steps of the derivation in order to see the modifications made in 4.3 to derive a generalized flow theory.
Most models are based on the simple form of the reaction rate equation eq.(3.2.1) (for activation over a single potential energy barrier):

$$\text{Rate} = \frac{d\rho_2}{dt} = \rho_1 C_{1f} - \rho_2 C_{1b} = \frac{\rho_1 - \rho_2 C_{1b}/C_{1f}}{1/C_{1f}}, \qquad (4.2.1)$$

being a poor approximation of eq.(4.2.13) and eq.(4.2.15) and will lead to variable activation parameters in different circumstances.
This is so, because for larger, noticible, plastic deformations, the reaction occurs over a system of energy barriers and systems of consecutive and parallel barriers have to be regarded.
For a two barrier system (fig.4.1) there is an intermediate stage of units being in steady state concentration. So:

$$\frac{d\rho_2}{dt} = 0 = -\rho_2(C_{2f} + C_{1b}) + \rho_1 C_{1f} + \rho_3 C_{2b}. \qquad (4.2.2)$$

The net numbers of units crossing the two barrier system is thus:

$$\text{Rate} = \rho_2 C_{2f} - \rho_3 C_{2b} = C_{2f}\frac{\rho_1 C_{1f} + \rho_3 C_{2b}}{C_{2f} + C_{1b}} - \rho_3 C_{2b} =$$

$$= \frac{\rho_1 - \rho_3 (C_{1b}/C_{1f}).(C_{2b}/C_{2f})}{1/C_{1f} + C_{1b}/(C_{1f}.C_{2f})}. \qquad (4.2.3)$$

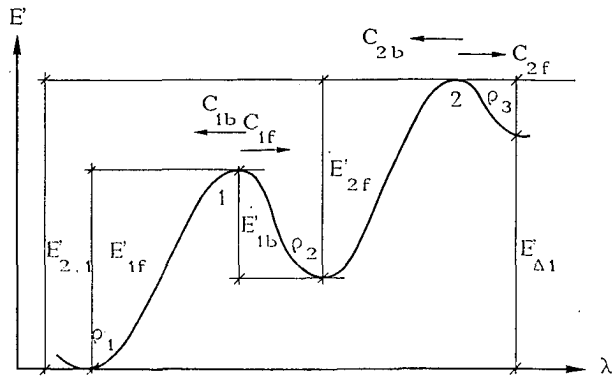

fig. 4.2 Two consecutive barriers [1]

For each obstacle i we have:

$$C_i = \varkappa_i \frac{k\,T}{h} \exp\left(-\frac{E_i}{k\,T}\right), \qquad (4.2.4)$$

or:

$$\frac{C_{ib}}{C_{i+1,f}} = \exp\left(\frac{E_{i+1,f} - E_{ib}}{kT}\right), \qquad (4.2.5)$$

and:

$$\frac{C_{1b}}{C_{2f}C_{1f}} = \frac{h}{\varkappa kT} \exp\left(\frac{E_{2f} - E_{1b} + E_{1f}}{kT}\right) = \frac{h}{\varkappa kT} \exp\left(\frac{E_{2,1}}{kT}\right) = \frac{1}{C_{2,1}}. \qquad (4.2.6)$$

Similarly:

$$\frac{C_{1b}C_{2b}}{C_{1f}C_{2f}} = \exp\left(\frac{E_{1f} - E_{1b} - E_{2b} + E_{2f}}{kT}\right) = \exp\left(\frac{E_{\Delta 1}}{kT}\right) \qquad (4.2.7)$$

Thus the rate becomes: (E = E' - W)

$$\text{Rate} = \frac{\rho_1 - \rho_3 \exp\left(\frac{E'_{\Delta 1} - W_{\Delta 1}}{kT}\right)}{1/C_{1,1} + 1/C_{2,1}}, \qquad (4.2.8)$$

with:

$$C_{1,1} = \varkappa \frac{kT}{h} \exp\left(- \frac{E'_{1,1} - W_{1,1}}{kT}\right), \tag{4.2.9}$$

$$C_{2,1} = \varkappa \frac{kT}{h} \exp\left(- \frac{E'_{2,1} - W_{2,1}}{kT}\right), \tag{4.2.10}$$

and

$$E_{\Delta 1} = (E' - W)_{1f} - (E' + W)_{1b} - (E' + W)_{2b} + (E' - W)_{2f} =$$

$$= (E'_{1f} - E'_{1b} - E'_{2b} + E'_{2f}) - (W_{1b} + W_{1f} + W_{2b} + W_{2f}) = E'_{\Delta 1} - W_{\Delta 1}. \tag{4.2.11}$$

$$E_{2,1} = E_{1f} - E_{1b} + E_{2f} = (E' - W)_{1f} - (E' + W)_{1b} + (E' - W)_{2f} =$$

$$= E'_{1f} - E'_{1b} + E'_{2f} - (W_{1f} + W_{2f} + W_{1b}) = E'_{2,1} - W_{2,1}, \tag{4.2.12}$$

$$C_{1,1} = C_{1f}.$$

In the same way is for n obstacles in series:

$$\text{Rate}_n = \frac{\rho_1 - \rho_{n+1} \exp(E_{\Delta 1}/kT)}{\sum_{i=1}^{n} \frac{1}{C_{i,1}}}, \tag{4.2.13}$$

with:

$$C_{i,1} = \varkappa \frac{kT}{h} \exp\left(- \frac{E_{i,1}}{kT}\right). \tag{4.2.14}$$

For m processes parallel:

$$\text{Rate}_{m,n} = \sum_{j=1}^{m} \left(\frac{\rho_1 - \rho_{n+1} \exp(E_{i,\Delta}/kT)}{\sum_{i=1}^{n} (1/C_{i,1})} \right)_j. \tag{4.2.15}$$

4.3 Derivation of a general creep- and damage- model by series approximation.

The general equations can be simplified to suitable forms for solutions of the rate equations as will be shown here.

It is possible to expand the total potential energy curve into (Fourier-) series and regard the process as a parallel acting system of symmetrical consecutive barriers.

Except of the first term, that is only symmetrical at loading to W_0 (see eq.(4.3.14), is in all series $E'_{\Delta 1} = 0$ (see fig.4.2) and because of the symmetry of the barriers in the series, all $E_{i,j}$'s and all $W_{i,j}$'s are equal.

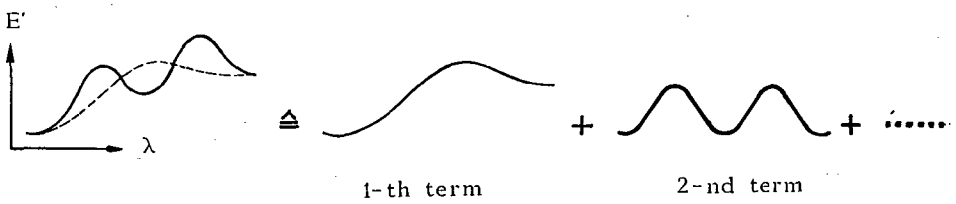

fig. 4.3.1 Series approximation of E'

By eq.(4.2.9): $$C_{1,1} = \varkappa \frac{kT}{h} \exp\left(-\frac{E' - W}{kT}\right). \qquad (4.3.1)$$

By eq.(4.2.10): $$C_{2,1} = \varkappa \frac{kT}{h} \exp\left(-\frac{E' - 3W}{kT}\right). \qquad (4.3.2)$$

Eq.(4.2.14) becomes: $$C_{i,1} = \varkappa \frac{kT}{h} \exp\left(-\frac{E' - (2i-1)W}{kT}\right). \qquad (4.3.3)$$

So: $$\sum \frac{1}{C_{i,1}} = \frac{1}{\varkappa \frac{kT}{h} \exp\left(-\frac{E'}{kT}\right)} \cdot \left(\frac{1}{\exp\left(\frac{W}{kT}\right)} + \frac{1}{\exp\left(\frac{3W}{kT}\right)} + \cdots + \frac{1}{\exp\left(\frac{(2i-1)W}{kT}\right)}\right) =$$

$$= \frac{1}{\varkappa \frac{kT}{h} \exp\left(-\frac{E'}{kT}\right)} \cdot \left(\frac{1}{\exp\left(\frac{W}{kT}\right)} + \frac{1}{\left(\exp\left(\frac{W}{kT}\right)\right)^3} + \cdots + \frac{1}{\left(\exp\left(\frac{W}{kT}\right)\right)^{(2i-1)}}\right) =$$

$$= \frac{1}{\varkappa \frac{kT}{h} \exp\left(-\frac{E'}{kT}\right)} \cdot \left(\frac{\frac{1}{\exp(W/kT)}\left(1 - \left(\frac{1}{\exp(W/kT)}\right)^{2i}\right)}{1 - 1/(\exp(W/kT))^2}\right) =$$

$$= \frac{1}{\varkappa \frac{kT}{h} \exp\left(-\frac{E'}{kT}\right)} \left(\frac{1 - \exp(-2iW/kT)}{\exp(W/kT) - (\exp(W/kT))^{-1}}\right) =$$

$$= \frac{1 - \exp(-2iW/kT)}{\varkappa \frac{kT}{h}\left(\exp\left(-\frac{E'}{kT}\right)\right) \cdot 2\left(\sinh\left(\frac{W}{kT}\right)\right)}. \qquad (4.3.4)$$

The rate is from eq.(4.2.11) and (4.2.13), with $E_{\Delta 1} = E'_{\Delta 1} - W_{\Delta 1} = -W_{\Delta 1} = -2iW$:

$$\text{Rate} = \frac{(\rho_1 - \rho_{n+1}\exp(-2iW/kT)) \cdot (2\varkappa \frac{kT}{h} \exp(E'/kT) \cdot \sinh(W/kT))}{1 - \exp(-2iW/kT)} =$$

$$= 2\varkappa \frac{kT}{h} \rho_1 \exp\left(-\frac{E'}{kT}\right) \cdot \sinh\left(\frac{W}{kT}\right). \qquad (4.3.5)$$

Equilibrium (Rate= 0) is only possible for W= 0 for these barriers and from symmetry of $E = E_f = E_b$, ρ_1 has to be equal to ρ_{n+1}.

Calling: $1/((\varkappa kT/h)\exp(-E'/kT)) = t_i$, the relaxation time of the i-th expanded term, eq.(4.3.5) can be written like a chemical reaction equation:

$$\frac{d\rho_{n+1}}{dt} = -\frac{d\rho_1}{dt} = \frac{2\rho}{t_i}\sinh\left(\frac{W_i}{kT}\right). \tag{4.3.6}$$

Now the work W, of a flow unit with area $\lambda_2.\lambda_3$ moving over a barrier over a distance 2λ, is (see 3.5):

$$W = f.\lambda_2.\lambda_3.\lambda = fV/2 = \sigma\lambda/N,$$

where V is the activation volume and N is the number of activated flow units per unit area. The concentration of flow units, or the number of activated volumes per unit volume, is:

$$\rho = N.\lambda_2.\lambda_3.2\lambda/\lambda_1.$$

Eq.(4.3.6) can now be written (with $\varphi_i = \lambda_i/N_i$):

$$\frac{d}{dt}\left(\frac{N.\lambda.\lambda_2.\lambda_3}{\lambda_1}\right) = 2\frac{N.\lambda_2.\lambda_3.\lambda}{t_i.\lambda_1}\cdot\sinh(\sigma_i.\varphi_i), \tag{4.3.7}$$

or, for a constant structure $N.\lambda_2.\lambda_3$:

$$\frac{d}{dt}\left(\frac{\lambda}{\lambda_1}\right) = 2\frac{\lambda}{t_i.\lambda_1}\cdot\sinh(\sigma_i.\varphi_i), \tag{4.3.8}$$

or because λ/λ_1 is a plastic strain ε:

$$\frac{d\varepsilon}{dt} = \dot{\varepsilon} = \frac{\varepsilon_0'}{t_i}\sinh(\sigma_i.\varphi_i) = \frac{1}{t_i'}\sinh(\sigma_i.\varphi_i),$$

with the apparant relaxation time $t_i' = t_i/\varepsilon_0'$ ($\varepsilon_0' = 1$ is assumed for cellulosic materials). So eq.(4.3.6) gets the form for no structural change:

$$\dot{\varepsilon} = \frac{1}{t_i}\sinh(\varphi_i.\sigma_i). \tag{4.3.9}$$

The form of the first expanded term of the series (see fig. 4.3.1) has to be taken symmetrical for the expanded W. So from eq.(4.2.1):

$$\text{Rate} = \varkappa\frac{kT}{h}\left(\rho_1.\exp\left(-\frac{E_{1f}' - W_1}{kT}\right) - \rho_{n+1}.\exp\left(-\frac{E_{1b}' + W_1}{kT}\right)\right). \tag{4.3.10}$$

For a creep process, it may be expected that the rate is zero for no external force (equilibrium) or $W_1 = 0$. So (4.3.10) becomes:

$$\rho_1\exp\left(-\frac{E_{1f}'}{kT}\right) = \rho_{n+1}\exp\left(-\frac{E_{1b}'}{kT}\right), \tag{4.3.11}$$

and eq.(4.3.10) can be written:

$$\text{Rate} = 2\varkappa\frac{kT}{h}\rho_1\exp\left(-\frac{E'_{1f}}{kT}\right).\sinh\left(\frac{W_1}{kT}\right),$$

$$\text{or:}\quad \dot{\varepsilon} = \frac{1}{t_1}\sinh(\sigma_1.\varphi_1). \tag{4.3.12}$$

For low stresses, $\sinh(\sigma.\varphi) \approx \sigma.\varphi$ and the behaviour is approximately Newtonian.

For structural changes, as in crack propagation, the crack extension force must overcome the thermodynamic surface energy. Further energy is needed to change the material near the crack surface (the new surface contains more defects) and to fracture strong ordered areas of bonds, crossing the surface, that cannot be broken by thermal activation at normal temperatures. So, calling these energies W_0, the crack is in an equilibrium state with zero velocity when $W = W_0$. Eq. (4.3.10) then gives:

$$\rho_1\exp\left(-\frac{E'_{1f} - W_0}{kT}\right) = \rho_{n+1}\exp\left(-\frac{E'_{1b} + W_0}{kT}\right).$$

So eq. (4.3.10) can be written:

$$\text{Rate} = \varkappa\frac{kT}{h}\left(\rho_1.\exp\left(-\frac{E'_{1f} - W_0}{kT}\right).\left(\exp\left(\frac{W_1 - W_0}{kT}\right) - \exp\left(-\frac{W_1 - W_0}{kT}\right)\right)\right) =$$

$$= 2\varkappa\frac{kT}{h}\rho_1.\exp\left(-\frac{E'_{1f} - W_0}{kT}\right).\sinh\left(\frac{W_1 - W_0}{kT}\right), \tag{4.3.13}$$

or, for a steady state process (ρ_1 = constant):

$$\dot{\varepsilon} = \frac{1}{t_1}\sinh\left(\frac{W_1 - W_0}{kT}\right), \tag{4.3.14}$$

with:

$$\frac{1}{t_1} = \varkappa\frac{kT}{h}\exp\left(-\frac{E'_{1f} - W_0}{kT}\right) \qquad \left(\approx \varkappa\frac{kT}{h}\exp\left(-\frac{E'_{1f} + E'_{1b}}{2kT}\right)\right),$$

and:

$$W_0 = (E'_{1f} - E'_{1b})/2 - kT.\ln(\sqrt{(\rho_1/\rho_{n+1})}) \approx (E'_{1f} - E'_{1b})/2.$$

Because of the long relaxation time t_0, that is to be expected for this first expansion term, the influence of W_0 will not be noticed and can be neglected for short term processes. Even at high stress levels this will be true as can be seen from the following.

For high stress:

$$\sinh((W_1 - W_0)/kT) \approx 0.5\ \exp((W_1 - W_0)/kT),$$

and:

$$\dot{\varepsilon} = \varkappa\frac{kT}{h}\exp\left(-\frac{E'_{if} - W_0}{kT}\right)\sinh\left(\frac{W_1 - W_0}{kT}\right) \approx \varkappa\frac{kT}{2h}\exp\left(\frac{-E'_{if} + W_1}{kT}\right) \approx$$

$$\approx \varkappa\frac{kT}{h}\exp\left(\frac{-E'_{if}}{kT}\right).\ \sinh\left(\frac{W_1}{kT}\right).$$

This is assumed for the next equations.

If there are different kinds of flow units acting together, the total applied stress is the sum of these components. So:

$$\sigma = \sum \sigma_i . x_i$$

where x_i is the fraction of the total an-elastic stress due to the i-th group of units. With $W_i = \sigma_i \varphi_i$:

$$\sigma = \sum_i \frac{x_i}{\varphi_i}\operatorname{arcsinh}(t_i\dot{\varepsilon}),$$

or:

$$\frac{\sigma}{\dot{\varepsilon}} = \sum_i \frac{x_i t_i}{\varphi_i}.\frac{\operatorname{arcsinh}(t_i\dot{\varepsilon})}{t_i\dot{\varepsilon}}. \qquad (4.3.15)$$

For the terms with $t_i\dot{\varepsilon} << 1$: $(\operatorname{arcsinh}(t_i\dot{\varepsilon})/t_i\dot{\varepsilon} = 1$,
and for terms with $t_i\dot{\varepsilon} >> 1$: $(\operatorname{arcsinh}(t_i\dot{\varepsilon})/t_i\dot{\varepsilon} = 0$.
So there remain a limited number of terms:

$$\frac{\sigma}{\dot{\varepsilon}} = \sum\frac{x_i . t_i}{\varphi_i} + \sum\frac{x_i}{\varphi_i\dot{\varepsilon}}\operatorname{arcsinh}(t_i\dot{\varepsilon}). \qquad (4.3.16)$$

The first term of (4.3.16) can be expressed in a mean value:

$$\sum\frac{x_i . t_i}{\varphi_i} = t_1\sum\frac{x_i}{\varphi_i} = t_1 x_1 \sum\frac{1}{\varphi_i} = t_1 x_1/\varphi_1, \qquad (4.3.17)$$

and eq.(4.3.16) gets the form of the generalized flow theory [1] consisting of separate symmetrical elements:

$$\frac{\sigma}{\dot{\varepsilon}} = \frac{x_1 t_1}{\varphi_1} + \frac{x_2 t_2}{\varphi_2}.\frac{\operatorname{arcsinh}(t_2\dot{\varepsilon})}{t_2\dot{\varepsilon}} + \frac{x_3 t_3}{\varphi_3}.\frac{\operatorname{arcsinh}(t_3\dot{\varepsilon})}{t_3\dot{\varepsilon}}. \qquad (4.3.18)$$

So, by series expansion, the assumptions of this generalized flow theory have now been proven:

a) The flow unit spectrum exists (as expanded terms) and may be approximated by a limited number of elements with distinct average relaxation times. (As experimentaly found [2], less than 3 groups are sufficient for a description of most materials).

b) The deformation rate of all units is the same (in accordance with the observations that there are no structural changes due to rate differences

during flow).

The first term of eq.(4.3.18) represents Newtonian behaviour. The others are non-Newtonian, or Newtonian in the low strain rate range.

The fysical meaning of the expansion of the potential energy curve is to regard the total process as a result of parallel acting simple processes. For instance, a dislocation may meet different kinds of obstacles and the mean waiting time per obstacle at the end of the process is the mean of the waiting times at the different obstacles. At higher stresses these

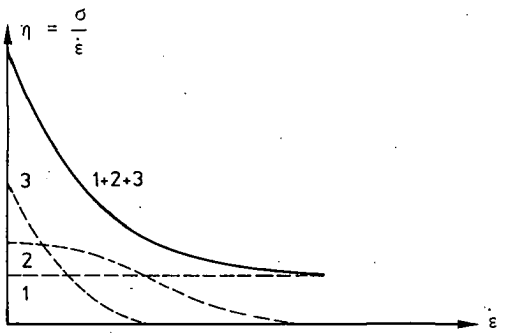

fig. 4.3.2 Viscosity-strain rate relation [1]

waiting times may change differently for the different obstacles and the apparent activation energy and volume may be stress dependant. Expansion means that groups of dislocations are supposed to meet only one type of obstacle. Each group meets another type of the same obstacles in succession, resulting in a number of parallel acting simple reactions. Hereby it is supposed that the interaction between the different mechanisms is not strong. In elementary reactions, the activation parameters (enthalpy, entropy) are often constant (for temperature) so that a simple description of the total rate process becomes possible.

An experimental verification (by relaxation tests) of this picture follows from [3] for metals. Those metals that where described with single barrier mechanisms, often had a stress dependant activation energy or volume. This was not the case for the metals that were described by two (so more than one) parallel symmetrical barriers. The enthalpy and entropy were also constant.

The same has be done for cotton [4] (that has a similar structure as wood). The two symmetrical barriers had constant, stress independant activation parameters.

4.4 Basic equations for fracture.

Eq.(4.3.18) applies for steady state processes, when the structure and bond density do not change. Crack initiation and propagation occur when the rate of bond breaking exceeds the rate of bond re-establishment, leading to structural changes. For this case eq.(4.3.6) does not lead to eq. (4.3.8) but can be written in the form:

$$\frac{d}{dt}\left(\frac{N\lambda}{\lambda_1}\right) = \frac{2N\lambda}{\lambda_1 t_r}\sinh\left(\frac{\sigma\lambda}{NkT}\right), \tag{4.4.1}$$

where the change of N may be due to primary bond breaking. If λ_1 can be regarded as a constant length of the flow segment, as can be expected if there is no change in flow unit density, then N can also be interpreted as the number of bonds along the flow segment and a change of N will be the change of the number of bonds along the segments. So N or λ may change in eq.(4.4.1) whether bond density changes (N) or change in free volume (λ) is expected to cause fracture. Both models give the same results because eq. 4.4.1 is for constant $\lambda = \lambda_0$ (and decreasing N), according to eq.(4.3.6):

$$-\frac{dN_1}{dt} = \frac{2N_1}{t_r}\sinh\left(\frac{\sigma\lambda_0}{N_1 kT}\right),$$

or:

$$\frac{d(1/N_1)}{dt} = \frac{1}{N_1}\cdot\frac{2}{t_r}\sinh\left(\frac{\sigma\lambda_0}{N_1 kT}\right). \tag{4.4.2}$$

For constant $N_1 = N_{n+1} = N$ and variable, increasing λ, eq.(4.3.6) leads to:

$$\frac{dN_{n+1}\lambda}{dt} = \frac{2N_1\lambda}{t_r}\sinh\left(\frac{\sigma\lambda}{N_1 kT}\right),$$

or:

$$\frac{d\lambda}{dt} = \frac{2\lambda}{t_r}\sinh\left(\frac{\sigma\lambda}{NkT}\right). \tag{4.4.3}$$

So eq.(4.4.2) in 1/N is exactly the same as eq.(4.4.3) in λ. The choise is thus possible to regard λ as a constant (as done for crystals and metals, (where λ is taken to be equal to the Burger's vector) or to take N as constant (when slip of the chains is expected to cause failure).
A third possibility for fracture is the change of λ_1 (by the part of the change of bond density along the segment or change in flow unit density that doesn't decrease the stressed area). Then eq.(4.4.1) becomes:

$$\frac{d(1/\lambda_1)}{dt} = \frac{2}{t_r\lambda_1}\sinh\left(\frac{\sigma\lambda}{N_1 kT}\right). \tag{4.4.4}$$

In the following it will be shown that both models eq.(4.4.2) and eq.(4.4.4) may give the same results. So that the simplest equation (4.4.4) can be used for applications. Because fracture occurs at higher stresses, eq. (4.4.2) can be written:

$$-\frac{dN_1}{dt} = \frac{2N_1}{t_r}\sinh\left(\frac{\sigma\lambda_0}{N_1kT}\right) \approx \frac{2N_1}{t_r}\exp\left(\frac{\sigma\lambda_0}{N_1kT}\right), \tag{4.4.5}$$

or for constant stress σ:

$$\int_{\sigma\lambda/N_0kT}^{\infty} \left(\frac{dN_1^{-1}}{N_1^{-1}}\exp\left(\frac{\sigma\lambda}{kT}N_1^{-1}\right)\right) = \frac{t_f}{t_r}, \tag{4.4.6}$$

where t_f is the lifetime of he specimen subjected to a constant stress. The integral in eq.(4.4.6) is the exponential integral: $-E_i(-\sigma\lambda/NkT)$ reducing for larger values of the variable to:

$$-E_i\left(-\frac{\sigma\lambda}{NkT}\right) \approx \frac{\exp(-\lambda\sigma/N_0kT)}{\sigma\lambda/N_0kT}. \tag{4.4.7}$$

So eq.(4.4.6) becomes:

$$t_f = t_r\frac{N_0kT}{\sigma\lambda}\exp\left(-\frac{\sigma\lambda}{N_0kT}\right) = \frac{N_0h}{\varkappa\sigma\lambda}\exp\left(\frac{E}{kT} - \frac{\sigma\lambda}{N_0kT}\right), \tag{4.4.8}$$

or:

$$\ln(t_f) = \ln\left(\frac{N_0h}{\varkappa\sigma\lambda}\right) + \frac{E}{kT} - \frac{\sigma\lambda}{N_0kT}. \tag{4.4.9}$$

In the same way eq.(4.4.4) can be integrated:

$$\int_{1/\lambda_{1o}}^{1/\lambda_{1m}} d(\ln(1/\lambda_1)) = \frac{t_f}{t_r}\exp\left(\frac{\sigma\lambda}{N_0kT}\right) = \ln\left(\frac{\lambda_{1o}}{\lambda_{1m}}\right), \tag{4.4.10}$$

or:

$$t_f = \frac{h}{\varkappa kT}\ln\left(\frac{\lambda_{1o}}{\lambda_{1m}}\right).\exp\left(\frac{E}{kT} - \frac{\sigma\lambda}{N_0kT}\right),$$

or:

$$\ln(t_f) = \ln\left(\frac{h}{\varkappa kT}\ln\left(\frac{\lambda_{1o}}{\lambda_{1m}}\right)\right) + \frac{E}{kT} - \frac{\sigma\lambda}{N_0kT} = \ln(t_0) + \frac{E}{kT} - \frac{\sigma\lambda}{N_0kT}, \tag{4.4.11}$$

giving the same form as eq.(4.4.9).

Eq.(4.4.11) gives a strain criterion for failure:

$$t_0 = \frac{h}{\varkappa kT}\ln\left(\frac{\lambda_{1o}}{\lambda_{1m}}\right) \tag{4.4.12}$$

or:

$$\frac{\lambda_{1o}}{\lambda_{1m}} = \frac{\varepsilon_m}{\varepsilon_o} = \exp\left(\frac{\varkappa kT}{h}t_0\right). \tag{4.4.13}$$

From tests [5] it is found that t_0 in eq.(4.4.11) or eq.(4.4.9) has a de-

finite value for the many materials tested, being the reciprocal of the natural oscillation frequency of atoms in solids. It is seen that t_0 is not constant in eq.(4.4.9) being the error of integrating with a constant (mean value) λ_1. This error diminishes when T approaches zero as can be seen in eq.(4.4.13):

$\lambda_{1o} \rightarrow \lambda_{1m}$ when $T \rightarrow 0$.

It is seen that the bond breaking model in this form, changing only the value of N, only applies near absolute zero temperature for small values of E' and $\sigma\lambda/N_0$ (because $E' = \sigma\lambda/N_0 = h/t_0$ for T->0), and so for wood, showing higher values of E' and $\sigma\lambda/N_0$, there will be always changes in $1/\lambda_1$. To show the amount of change of N and $1/\lambda_1$, eq.(4.4.1) can be written:

$$\frac{d(\lambda/N\lambda_1)}{dt} = \frac{2\lambda}{N\lambda_1 t_r}\sinh\left(\frac{\sigma\lambda}{kTN}\right) \approx \frac{\lambda}{N\lambda_1 t_r}\exp\left(\frac{\sigma\lambda}{kTN}\right) \quad \rightarrow \quad (4.4.14)$$

$$\frac{d}{dt}\left(\ln\left(\frac{\lambda}{N}\right)\right) + \frac{d}{dt}\left(\ln\left(\frac{1}{\lambda_1}\right)\right) = \frac{1}{t_r}\exp\left(\frac{\sigma\lambda}{NkT}\right) \quad \rightarrow \quad (4.4.15)$$

$$(1 + A)\frac{d}{dt}\left(\ln\left(\frac{1}{\lambda_1}\right)\right) = \frac{1}{t_r}\exp\left(\frac{\sigma\lambda}{NkT}\right), \quad (4.4.16)$$

where A is the mean value of: $\dfrac{d(\ln(1/\lambda_1))/dt}{d(\ln(\lambda/N))/dt}$ and:

$A = 0$, when λ_1 is constant.

$$\int_{\lambda/N_0}^{\infty} \frac{d(\ln(\lambda/N))}{\exp(\sigma\lambda/NkT)} = \int_0^{t_f} \frac{dt}{(1+A)t_r} \rightarrow E_1\left(\frac{\sigma\lambda}{N_0 kT}\right) = \frac{t_f}{(1+A)t_r} \rightarrow \frac{\exp(-\sigma\lambda/N_0 kT)}{\sigma\lambda/N_0 kT} \approx$$

$$\approx \frac{t_f kT}{(1+A)h}\exp\left(-\frac{E'}{kT}\right). \quad (4.4.17)$$

Or with $\nu = 1/t_0$:

$$\exp\left(\frac{E'}{kT} - \frac{\sigma\lambda}{N_0 kT}\right) = \frac{1}{1+A}\cdot\frac{t_f}{t_0}\cdot\frac{kT}{h\nu}\cdot\frac{\sigma\lambda}{N_0 kT} \rightarrow$$

$$\frac{E'}{kT} - \frac{\sigma\lambda}{N_0 kT} = \ln\left(\frac{t_f}{t_0}\right) + \ln\left(\frac{kT}{h\nu}\cdot\frac{\sigma\lambda}{N_0 kT}\cdot\frac{1}{1+A}\right).$$

According to the measurements, see fig. 4.4.1, is, with $kT/h\nu \approx 1$:

$$\ln\left(\frac{\sigma\lambda}{N_0 kT(1+A)}\right) = 0 = \ln(1) \rightarrow 1+A = \frac{\sigma\lambda}{N_0 kT}. \quad (4.4.18)$$

Because $\sigma\lambda/N_0 kT \gg 1$ for wood, is: $A \gg 1$ and the change of $1/\lambda_1$ domi-

nates the change of N, and N may be regarded as constant when a maximum strain condition is used for the end state.
The improbable results of the bond breaking model eq.(4.4.9) shows that the change of N will be different. It is seen, that eq.(4.4.8) and eq.(4.4.11) contain N_0, the constant initial value of N and not the variable value of N. So the result of the process is not influenced by the path followed and it is possible to regard steps in the total process where $1/\lambda_1$ changes at constant N_0, followed bij a step where $1/\lambda_1$ is constant and N changes. These steps may be infinitely small. Then t_f according to eq.(4.4.11) will be shortened by the bondbreaking process according to eq.(4.4.8), and the time to failure is determined by the difference of the times of both processes. The result of the subtraction of both equations gives:

$$t_f = \left(\frac{h}{\varkappa kT}\cdot\ln\left(\frac{\lambda_{10}}{\lambda_{1m}}\right) - \frac{N_0 h}{\varkappa\sigma\lambda}\right)\cdot\exp\left(\frac{E'}{kT} - \frac{\sigma\lambda}{N_0 kT}\right)$$

So for this case:

$$t_0 = \frac{h}{\varkappa kT}\cdot\ln\left(\frac{\lambda_{10}}{\lambda_{1m}}\right) - \frac{N_0 h}{\varkappa\sigma\lambda},$$

or:

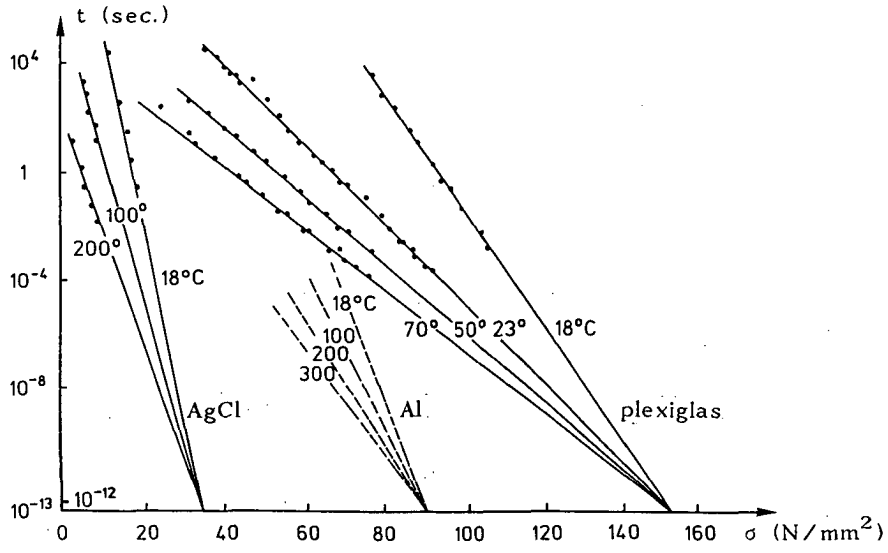

fig. 4.4.1 Stress and temperature dependence of the lifetime for some materials [5]

$$\ln\left(\frac{\lambda_{10}}{\lambda_{1m}}\right) = \frac{\varkappa kTt_0}{h} + \frac{N_0 kT}{\sigma\lambda},$$

and it is seen that there is a necessary ultimate strain condition for failure, determined by the point where all bonds are failed. Because the value of $kTN_0/\sigma\lambda$ is small for wood, there is a minor difference with the strain condition eq.(4.4.13).

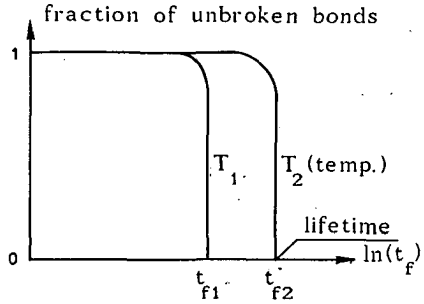

fig. 4.4.2 Lifetime of the bonds [8]

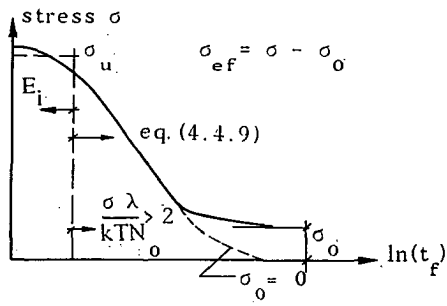

fig. 4.4.3 Long term strength

In the derivations above it is assumed that the initial value of $\lambda/N\lambda_1$ is small. When this initial value is not small and $\lambda/N\lambda_1$ doesn't change much with respect to the initial value, it must be possible to regard a mean value of $\lambda/N\lambda_1$ in the right hand side of eq.(4.4.14). Integration then gives:

$$\frac{d}{dt}\left(\frac{\lambda}{\lambda_1 N}\right) \approx \frac{\lambda}{t_r \lambda_{10} N_0} \exp\left(\frac{\sigma\lambda}{N_0 kT}\right) \quad \rightarrow \quad (4.4.19)$$

$$\frac{\lambda}{\lambda_1 N} = \frac{t_f}{t_r} \cdot \frac{\lambda}{\lambda_{10} N_0} \exp\left(\frac{\sigma\lambda}{N_0 kT}\right) + \frac{\lambda}{N_0 \lambda_{10}} \quad \rightarrow$$

$$\left(\frac{\lambda}{N_f \lambda_1} - \frac{\lambda}{N_0 \lambda_{10}}\right) \cdot \frac{N_0 \lambda_{10}}{\lambda} = \frac{t_f}{t_0} \cdot \frac{kT}{h\nu} \cdot \exp\left(-\frac{E}{kT} + \frac{\sigma\lambda}{kTN_0}\right) \quad \rightarrow$$

$$\frac{E}{kT} - \frac{\sigma\lambda}{kTN_0} \approx \ln\left(\frac{t_f}{t_0}\right) - \ln\left(\frac{N_0}{N_f} - 1\right) = \ln\left(\frac{t_f}{t_0}\right) - \ln\left(\frac{\varepsilon_f}{\varepsilon_0} - 1\right). \quad (4.4.20)$$

According to fig.4.4.1, the left term of this equation is equal to: $\ln(t_f/t_0)$ leading to $N_f = 0.5 \cdot N_0$, as experimentally found for fracture (i.e. the crack length is about the crack distance, or the intact area has reduced to 0.5 times the initial area when instable crack propagation starts).

Because λ/λ_1 is the strain, it is also possible to interprete this as an

ultimate strain condition $\varepsilon_f/\varepsilon_0 = 2$ for this slip model. This slip model is the same as discussed in 4.3. In [6] this model was used and as has to be expected from the derivations above, it was found that a maximum shear strain condition has to be applied. This was compaired by other tests [7] with the bond fracture model. Both models gave almost the same results as can be expected from the derivations above.

4.5 Fracture at constant loading rate and at creep loading

Numerical integration of the bond breaking eq.(4.4.2) [8] for constant loading rate is given in fig. 4.4.2, showing also the possibility of a constant value of N during the lifetime. This was also shown in 4.4 and it is sufficient to use eq.(4.4.4). For a constant loading rate $\sigma = \dot{\sigma}\cdot t$ (with $\dot{\sigma}$ = constant) this equation is:

$$\frac{d}{dt}(\ln(1/\lambda_1)) = \frac{2}{t_r}\sinh\left(\frac{\dot{\sigma}\lambda t}{NkT}\right), \tag{4.5.1}$$

or:

$$\ln\left(\frac{\lambda_{10}}{\lambda_{1m}}\right) = \frac{2NkT}{t_r\lambda\dot{\sigma}}\left(\cosh\left(\frac{\dot{\sigma}\lambda t_f}{NkT}\right) - 1\right) \approx \frac{NkT}{t_r\lambda\dot{\sigma}}\exp\left(\frac{\dot{\sigma}\lambda t_f}{NkT}\right)$$

for higher stresses. With $\dot{\sigma}.t_f = \sigma_u$ this is:

$$\ln\left(\frac{h}{\varkappa kT}\cdot\frac{\sigma\lambda}{NkT}\cdot\ln\left(\frac{\lambda_{10}}{\lambda_{1m}}\right)\right) = -\frac{E}{kT} + \frac{\sigma\lambda}{NkT}. \tag{4.5.2}$$

So:

$$\ln\left(t_f\cdot\frac{NkT}{\sigma_u\lambda}\right) = \ln\left(\frac{h}{\varkappa kT}\ln\left(\frac{\lambda_{10}}{\lambda_{1m}}\right)\right) + \frac{E}{kT} - \frac{\sigma_u\lambda}{NkT} =$$

$$= \ln(t_0) + \frac{E}{kT} - \frac{\sigma_u\lambda}{NkT}. \tag{4.5.3}$$

This equation is the same as eq.(4.4.11). So the short-term failure time t_s is equivalent to a creep failure at level σ_u and life-time t_c:

$$t_c = t_s\cdot\frac{NkT}{\lambda\sigma_u} = \frac{NkT}{\lambda\dot{\sigma}}.$$

The normalized creep strength (creep strength divided by the short-term strength σ_s) is:

$$\frac{\sigma}{\sigma_s} = \frac{\frac{EN}{\lambda} - \frac{NkT}{\lambda}\ln\left(\frac{t_f}{t_0}\right)}{\frac{EN}{\lambda} - \frac{NkT}{\lambda}\ln\left(\frac{t_c}{t_0}\right)} = 1 - \frac{\ln(t_f/t_c)}{\frac{E}{kT} - \ln\left(\frac{t_c}{t_0}\right)} = 1 - \frac{NkT}{\sigma_s\lambda}\ln\left(\frac{t_f}{t_c}\right). \tag{4.5.4}$$

For wood polymers the same applies with: $t'_0 = t_0 \cdot \exp(-S_0/k)$ and $E' = H' - S'T$ with $H' = H_0 - c\omega$ and $S' = S_0 + b\omega$ giving:

$$\sigma\lambda = NH_0 - Nc\omega - Nb\omega T - NkT.\ln\left(\frac{t_f}{t'_0}\right). \qquad (4.5.5)$$

For wood, eq.(4.5.4) is one line (see e.g. [9]) for different wood species, moisture contents, stress states (bending, shear, compression etc.) and types of loading, indicating one common strength determining element. This will be the cellulose because the structure of cellulose is the same for all species. So $\sigma_s\lambda/NkT = n$ has to be constant, independent of the density and moisture content. Extrapolation of eq.(4.5.4) to $\sigma = 0$, at $t_f = t_{fm}$, shows that t_{fm} is constant because t_c is constant. Because t_s is a chosen time of the constant short term strength, is $t_c = t_s/n$ also constant. Extrapolation of eq.(4.5.5) to $\sigma = 0$ gives:

$$NH_0 - NkT.\ln\left(\frac{t_{fm}}{t'_0}\right) = Nc\omega + Nb\omega T.$$

Because the left side of this equation is independent of the moisture content c and b must be zero (or there is equilibrium for the stress independent part of the free energy due to the moisture content $\Delta H'_\omega = T\Delta S'_\omega$). The measured value [9] of the slope of this line, for $t \approx 3$ sec., (and not too long lifetimes at 20 °C) is:

$$\frac{d(\sigma/\sigma_s)}{d(\ln(t_s))} = \frac{NkT}{\sigma_s\lambda} = \frac{1.03}{17.1\ln(10)} = \frac{1}{38.2}.$$

So:

$$n = \frac{\sigma_s\lambda}{NkT} = 38. \qquad (4.5.6)$$

This is comparable with the measured value of [10], if the equation is transformed to the 5 min. strength, giving the right measured value of 34 then.

From the foregoing considerations it is seen that more general eq.(4.4.1) can be written:

$$\frac{d}{dt}\left(\frac{\lambda}{N\lambda_1}\right) = \frac{2}{t_r}\left(\frac{\lambda}{N\lambda_1}\right)\sinh\left(\frac{\sigma\lambda_1}{kT}\frac{\lambda}{\lambda_1 N}\right), \qquad (4.5.7)$$

or:

$$\frac{dL}{dt} = C_1 L.\ \sinh(C_2\sigma\lambda_1 L). \qquad (4.5.8)$$

Including in L the starting value of L and the not changing fraction of flow units with constant structure, L has the form:

$$L = A + B\varepsilon.$$

In eq.(4.5.8) is L increasing and λ_1 decreasing, so:

$$L\lambda_1 = (A+B\varepsilon)\cdot(C-D\varepsilon) = AC-(DA-BC+BD\bar{L})L \approx \varphi(1 - c\varepsilon).$$

DA > BC because of the more rapid decrease of λ_1.
Because L is proportional to the plastic strain ε, a more general form of eq.(4.5.8) is:

$$\dot{\varepsilon} = (C_1 + C_2\varepsilon)\sinh(\sigma\varphi(1 - C_3\varepsilon)). \qquad (4.5.9)$$

As shown before, C_3 can be neglected if a maximum strain condition for failure is used. The small change of C_3, follows directly from eq.(4.4.1) because the change of λ_1 is dominating in this equation and λ_1 doesn't appear in the sinh-function.

The effect of constant moisture content can be regarded as an equilibrium of a transition pocess of mechanical properties. As shown before, the main influence of a change of the content is the change of the activation volume of wood. The activation volume is linear dependent on the moisture content ω as confirmed by tests in [11].
Eq.(4.5.5) can now be written:

$$\sigma_u\lambda = \sigma_u(\lambda_0 + \lambda_1\omega(T - T_0)) = NH - kTN.\ln\left(\frac{t_f}{t'_0}\right), \qquad (4.5.10)$$

in accordance with 3.4 and the data of [11]. See fig. 4.5.2, where the modified activation volume $V = \lambda/N$ is given. (The deviation of the theory at 100 °C indicates that more than one mechanism is acting at higher temperatures).
A first estimate of the numerical values of T_0 and C_0/ω_m in:

$$\frac{V}{V_0} = 1 + C_0\frac{\omega}{\omega_m}(T - T_0)$$

are: (taken from the picture of [11] without the possibility of correction of the times to failure, that are not given and are probably not the same in all tests):

$$T_0 = 265\,^{\circ}K \text{ and } C_0/\omega_m = 0.145.$$

With these values, the lines in fig. 4.5.1, given by eq.(4.5.10), are:

$$\sigma_u = \frac{HN - NkT.\ln(t_f/t'_0)}{\lambda_0(1 + C_0\frac{\omega}{\omega_m}(T-T_0)} = \frac{193 - 0.35T}{1 + 0.145\omega(T- 265)},$$

showing that the straight line for $\omega = 0$, as well as the curved line for

ω = 0.3, can be given by one equation.

If it is assumed that the time of the short term tests is about 10 minutes, giving an equivalent step strength of about 20 sec, then:

$(NR/\lambda_0)\cdot\ln(20/10^{-13})$ = 0.35, or: $NR/\lambda_0 = 1.06\cdot10^{-2}$ and the enthalpy is:

$H' = 193\cdot\lambda_0/N = 193\cdot1.987\cdot10^{-3}/1.06\cdot10^{-2} = 36$ kcal/mol.

$n = \sigma\lambda_0/NRT \approx 93/(1.06\cdot10^{-2}\cdot293) = 30.$

According to [9] and [11], $t_0' = t_0$, or $S' = 0$ is assumed.

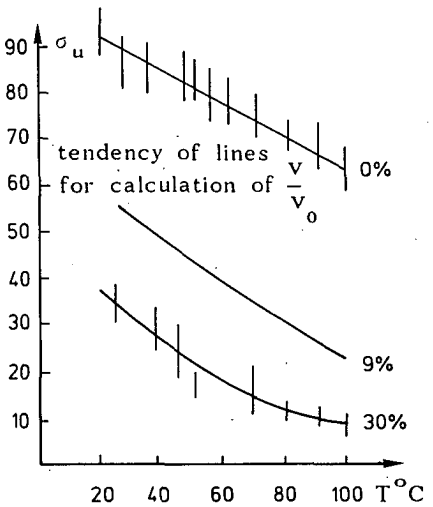

fig. 4.5.1 Compression strength of oak [11]

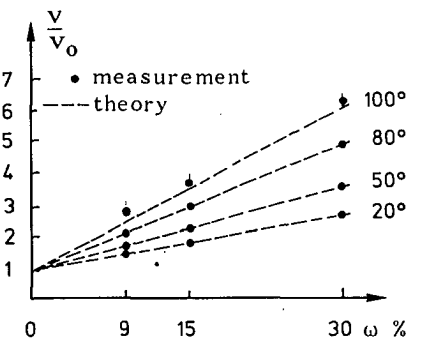

fig. 4.5.2 Activation volume

The form of the equation of $V = \lambda/N$ indicates a transition temperature of T_0 = 265 K = - 8 °C. Below this temperature is $V = V_0$ for tension, in agreement with the reported values of the tensile strength in [12] at low temperatures showing no influence of temperature and moisture content. For dry wood, ω = 0, this transition disappeares (and is not noticible at low m.c.). Information about the mechanism that is determining for compression at low temperatures can be obtained by a fit of the measured values of p.e. [12]. The steep descent of the strength curves for $\omega = \omega_m$, indicates a small value of λ_0/N and therefor λ_0/N can be neglected as a first approximation. (For $T \to 0$, this is not allowed).

With $\lambda/N = \omega\lambda_1 T/N$, eq.(4.5.2) becomes with $\omega = \omega_m$:

$$\sigma_u = \frac{HN}{\omega_m\lambda_1 T} + \frac{Nk}{\omega_m\lambda_1}\ln\left(t_0'\frac{\omega_m\lambda_1\dot{\sigma}}{Nk}\right), \qquad (4.5.13)$$

or scaled with respect to 20 °C or 293 K (Kelvin):

$$\sigma_u = \frac{HN}{\omega_m \lambda_1 293} + \frac{Nk}{\omega_m \lambda_1} \ln\left(t_0' \frac{\omega_m \lambda_1 \dot{\sigma}}{Nk}\right) + \frac{HN}{\omega_1 \lambda_1 T} - \frac{HN}{\omega_m \lambda_1 293} =$$

$$= \sigma_{u,20}\left(1 + \frac{HN}{\sigma_{u,20} \lambda_1 \omega_m}\left(\frac{1}{T} - \frac{1}{293}\right)\right). \qquad (4.5.14)$$

From the data of [12], the compressive strength parallel to the grain of saturated wood (see fig. 4.5.3):

$$\frac{\sigma_u}{\sigma_{u,20}} = 1 + 845\left(\frac{1}{T} - \frac{1}{293}\right).$$

So:

$$\frac{HN}{\sigma_{u,20} \omega_m \lambda_1} = 845,$$

or:

$$\frac{HN}{\sigma_{u,20} \omega_m \lambda_1 293} = 2.88.$$

Eq.(4.5.3) becomes:

$$\frac{\sigma_u \lambda}{HN} = 1 + \frac{kT}{H}\ln\left(\frac{t_0'}{t_f} \cdot \frac{\sigma_u \lambda}{NkT}\right) \rightarrow \frac{1}{2.88} = 1 + \frac{2*0.29}{H}\ln\left(\frac{t_0'}{t_f} \cdot \frac{H}{2*0.293*2.88}\right),$$

giving a value of H' of about 30 kcal/mole, (if $t_0'/t_f = 10^{-13}/600$ is a reasonable estimate). For dry wood, λ/N is constant and eq.(4.5.4) is nearly a straight line with respect to T because the influence of the temperature on t_c is small in the ln-function (see fig. 4.5.4). The enthalpy H' is about 36 kcal./mol, as found before.

Compression strength // [12]

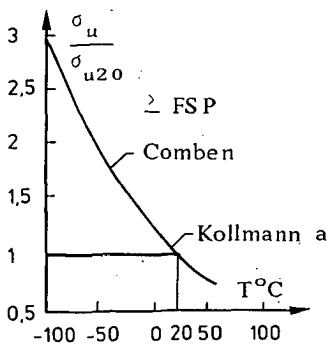

fig. 4.5.3 Saturated wood

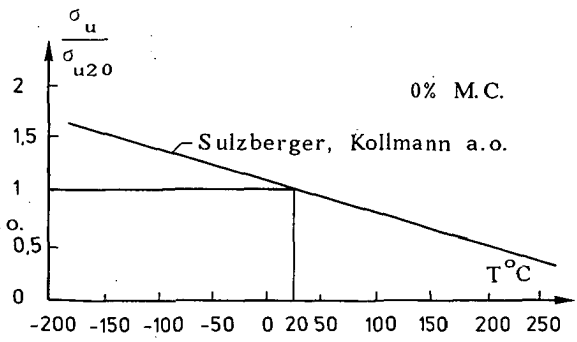

fig. 4.5.4 Dry wood

4.6 Power approximation of the rate equations.

As shown in 4.3, a range of successive processes can be given by eq. (4.3.5):

$$\text{Rate} = 2\varkappa\frac{kT}{h}\rho_1\exp\left(\frac{-E}{kT}\right)\cdot\sinh\left(\frac{W}{kT}\right), \tag{4.6.1}$$

or for higher values of W (higher stresses):

$$\dot{\varepsilon} = \dot{\varepsilon}_0\exp\left(\frac{W}{kT}\right) \;\rightarrow\; \frac{\dot{\varepsilon}}{\dot{\varepsilon}_1} = \exp\left(\frac{\sigma\lambda}{NkT} - \frac{\sigma_1\lambda}{NkT}\right) \approx 1 + \frac{\sigma\lambda}{NkT} - \frac{\sigma_1\lambda}{NkT}. \tag{4.6.2}$$

The experimental power equation, as used in fracture mechanics, is:

$$\frac{\dot{\varepsilon}}{\dot{\varepsilon}_1} = \left(\frac{\sigma}{\sigma_1}\right)^n. \tag{4.6.3}$$

This can be written for high enough stresses:

$$\frac{\dot{\varepsilon}}{\dot{\varepsilon}_1} \approx \left(1 - \frac{\sigma_1 - \sigma}{\sigma_1}\right)^n \approx 1 - n\frac{\sigma_1 - \sigma}{\sigma_1} = 1 - n\left(1 - \frac{\sigma}{\sigma_1}\right) \tag{4.6.4}$$

so:

$$n \approx \frac{\sigma_1\lambda}{NkT}. \tag{4.6.5}$$

It is shown in 4.5 that $\sigma_1\lambda/NkT$ is constant (for constant T), but dependent on the scaling (i.e. the choise of the 1-sec.-strength or the 5-min.-strength). It is now shown that the empirical power form of the rate equation (4.6.3), is identical to the theoretical expression for activation over consecutive barriers if n is not too low, see also eq.(5.3.8). If there is a lower bound of stress σ_0 where flow can be ignored: $\dot{\varepsilon} = 0$, then the effective stress $\sigma - \sigma_0$, has to be taken in eq.(4.6.3).
As derived in 4.5, the structural changes can be given by adding a linear term in ε. This is also in conformity with dislocation mobility studies and other experiments. Eq.(4.6.3) becomes:

$$\dot{\varepsilon} = (C + B\varepsilon)\left(\frac{\sigma - \sigma_0}{\sigma_1}\right)^n. \tag{4.6.6}$$

For wood there are probably two main processes for longer times:

$$\dot{\varepsilon} = C_1(1 + B_1\varepsilon)\left(\frac{\sigma - \sigma_0}{\sigma_1}\right)^n + C_2(1 + B_2\varepsilon)\left(\frac{\sigma - \sigma_0}{\sigma_1}\right)^m. \tag{4.6.7}$$

In the first process, the term $B_1C_1\cdot\varepsilon$ is probably small and a mean value may be taken. The second process is only noticeble at low stresses and after a long time and shows a long delay time. So here $C_2B_2\cdot\varepsilon$ dominates and a mean value of the stress may be taken (because of the limited

stress range where this process is dominating). So eq.(4.6.7) becomes:

$$\dot{\varepsilon} = C_1\left(\frac{\sigma - \sigma_0}{\sigma_1}\right)^n + \varepsilon C_2 B_2\left(\frac{\bar{\sigma} - \sigma_0}{\sigma_1}\right)^m \qquad (4.6.8)$$

Because the damage δ is proportional to the plastic deformation ε this can be written:

$$\frac{d\delta}{dt} = C_1\left(\frac{\sigma - \sigma_0}{\sigma_1}\right)^n + C_3\delta, \qquad (4.6.9)$$

being the damage model of [13]. For creep-to-failure tests (σ = constant), a fit of the data of [13] gives n = 36 assuming $\sigma_0 = 0$. For $\sigma_0 = 0.48$, n = 34 is found in [10], giving about the same value of n. This is in accordance with the previous mentioned values (eq.(4.5.6)) confirming this interpretation of the power law.

Short term behaviour is also determined by two main processes, as follows from the experiments of [14], where two values of n are given: $n \approx 62$ for controlled crack growth tests, to $n \approx 65$ in constant strain rate tests, and $n \approx 30$ in constant load tests to failure. In other experiments also values of n = 25 to 39 are mentioned. Analysing the creep values of [15] in [16], the existence of two parallel barriers was clearly demonstrated. The quick process had a high internal stress (forward activation) and an activation energy of approximate 50 kcal/mole. The slower process was approximately symmetrical and had an activation energy of about 21 kcal/mole.

The quick process, that was determining in the first stage of the loading may be associated with the first determining crack propagation process of [14] with $n \approx 62$ and the second process may be associated with the slower process with $n \approx 30$. The activation energy of this process is comparable with values found in [17], where from creep tests at different temperatures for bending: H'= 22 kcal/mole to 24.4 kcal/mole, depending on the temperature range, have been found. From normal-to-grain relaxation tests 23 kcal/mole was reported for wet beechwood in [18]. This energy is often regarded to be the energy of cooperative hydrogen bond breaking. The activation energy of 50 kcal/mole is high enough for C-O--bond or C-C-bond rupture.

The estimated value of H' of about 36 kcal/mole in 4.5, may be the result of a mixture of primary and secondary bond breaking at the same apparent activation volume.

Because the density of the cell wall is about 1.6/.35 times higher than

the mean density of wood, an estimate of the real stress on the sites is: $f = (1.6/.35)\cdot 20 = 90\ N/mm^2$, and is, for n = 30:

$\lambda\cdot\lambda_2\cdot\lambda_3 = 30\cdot kT/f = 30\cdot 1.39\cdot 10^{-20}\cdot 293/91 = 1.347\cdot 10^{-18}\ mm^3$.

So λ is of the order of: $(1.347\cdot 10^{-18})^{0.33} = 1.1\cdot 10^{-6}$ mm = 1.1 nm, or 1 cellobiose unit (see fig. 2.1.2).

More extented derivations of the theory of chapter 3, 4 and 5 can be found in [19] to [24].

4.7 References

[1] Deformation kinetics. A.S. Krausz, H.Eyring 1975 John Wiley & Sns.

[2] Rheology, Theory and Applications. T.Ree, H. Eyring 1958 New York.

[3] Kinetics of stress relaxation in metals. J.F. Wilaon, N.R. Wilson, Transac. of the Soc. of Rheol. 1011, 399-418 1966.

[4] Mechanical Prop. of Textiles J.A.Lasater, E.L.Nimer, H.Eyring Text. Res. J. 23- 237- 1953.

[5] Kinetic Concept of the strength of Solids S.N. Zhurkov Int.J.Fract. Mech.I, 311, 1965.

[6] J.Polym.Sci. 20,447 1956 B. Coleman.

[7] Int.J.Fract.Mech. 6,33 1970 and J.Fract.Mech. 5, 57,1969 C.B.Henderson P.H.Graham, C.N.Robinson.

[8] Influence of Heat on Creep of Dry D.-Fir. E.L.Schaffer For.Prod. Lab. Madison, Wisconsin.

[9] Bestimmung der Dauerfestigk. v. Holzkonstr. e.v. J.M. Ivanov Holztechnol. 14-1973-4.

[10] Duration of Load Test Data Analysis R.O. Foschi, J.D. Barrett pap. G4 IUFRO-Meeting 1980 Oxford, England.

[11] Ueber die Abhangigkeit der Festigk. d. Holzes v. d. Feuchte. J.M. Ivanov Holztechnologie 22 1981 1.

[12] Effect of Moisture Content and Temperature. Gerhards Wood and Fiber Jan. 1982 14 1.

[13] First Int. Confer. on Wood Fracture. 1978 Banff, Alberta Canada R.O. Foschi and J.D. Barrett.

[14] Effect of Constant Deformation Rate on Strength $\perp$ grain of D.-Fir. S. Mindess, Nadeau, Barrett, Wood Science 8 nr 4 1976.

[15] Creep and Stress relaxation in Wood during Bending. P.U.A. Grossman, R.S.T. Kingston Austr.J.Appl.Sci., 1963,14,305-17.

[16] Time depend. Deformation of Wood etc. A. v.d.Wiel Report 4-84-4-Ha-17 Stevin Lab. Techn. Univ. Delft.

[17] Studies on Thermal Softening of Wood III O.Sawake, 1974, J.Jap. Wood Res.Soc. 20 (11):517-522.

[18] Studies on Rheological Properties of Wood. T.Yamada et al. 1961 J.Jap Wood Res. Soc. 7 (2):63 - 72.

[19] Theory of deformation processes and lifetime of wood T.A.C.M. van der Put, Rep. 4-85-5 HA-21 Stevin Lab. TU-Delft.

[20] A model of deformation and damage processes based on deformation kinetics, Lecture for the EC-meeting, Palaiseau, Oct. 1985. Rep. 4-85-9 HA-22, T.A.C.M. van der Put, Stevin Lab. TU-Delft.

[21] Reaction kinetics of bond exchange of deformation and damage processes in wood. Proceed. or the IUFRO S 5.02 Conf. Sept. 1986, Firenze, Italy. and Rep. 4-86-11 HA-28, T.A.C.M. van der Put, Stevin Lab. TU-Delft.

[22] Equations for parameter estimation for a deformation kinetics model EC-BOS-129-NL, Rep. 4-86-13, HA 29, T.A.C.M. van der Put, TUD.

[23] Investigation of a lifetime theory based on thermodynamics, Lect. CEC-meeting Munchen april 1987, T.A.C.M. van der Put.

[24] A rheological model based on the theory of molecular deformation kinetics, T.A.C.M. van der Put, Delft Progress Report, Vol. 12, nr. 4, Delft Univers. Press. 1988.

5. SOLUTION AND DISCUSSION OF THE DERIVED MODEL-EQUATIONS FOR DIFFERENT LOADING PATHES

5.1 Introduction

In 4, the mathematical derivation of a creep and damage model is given, solely based on the reaction equations of plastic deformation at the deformation sites and the transmission of stresses by the surrounding elastic material. Hereby, only the end state or the flow process is regarded where there is no more internal elastic stress redistribution among the parallel processes and only the last strength determining process has an influence. To describe the whole creep and damage history, the change of the elastic stresses on the the sites has to be regarded.
This leads to the following equations (with an elastic part ε_e and a viscous part ε_v):

$$\frac{d\varepsilon}{dt} = \dot{\varepsilon} = \dot{\varepsilon}_{ei} + \dot{\varepsilon}_{vi} = \frac{\dot{\sigma}_i}{K_i} + (A_i + B_i\varepsilon_i)\sinh(\sigma_i\varphi_i(1 - C_i\varepsilon_i)) \qquad (5.1.1)$$

This can be visualized by a parallel system of Maxwell elements, where σ_i is the stress on element i; ε_i is the strain of the non-linear dashpot and K_i is the spring constant. The terms with B_i and C_i give the small structural changes. As discussed in 4, $C_i\varepsilon_i$ is very small and can be neglected. So hardening is due to the influence of the parallel elements and σ_i has the form of $\sigma_i = \sigma - M\varepsilon$, where M is proportional to the spring constants of the parallel elements and $M\varepsilon >> C_i\varepsilon_i$, during most of the lifetime, it will hardly be possible to measure C_i.

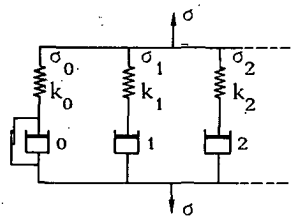

fig. 5.1 Parallel system of Maxwell units.

In most experiments, one of the processes controls the overall behaviour and only three elements (springs $K_0 + K_1$; K_2; and dashpot 2) have to be

regarded (dashpots 0 and 1 are then rigid; see fig.5.1). During the deformation, the loading of the springs changes (transient flow) until all Maxwell elements flow. Then the behaviour can be described by a single Maxwell element.
In the following the solutions of this equation for the different loading types will be given.

5.2 Constant strain rate test

In fig. 5.2, a three-element model is given of one dominating process controlling the overall rate. For the Maxwell unit at constant strain rate $\dot{\varepsilon} = c$, is $\dot{\varepsilon} = \dot{\varepsilon}_e + \dot{\varepsilon}_v = c$ or, when the structural change can be neglected (B and C in eq.5.1.1):

$$\dot{\varepsilon} = \dot{\varepsilon}_e + \dot{\varepsilon}_v = \frac{\dot{\sigma}_v}{K_1} + A.\sinh(\varphi\sigma_v). \tag{5.2.1}$$

The solution of this equation is:

$$\sigma_v = \frac{1}{\varphi}\cdot \ln\left(\beta + \left(\sqrt{1+\beta^2}\right).\tanh\left(\frac{\sqrt{1+\beta^2}}{2}A\varphi K_1(t - C)\right)\right), \tag{5.2.2}$$

with: $\beta = \frac{\dot{\varepsilon}}{A}$ and: $-\sqrt{1+\beta^2}\cdot\frac{A}{2}\cdot\varphi K_1 C = \operatorname{arctanh}\left[\frac{1-\beta}{\sqrt{1+\beta^2}}\right]$, (5.2.3)

if the initial value $\sigma_{v0} = 0$.
In fig.(5.3), the stress - time relation of the model is given. For wood K_1 and σ_v are small and the line of fig. 5.3 is approximated by a single straight line. This leads to a mean modulus of elasticity μ:

$$\mu = \frac{\sigma_m}{\varepsilon_m} = \frac{K_2\varepsilon_m}{\varepsilon_m} + \frac{\sigma_{v\infty}}{\varepsilon_m} = K_2 + \frac{1}{\varphi\varepsilon_m}\cdot\ln\left(\beta + \sqrt{1+\beta^2}\right) \approx K_2 + \frac{1}{\varphi\varepsilon_m}\ln(2\beta),$$

or:

$$\mu = K_2 + \frac{1}{\varphi\varepsilon_m}(\ln(2/A) + \ln(\dot{\varepsilon})). \tag{5.2.4}$$

So the dependence of μ on the strain rate $\dot{\varepsilon}$ is:

$$\mu - \mu_0 = \frac{1}{\varphi\varepsilon_m}(\ln(\dot{\varepsilon}) - \ln(\dot{\varepsilon}_0),$$

or:

$$\mu = \mu_0\left(1 + \frac{1}{\mu_0\varphi\varepsilon_m}(\ln(\dot{\varepsilon}) - \ln(\dot{\varepsilon}_0)\right), \tag{5.2.5}$$

with: $\mu_0\varphi\varepsilon_m = K_2\varphi\varepsilon_m + \ln(2\beta_0)$. (5.2.6)

Eq.(5.2.5) is equal to the experimental equation given in [1]. Because $K_2\varphi\varepsilon_m$ is dominating in eq.(5.2.6), $K_2\varphi\varepsilon_m$ is approximately constant and

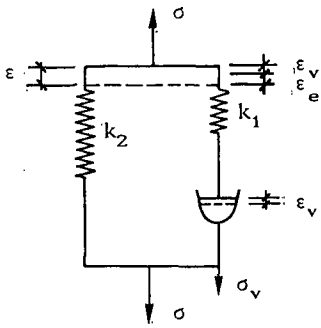

fig. 5.2 Three element model

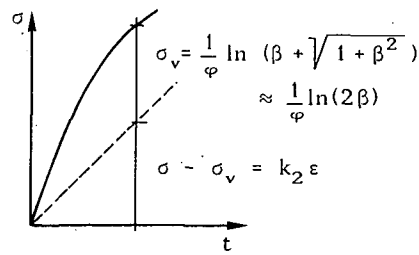

fig. 5.3 Early flow of wood

φ is inversely proportional to $K_2\varepsilon_m$. Because $\mu_0\varphi\varepsilon_m \approx \sigma_m\varphi = n$, a value of $n \approx 12$ applies for green wood and $n \approx 36$ at 10 % m.c. as also has been found for fracture. It can be concluded that there is a small flow process in wood during loading at normal speeds.
Because usely β is much greater than 1, eq.(5.2.2) can be approximated by:

$$\sigma_v\varphi \approx \ln(\beta + \beta\tanh(\tfrac{\beta}{2}A\varphi K_1(t-C)) \text{ or with: } \gamma = \tfrac{\beta}{2}A\varphi K_1 \text{ and: } \tanh(-\gamma C) = \frac{1-\beta}{\beta}$$

this is:

$$\sigma_v\varphi \approx \ln\Big(\beta + \beta\frac{\tanh(\gamma t) + \tanh(-\gamma C)}{1 + \tanh(\gamma t)\cdot\tanh(-\gamma C)}\Big) = \ln\Big(\frac{1+\tanh(\gamma t)}{1 + \frac{1-\beta}{\beta}\tanh(\gamma t)}\Big) =$$

$$= \ln\Big(\frac{\exp(2\gamma t)}{1+\frac{1}{2\beta}(\exp(2\gamma t)-1)}\Big),$$

or:

$$\sigma_v\varphi \approx \ln\Big(\frac{2\beta}{1 + 2\beta\exp(-2\gamma t)}\Big) = \ln(2\beta\alpha), \qquad (5.2.7)$$

with: $1/\alpha \approx 1 + 2\beta\exp(-\beta A\varphi K_1 t_m) = 1 + 2\beta\exp(-\varphi\sigma_{1e})$,
because: $\beta A\varphi K_1 t_m = \dot{\varepsilon}\varphi K_1 t_m = \varphi K_1\varepsilon_m = \varphi\sigma_{1e}$.

$\sigma_{1e} = K_1\varepsilon_m$, is the maximal potential elastic stress on element 1.
It is seen that the experimental law eq.(5.2.5) holds for relative long values of t_m when: $2\beta \ll \exp(\varphi\sigma_{1e})$ or for relatively slow rates. For extremely high rates is: $\sigma_v\varphi \approx \sigma_e\varphi$. Further: $\varphi(\sigma_v - \sigma_e) = \ln(1-\alpha)$, or: $\alpha = 1 - \exp(\varphi(\sigma_v - \sigma_e)) = 1 - \exp(-\varphi\varepsilon_v K_1)$.

If all Maxwell elements of fig. 5.1 flow, a description by a *single* (dominating) Maxwell element is possible (neglecting the small, almost constant,

stress in K_1 in fig. 5.2). If B and C in eq.(5.1.1) are zero, then eq.(5.2.1) applies, represented by fig. 5.4.

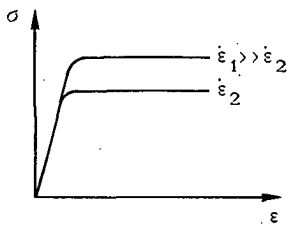

fig. 5.4 Non-linear Maxwell element

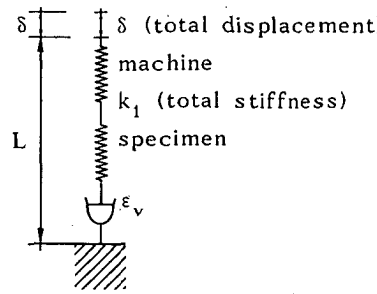

fig. 5.5 Flow of all elements

For a machine - specimen combination in a test, the crosshead displacement is (fig. 5.5):

$$\frac{\delta}{L} = \frac{\sigma}{K_1} + \varepsilon_v$$

and the constant crosshead rate $\dot{\delta} = c$ becomes:

$$\dot{\delta} = L\left(\frac{\dot{\sigma}}{K_1} + \dot{\varepsilon}_v\right). \quad \text{So:} \quad \dot{\varepsilon}_v = \frac{\dot{\delta}}{L} - \frac{\dot{\sigma}}{K_1} = \frac{\dot{\delta}}{L}\left(1 - \frac{L}{K_1}\cdot\frac{d\sigma}{d\delta}\right).$$

or:

$$\frac{d\sigma}{d\delta} = \frac{K_1}{L} - \frac{K_1}{c}\cdot\dot{\varepsilon}_v = \frac{K_1}{L} - \frac{K_1}{L}A'T\left(\rho_0 + B'\left(\frac{\delta}{L} - \frac{\sigma}{K_1}\right)\right)\sinh\left(\varphi\sigma\left(1 - C\frac{\delta}{L} + C\frac{\sigma}{K_1}\right)\right). \tag{5.2.8}$$

The analogues power equation for this case has the form:

$$\frac{d\sigma}{d\delta} = C_0 - (C_1 + C_2\delta - C_3\sigma)\cdot\left(\frac{\sigma + C_4\varepsilon_v}{\sigma_0}\right)^n. \tag{5.2.9}$$

Both equations (5.2.8) and (5.2.9) cannot be integrated to a functional form. The results of numerical integration are shown in fig. 5.6 and 5.7. Clear wood in compression // shows a behaviour like in fig. 5.4, indicating no hardening and no yield drop. So B' and C in eq.(5.2.8) may be neglected. For timber (with knots) in compression along the grain however there is a small yield drop, superposed on the behaviour of the clear wood between the knots, indicating the acting of another (tensional) Maxwell element (crack propagation in grain direction at the knots). So knots act like flow units with a low density.

For wood in tension // there is a high yield drop, indicating that B' in

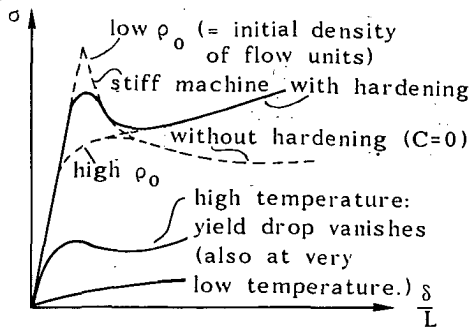

fig. 5.6 Yield drop eq.(5.2.8)

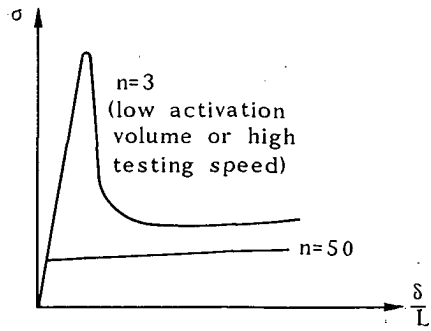

fig. 5.7 Influence of n, eq.(5.2.9)

eq.(5.2.8) is dominating by a low initial flow unit density ρ_0. Measurements show that this is not caused by a low value of n. There is also no indication of hardening so that the differential-equation for this case becomes:

$$\dot{\varepsilon} = \frac{\dot{\sigma}_v}{K_1} + B\varepsilon_v \sinh(\varphi\sigma_v). \qquad (5.2.10)$$

Taking the solution of this equation in the form: $\sigma_v = K_1\varepsilon - f(t)$, or: $\dot{\sigma}_v = K_1\dot{\varepsilon} - \dot{f}$, then:

$$\varepsilon_v = \varepsilon - \frac{\sigma_v}{K_1} = \varepsilon - \varepsilon + \frac{f}{K_1} = \frac{f}{K_1}, \qquad (5.2.11)$$

and the differential equation is:

$\dot{f} - Bf\sinh(\varphi(K_1\varepsilon - f)) = 0$, or for higher stresses where f is noticeble:

$$\dot{f} - \frac{Bf}{2}\exp(\varphi(K_1\dot{\varepsilon}t - f)) = 0, \qquad (5.2.12)$$

or:

$$\exp(\varphi f)\frac{d(\ln(\varphi f)}{dt} = \frac{B}{2}\exp(\varphi K_1\dot{\varepsilon}t). \qquad (5.2.13)$$

Now is: $\int_{x_0}^{x}\exp(x).d(\ln(x)) = \int_{-\infty}^{x}\exp(x).d(\ln(x)) - \int_{-\infty}^{x_0}\exp(x).d(\ln(x)) = E_i(x) - E_i(x_0)$.

So eq.(5.2.13) has as solution:

$$E_i(\varphi f) - E_i(\varphi f_0) = \frac{B}{2\varphi K_1\dot{\varepsilon}}\cdot(\exp(\varphi K_1\dot{\varepsilon}t) - 1) \quad \rightarrow \qquad (5.2.14)$$

$$\frac{\exp(\varphi f)}{\varphi f} \approx \frac{B}{2\varphi K_1\dot{\varepsilon}}(\exp(\varphi K_1\dot{\varepsilon}t) - 1) + E_i(\varphi f_0) \approx \frac{B}{2\varphi K_1\dot{\varepsilon}}(\exp(\varphi K_1\dot{\varepsilon}t) - 1) + \frac{\exp(\varphi f_0)}{\varphi f_0}$$

or:

$$\varphi f = \ln(\varphi f) + \ln\Big(\frac{B}{2\varphi K_1\dot{\varepsilon}}(\exp(\varphi K_1\dot{\varepsilon}t) - 1) + \frac{\exp(\varphi f_0)}{\varphi f_0}\Big) =$$

$$= \varphi f_0 + \ln\Big(\frac{Bf\varphi}{2\varphi K_1\dot{\varepsilon}}(\exp(\varphi K_1\dot{\varepsilon}t) - 1)\cdot\exp(-\varphi f_0) + \frac{\varphi f}{\varphi f_0}\Big) \approx$$

$$\approx \varphi f_0 + \ln\Big(\frac{Bf}{2\dot{\varepsilon}K_1}\cdot(\exp(\varphi K_1\dot{\varepsilon}t) - 1)\cdot\exp(-\varphi f_0) + 1\Big). \qquad (5.2.15)$$

For larger values of the time t this approaches to:

$$\varphi f \approx \ln\Big(\frac{Bf}{2\dot{\varepsilon}K_1}\cdot(\exp(\varphi K_1\dot{\varepsilon}t)\Big) = \varphi K_1\dot{\varepsilon}t - \ln\Big(\frac{2\dot{\varepsilon}K_1}{Bf}\Big)$$

or:

$$\sigma_v\varphi = \ln(2\beta\alpha) \quad \text{with: } \beta = \frac{\dot{\varepsilon}}{B}, \text{ and } \alpha = \frac{1}{\varepsilon_v} \qquad (5.2.16)$$

and the result is comparable to the case with the initial high flow unit density eq.(5.2.7). Because the process is small, showing only a very slight curvature of the loading line, parameter estimation is not possible with rate tests and a parabolic form of the line will be assumed.
For small values of φf, eq.(5.2.14) is approximately:

$$\ln(\varphi f) = \ln(\varphi f_0) + \frac{B}{2\varphi K_1\dot{\varepsilon}}(\exp(\varphi K_1\dot{\varepsilon}t) - 1) \qquad (5.2.17)$$

or:

$$\varepsilon_v = \varepsilon_{v0}\cdot\exp\Big(\frac{B}{2\varphi K_1\dot{\varepsilon}}(\exp(\varphi K_1\dot{\varepsilon}t) - 1)\Big). \qquad (5.2.18)$$

For loading at a constant rate to a stress level σ_m at a strain ε_m this equation gets the form:

$$\varepsilon_v = \varepsilon_{v0}\cdot\exp(C\sigma_m), \qquad (5.2.19)$$

if $\varphi\varepsilon_m$ is constant for different values of ε_m. So ε_v increases exponential with the stress. When $\exp(C\sigma)$ is approaced by a parabola then, neglecting $\varepsilon_{v0}\sigma$, this equation can be given as:

$$\frac{\varepsilon_{v1}}{\sigma_1} - \frac{\varepsilon_{v2}}{\sigma_2} \approx C(\sigma_1 - \sigma_2). \qquad (5.2.20)$$

5.3 Constant loading rate test

For the three - element model of fig. 5.2 is for this case: $\dot{\sigma}$ = constant and as shown before B_i and C_i of eq.(5.1.1) may be neglected.
Because: $\sigma = K_2\varepsilon + \sigma_v$, is: $\dot{\varepsilon} = \dot{\sigma}/K_2 - \dot{\sigma}_v/K_2$, and eq.(5.2.1) becomes:

$$\frac{\dot{\sigma}}{K_2} = \dot{\sigma}_v\left(\frac{1}{K_1} + \frac{1}{K_2}\right) + A\sinh(\varphi\sigma_v), \tag{5.3.1}$$

having a simular form as eq.(5.2.1) and the solution is identical if β is taken as:

$\beta = \frac{\dot{\sigma}}{AK_2}$, and: $\frac{1}{K_1}$ is replaced by: $\frac{1}{K} = \frac{1}{K_1} + \frac{1}{K_2}$. So:

$$\varepsilon = \frac{\dot{\sigma}t}{K_2} - \frac{1}{\varphi K_2}\ln\left(\beta + (\sqrt{1+\beta^2}).\tanh\left(\frac{\sqrt{1+\beta^2}}{2}A\varphi K(t - C)\right)\right) \tag{5.3.2}$$

with the same value of C as given in eq.(5.2.3). The same approximation is possible as for the constant strain rate test. So $\sigma_v\varphi = \ln(2\beta)$. Comparing two stresses with different loading rates at the same strain this gives:

$$\sigma_1 - \sigma_2 = K_2\varepsilon + \sigma_{v1} - K_2\varepsilon - \sigma_{v2} = \frac{1}{\varphi}(\ln(\beta_1) - \ln(\beta_2)) = \frac{1}{\varphi}\ln(\dot{\sigma}_1/\dot{\sigma}_2) =$$

$$= \frac{1}{\varphi}\ln\left(\frac{\dot{\sigma}_1 t_1}{\sigma_2 t_2}.\frac{t_2}{t_1}\right) = \frac{1}{\varphi}\ln\left(\frac{\sigma_1 t_2}{\sigma_2 t_1}\right) = \frac{1}{\varphi}\ln\left(\frac{t_2}{t_1}\right) + \frac{1}{\varphi}\ln\left(\frac{\sigma_1}{\sigma_2}\right)$$

or because the last term is neglectable:

$$\frac{\sigma_1}{\sigma_2} = 1 + \frac{1}{\varphi\sigma_2}\ln(t_2) - \frac{1}{\varphi\sigma_2}\ln(t_1) = C_1 - C_2\ln(t_1). \tag{5.3.3}$$

This is equal to the experimental equation given in p.e. [2] and [3], suggesting failure at the same strain. This has to follow from the description of the end state. In that case, when all elements flow (fig. 5.5), the elastic strain rate is zero and the rate equation is:

$\dot{\varepsilon}_v \approx A\sinh(\varphi\dot{\sigma}t)$, or integrated:

$$\varepsilon_v = \frac{A}{\dot{\sigma}\varphi}(\cosh(\dot{\sigma}\varphi t) - 1).$$

For higher values of $\dot{\sigma}\varphi t$ this becomes:

$$\varepsilon_v = \frac{A}{\dot{\sigma}\varphi}(\frac{1}{2}\exp(\dot{\sigma}\varphi t) - 1) \tag{5.3.4}$$

or with: $\sigma = \dot{\sigma}t$,

$$\sigma = \frac{1}{\varphi}\ln(2 + \frac{2\dot{\sigma}\varphi\varepsilon_v}{A}) \approx \frac{1}{\varphi}\ln(\frac{2\dot{\sigma}\varphi\varepsilon_v}{A}). \tag{5.3.5}$$

The strength is reached for $\varepsilon_v = \varepsilon_{vu}$. So σ_1 and σ_2 at the rates $\dot{\sigma}_1$ and $\dot{\sigma}_2$ are related by:

$$\sigma_1 - \sigma_2 = \frac{1}{\varphi}\ln\left(\frac{1 + \dot{\sigma}_1 c}{1 + \dot{\sigma}_2 c}.\frac{\dot{\sigma}_2}{\dot{\sigma}_1}\right) + \frac{1}{\varphi}\ln\left(\frac{\sigma_1 t_2}{\sigma_2 t_1}\right) \approx \frac{1}{\varphi}\ln\left(\frac{t_2}{t_1}\right)$$

or:

$$\frac{\sigma_1}{\sigma_2} = 1 + \frac{1}{\varphi\sigma_2}\ln(t_2) - \frac{1}{\varphi\sigma_2}\ln(t_1) = C_1 - C_2\ln(t_1),$$

what is equal to eq.(5.3.3) and gives an explanation of the experimental law given in [2], [3] etc., where C_1 = 1.2 to 1.3 and $1/C_2$ = n = 27 for compression and 31 for bending. If 1/n is approximately linear dependent on the moisture content as suggested in [1], then these values indicate a moisture content of 13%.

The same result is obtained by integration of eq.(5.3.6), where only the hardening term is neglected.

$$\dot{\varepsilon}_v = (A + B\varepsilon_v)\sinh(\varphi\dot{\sigma}t) \qquad (5.3.6)$$

Only the ultimate strain ε_{vu} will have another value.

The alternative power representation becomes ($\dot{\sigma}$ = constant):

$$\dot{\varepsilon}_v = (A + B\varepsilon_v)\left(\frac{\dot{\sigma}}{\sigma_0}\right)^n t^n. \qquad (5.3.7)$$

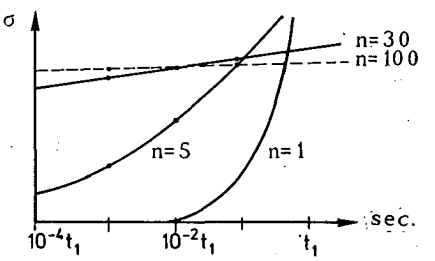

fig. 5.8 Influence of the rate of loading or time to loading to the same strain [4]

This is easy to integrate and the results are given in fig.(5.8).

It can be seen from this figure, that for small values of n (n > 1), there is a strong influence of the loading rate on the level of the flow stress. For high values of n (e.g. n = 30 as for wood), there is only a small influence and there is a linear relation between the strength and log(time to failure) as is also derived before.

For small values of n, the derivation of n in 4.6, is not general enough. From:

$$\frac{\dot{\varepsilon}}{\varepsilon_u} = \left(\frac{\sigma}{\sigma_u}\right)^n,$$

it follows that: $\ln(\dot{\varepsilon}) = \ln(\dot{\varepsilon}_u) - \ln(\sigma_u^n) + n.\ln(\sigma)$.

So: $\frac{d(\ln(\dot{\varepsilon}))}{d(\ln(\sigma))} = n$,

Applying this operation $\frac{d(\ln(\dot{\varepsilon}))}{d(\ln(\sigma))}$ to: $\dot{\varepsilon} = A.\sinh(\varphi\sigma)$ gives:

$$n = \frac{\sigma\varphi}{\tanh(\sigma\varphi)} . \qquad (5.3.8)$$

So for small values of $\sigma\varphi$ is $n = 1$, and for large values is $n \approx \sigma\varphi$.
So: $n \approx \sigma\varphi \geq 1$.
For wood there is an indication that there is an element with a small value of n, as will be shown later. This is only noticeble at very high loading speeds.

5.4 Creep and creep recovery

For the three - element model (fig.5.2), neglecting structural changes, the force on the Maxwell element is determined by eq.(5.2.1).
For the parallel spring K_2 is:

$$\dot{\varepsilon} = \frac{\dot{\sigma}_2}{K_2} = \frac{1}{K_2} \cdot \frac{d(\sigma - \sigma_v)}{d(t)} = \frac{\dot{\sigma} - \dot{\sigma}_v}{K_2} .$$

Because for creep $\dot{\sigma} = 0$, is: $\dot{\varepsilon} = - \frac{\dot{\sigma}_v}{K_2}$,
and eq.(5.2.1) becomes:

$$\frac{\dot{\sigma}_v}{K_1} + A\sinh(\varphi\sigma_v) = - \frac{\dot{\sigma}_v}{K_2}$$

or:

$$\dot{\sigma}_v + KA\sinh((\varphi\sigma_v) = 0 \qquad (5.4.1)$$

where $1/K = 1/K_1 + 1/K_2$.

With the boundary condition: $\varepsilon_\infty = \frac{\sigma}{K_2}$, is: $\sigma_v = \sigma - K_2\varepsilon = K_2(\varepsilon_\infty - \varepsilon)$.

The solution of eq.(5.4.1) is:

$$\ln\left(\tanh\left(\frac{\varphi K_2}{2}(\varepsilon_\infty - \varepsilon)\right)\right) = - \varphi KAt + \ln\left(\tanh\left(\frac{\varphi K_2}{2}(\varepsilon_\infty - \varepsilon_0)\right)\right)$$

or, because $\operatorname{arctanh}(x) = \frac{1}{2}\ln(\frac{1+x}{1-x})$, this can be written as:

$$\varepsilon_\infty - \varepsilon = \frac{1}{\varphi K_2}\ln\left(\coth\left(- \frac{1}{2}\ln\left(\tanh\left(\frac{K_2\varphi}{2}(\varepsilon_\infty - \varepsilon_0)\right)\right) + \frac{1}{2}K\varphi At\right)\right). \qquad (5.4.2)$$

In the early part of the test this reduces to the logarithmic form:

$$\varepsilon_\infty - \varepsilon = -\frac{1}{\varphi K_2}\ln\Big(-\frac{1}{2}\ln\Big(\tanh\Big(\frac{K_2\varphi}{2}(\varepsilon_\infty - \varepsilon_0)\Big)\Big) + \frac{1}{2}K\varphi At\Big) \qquad (5.4.3)$$

or:

$$\varepsilon = \varepsilon_0 + \frac{1}{\varphi K_2}\ln\Big(1 + \frac{K\varphi At}{\ln(\coth(\varphi\sigma_{v0}/2))}\Big). \qquad (5.4.4)$$

For sufficient large values of x is: $\ln(\coth(x)) = 2\operatorname{arctanh}(\exp(-2x) \approx = 2\exp(-2x)$.

Eq.(5.4.4) then becomes:

$$\varepsilon = \varepsilon_0 + \frac{1}{\varphi K_2}\ln\Big(1 + \frac{K\varphi At\exp(\varphi\sigma_{v0})}{2}\Big). \qquad (5.4.5)$$

A fit of this equation is not found in literature. Our tests show however that the form of eq.(5.4.4) or (5.4.5) is right, also for small times. The fit is mostly done for larger times (neglecting 1 in the last term) giving:

$$\varepsilon = C_1 + C_2\ln(t). \qquad (5.4.6)$$

After longer times, the influence of a second mechanism with a long relaxation time is noticeble and because: $\ln(1 + cx) \approx cx$, for small values of cx, an additional term: $C{\cdot}t$ in eq. (5.4.6) is sometimes used to account for the influence of a slow process. According to eq.(5.4.5) is: $C{\cdot}t = K\varphi At\exp(\varphi\sigma_{v0})/(2\varphi K_2)$. However this only describes the beginning of the process. For the whole process at very long times and sufficient high values of $\sigma_{v0}\varphi/2$, as for wood, eq.(5.4.2) can be written:

$$\varepsilon_\infty - \varepsilon = \frac{1}{\varphi K_2}\ln(\coth(K\varphi At/2)) \approx \frac{2}{\varphi K_2}\exp(-K\varphi At)$$

or:

$$\varepsilon = \varepsilon_0' + \frac{2}{\varphi K_2}\big(1 - \exp(-K\varphi At)\big). \qquad (5.4.7)$$

So the behaviour becomes quasi Newtonian after long times. Eq.(5.4.1) can be expected to be quasi Newtonian for low stresses, because then $\sinh(x) = x$. This equation then becomes:

$$\dot{\sigma}_v + KA\varphi\sigma_v = 0$$

with the solution:

$$\varepsilon - \varepsilon_0 = (\varepsilon_\infty - \varepsilon_0){\cdot}(1 - \exp(-KA\varphi t)).$$

Also from the solution of eq.(5.4.1) this equation follows if the creep strain ε is very small. It is seen that test results, in not to long time ranges, can be fitted by Newtonian equations as often is done. This, however will give an underestimation of the relaxation times because it is implicitely assumed that the creep is in the end state within the measuring time t or that the total creep strain is small.

When $B_i\varepsilon_i$ dominates A_i in eq.(5.1.1) and A_i can be neglected, then eq. (5.2.1) of the three element model of fig. 5.2 becomes:

$$\dot{\varepsilon} = \frac{\dot{\sigma}_v}{K_1} + B\varepsilon_v \sinh(\varphi\sigma_v). \tag{5.4.8}$$

Because: $\varepsilon = \frac{\sigma_2}{K_2} = \frac{\sigma - \sigma_1}{K_2} = \frac{\sigma}{K_2} - \frac{K_1}{K_2}(\varepsilon - \varepsilon_v)$,

or:

$$\varepsilon_v = \frac{K_1 + K_2}{K_1}\varepsilon - \frac{\sigma}{K_1},$$

is:

$$\dot{\varepsilon}_v = \frac{K_1 + K_2}{K_1}\dot{\varepsilon} - \frac{\dot{\sigma}}{K_1} = B\varepsilon_v \sinh(\varphi\sigma_v) \approx \frac{B\varepsilon_v}{2} \cdot \exp(\varphi\sigma_v) = \frac{B\varepsilon_v}{2} \cdot \exp(\varphi(\sigma - K_2\varepsilon)),$$

giving: $(K_1 + K_2)\dot{\varepsilon} = \dot{\sigma} + B\left((K_1 + K_2)\frac{\varepsilon}{2} - \frac{\sigma}{2}\right)\exp(\varphi(\sigma - K_2\varepsilon))$. (5.4.9)

For creep is σ = constant, or $\dot{\sigma} = 0$, so: $\dot{\varepsilon} = \frac{B}{2}\left(\varepsilon - \frac{\sigma}{K_1 + K_2}\right)\exp(\varphi\sigma - \varphi K_2\varepsilon)$

or:

$$\frac{d(\varphi K_2\varepsilon)}{\varphi K_2(\varepsilon - \frac{\sigma}{K_1+K_2})} \cdot \exp\left(\varphi K_2\varepsilon - \frac{\varphi K_2\sigma}{K_1+K_2}\right) = \frac{B}{2}\left(\exp(\varphi\sigma - \frac{\varphi\sigma K_2}{K_1+K_2})\right) \cdot d(t),$$

having the form: $\int_{x_0}^{x} \frac{d(x)}{x}\exp(x) = \int_{-\infty}^{x} \frac{d(x)}{x}\exp(x) - \int_{-\infty}^{x_0} \frac{d(x)}{x} = E_i(x) - E_i(x_0)$

or:

$$E_i\left(\varphi K_2(\varepsilon - \frac{\sigma}{K_1+K_2})\right) - E_i\left(\varphi K_2(\varepsilon_0 - \frac{\sigma}{K_1+K_2})\right) = \frac{Bt}{2}\exp\left(\frac{\varphi\sigma K_1}{K_1+K_2}\right) \tag{5.4.10}$$

so:

$$\varepsilon = \frac{\sigma}{K_1+K_2} + \frac{1}{\varphi K_2} \cdot E_i^{-1}\left(\frac{Bt}{2}\exp\left(\frac{\varphi\sigma K_1}{K_1+K_2}\right) + E_i\left(\frac{K_1K_2\varphi\varepsilon_{v0}}{K_1+K_2}\right)\right). \tag{5.4.11}$$

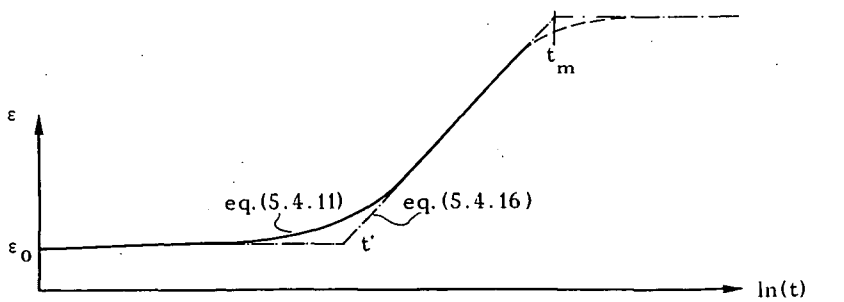

fig. 5.9 Irrecoverable creep (eq.(5.4.11))

For larger values of x is: $E_i(x) \approx \frac{\exp(x)}{x}$, and for small values is: $E_i(x) \approx$

= 0.577 + ln(x). So for small times and small dislocation densities equation (5.4.10) becomes:

$$\ln(\varphi K\varepsilon_v) = \frac{B}{2}\cdot t\cdot\exp\left(\frac{\varphi\sigma K}{K_2}\right) + \ln(\varphi K\varepsilon_{v0}) \qquad (5.4.12)$$

or:

$$\varepsilon = \frac{\sigma}{K_1+K_2} + \frac{K\varepsilon_{v0}}{K_2}\exp\left(\frac{B}{2}\cdot t\cdot\exp\left(\frac{\varphi\sigma K_1}{K_1+K_2}\right)\right).$$

So there is a small exponential increase of the deformation during the first stage of the creep (delay time), as measured in e.g. [5], if the initial dislocation density is small (see fig. 5.9). At still smaller times eq.(5.4.12) can also be written:

$$\ln(\varepsilon_v/\varepsilon_{v0}) = \ln\left(\frac{\varepsilon_v-\varepsilon_{v0}}{\varepsilon_{v0}} + 1\right) \approx \frac{\varepsilon_v-\varepsilon_{v0}}{\varepsilon_{v0}} = \frac{B}{2}\cdot t\cdot\exp\left(\frac{\varphi\sigma K}{K_2}\right)$$

and because $(\varepsilon_v - \varepsilon_{v0}):(\varepsilon - \varepsilon_0) = c$, this is: $\varepsilon - \varepsilon_0 = \frac{\varepsilon_{v0}}{c}\cdot\frac{B}{2}\cdot t\cdot\exp\left(\frac{\varphi\sigma K}{K_2}\right)$ (5.4.13)

($c = 1 + K_2/K_1$). Because ε_{v0} increases quadratic with σ at loading to the creep level, eq. (5.4.13) shows for shorter times a small initial quadratic increase of the creep with σ as measured in p.e. [6] ($\varphi\sigma$ is constant). Eq.(5.4.10) becomes for larger times:

$$\frac{\exp\left(\varphi K_2\left(\varepsilon - \frac{\sigma}{K_2+K_1}\right)\right)}{\varphi K_2\left(\varepsilon - \frac{\sigma}{K_2+K_1}\right)} \approx \frac{B}{2}t\cdot\exp\left(\frac{\varphi\sigma K_1}{K_2+K_1}\right) + \ln\left(\varphi K_2\left(\varepsilon_0 - \frac{\sigma}{K_2+K_1}\right)\right)$$

or:

$$\varphi K_2\left(\varepsilon - \frac{\sigma}{K_1+K_2}\right) = \ln\left(\frac{\varphi K_1K_2\varepsilon_v}{K_1+K_2}\right) + \ln\left(\frac{B}{2}\cdot t\cdot\exp\left(\frac{\varphi\sigma K_1}{K_1+K_2}\right) + \ln\left(\frac{\varphi K_1K_2\varepsilon_{v0}}{K_1+K_2}\right)\right).$$

So for very small values of: $\varepsilon - \sigma/(K_1 + K_2) = K_1\varepsilon_v/(K_1 + K_2)$ the double log-plot applies in stead of the semi log-plot. For larger values, with $1/K = 1/K_1 + 1/K_2$ this equation becomes:

$$\varepsilon = \frac{\sigma}{K_1+K_2} + \frac{1}{\varphi K_2}\ln(\varphi K\varepsilon_v) + \frac{1}{\varphi K_2}\ln\left(\frac{B}{2}\cdot t\cdot\exp\left(\frac{\varphi\sigma K}{K_2}\right) + \ln(\varphi K\varepsilon_{v0})\right). \qquad (5.4.14)$$

Because $\varphi K\varepsilon_{v0}$ is a small value, $\ln(\varphi K\varepsilon_{v0})$ is a high negative value. If this is replaced by the, during the initial creep stage, increased value ε_{v1} according to eq.(5.4.12), eq.(5.4.14) becomes:

$$\varepsilon = \frac{\sigma}{K_1+K_2} + \frac{1}{\varphi K_2}\ln(\varphi K\varepsilon_v) + \frac{1}{\varphi K_2}\ln\left(\frac{B}{2}\cdot(t-t_1)\cdot\exp\left(\frac{\varphi\sigma K}{K_2}\right) + \ln(\varphi K\varepsilon_{v1})\right)$$

or:

$$\varepsilon = \frac{\sigma}{K_2} + \frac{1}{\varphi K_2}\ln\left(\frac{B}{2}\varphi K\varepsilon_v\right) + \frac{1}{\varphi K_2}\ln\left(t - t_1 + \frac{2}{B}(\ln(\varphi K\varepsilon_{v1}))\cdot\exp\left(\frac{-\varphi\sigma K}{K_2}\right)\right). \qquad (5.4.15)$$

Because the second term on the right hand side is of minor importance, a mean value of ε_v ($\bar{\varepsilon}_v$) can be used and because $\sigma/K_2 = \varepsilon_0 + \sigma_{v0}/K_2 = \varepsilon_0 + (1/\varphi K_2)\ln(\exp(\varphi\sigma_{v0}))$, the equation can be written:

$$\varepsilon = \varepsilon_0 + \frac{1}{\varphi K_2}\ln\left(1 + \frac{\varphi K B\bar{\varepsilon}_v \exp(\varphi\sigma_{v0})}{2}\cdot(t - t')\right) \qquad (5.4.16)$$

where $t' = t_1 + \frac{2}{B}\cdot\exp(-\varphi\sigma_{v0})\cdot\left(\frac{1}{\varphi K\bar{\varepsilon}_v} - \ln(\varphi K\varepsilon_{v1})\right)$ is not far from t_1.

For long times $t >> t_1$, eq.(5.4.15) becomes:

$$\varepsilon = \frac{\sigma}{K_2} + \frac{1}{\varphi K_2}\ln\left(\frac{\varphi K B\bar{\varepsilon}_v}{2}\right) + \frac{1}{\varphi K_2}\ln(t) \qquad (5.4.17)$$

or:

$$-\varphi\sigma_1 = \ln(\varphi K B\bar{\varepsilon}_v/2) + \ln(t).$$

So the stress on element 1, σ_1, is zero at time: $t = t_m = 2/(\varphi K B\bar{\varepsilon}_v)$ and eq.(5.4.17) turns to:

$$\varepsilon = \varepsilon_m + \frac{1}{\varphi K_2}\ln\left(\frac{t}{t_m}\right) \qquad (5.4.18)$$

where $\varepsilon_m = \sigma/K_2$, when all the stress σ is on element 2 and the maximal strain is reached. (Of course ε is not the real strain for $t \to t_m$, but the extrapolation of the straight line approximation to ε_m, see fig.5.9).
For higher initial values eq.(5.4.10) becomes:

$$\frac{\exp(\varphi K\varepsilon_v)}{\varphi K\varepsilon_v} = \frac{\exp(\varphi K\varepsilon_{v0})}{\varphi K\varepsilon_{v0}} + \frac{B}{2}\cdot t\cdot\exp\left(\frac{\varphi K\sigma}{K_2}\right) \qquad (5.4.19)$$

or:

$$\varepsilon = \varepsilon_0 + \frac{1}{\varphi K_2}\ln\left(\frac{\varepsilon_v}{\varepsilon_{v0}}\right) + \frac{1}{\varphi K_2}\ln\left(1 + \frac{\varphi K\varepsilon_{v0}B}{2}\cdot t\cdot\exp(\varphi\sigma - \varphi K_2\varepsilon_0)\right)$$

or, because of the minor influence of the second term on the right hand side:

$$\varepsilon = \varepsilon_0 + \frac{1}{\varphi K_2}\ln\left(1 + \frac{K}{2}\varphi B\bar{\varepsilon}_v t\cdot\exp(\varphi\sigma_{v0})\right) \qquad (5.4.20)$$

what is comparable with eq.(5.4.5) as can be expected for higher initial dislocation densities.
The behaviour according to fig. 5.9 is measured for wood. Because this is probably related to the cellulose, test results of dry summerwood fibers of pine holocellulose pulp will also be discussed [5].
In fig. 5.10, the average creep compliance of 50 fibre bundles is given for different initial stresses. As follows from the very different values of the initial compliances and from the not decelerating curves, flow with-

out hardening must have been occurred. The kinked lines indicate two processes and a description is possible with two Maxwell elements. Because one process is slower than the other, a three-element model approach (one Maxwell element and one spring) is possible. The line with the small slope is the quick process and as before, structural changes can be neglected (eq.(5.4.1)). The line with the steep slope, shows a strong delay time (see fig. 5.9) and will follow eq.(5.4.8).

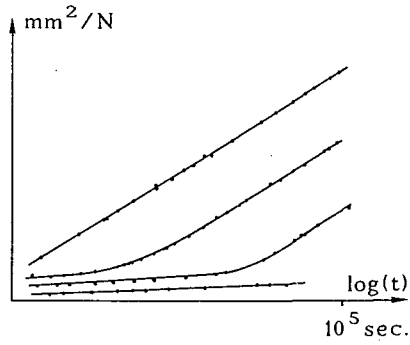

fig. 5.10 Creep compliance [5]

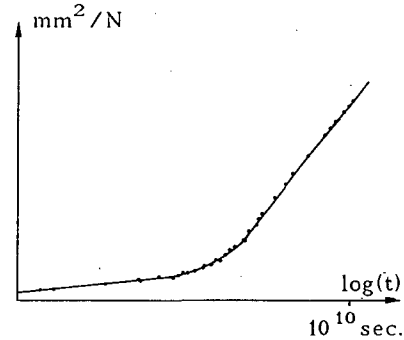

fig. 5.11 Master creep curve [5]

As seen in fig. 5.11, the lines can be moved horizontally along the log(t) axis, to form one curve (giving the behaviour after long times at the lowest given stress).

The line with the small slope is accordingly to eq.(5.4.4) and the line with the steep slope is given by eq.(5.4.16). It appears that in these equations, $1/\varphi\sigma K_2$ is constant or $1/\varphi K_2$ is proportional to σ, as also can be seen for creep of wood at lower stress levels. So $\sigma\cdot\varphi$ is constant, indicating that the number of creeping mechanisms per unit area increases with increasing initial stress. Except for cellulosic materials, this property is also found in other materials, like metals and rubbers [4].

The compliance according to eq.5.4.4 is for longer times:

$$\frac{\varepsilon}{\sigma} = \frac{\varepsilon_0}{\sigma} + \frac{1}{\sigma\varphi K_2}\ln\left(\frac{K\varphi At}{2}\exp(\varphi\sigma_{v0})\right) = \frac{\varepsilon_0}{\sigma} + \frac{1}{\sigma\varphi K_2}\ln\left(\frac{t}{t'}\right) \qquad (5.4.21)$$

where $1/\sigma\varphi K_2$ is constant.

For a horizontal shift of a creep - line along the time axis due to an higher stress level: $\sigma_b > \sigma_a$ it is necessary that ε_b/σ_b at time t_b has to

be equal to ε_a/σ_a at time t_a. So it follows from eq.(5.4.21):

$$\frac{\varepsilon_a}{\sigma_a} - \frac{\varepsilon_b}{\sigma_b} = 0 = \frac{\varepsilon_{0a}}{\sigma_a} - \frac{\varepsilon_{0b}}{\sigma_b} + \frac{1}{\sigma\varphi K_2}\Big(\ln(t_a) - \ln(t_b) - \ln(t'_a/t'_b)\Big).$$

So:

$$\ln(t_a) - \ln(t_b) = -\frac{\sigma\varphi K_1 K_2}{K_1 + K_2}\Big(\frac{\varepsilon_{v0a}}{\sigma_a} - \frac{\varepsilon_{v0b}}{\sigma_b}\Big) - \ln\Big(\frac{\varphi_b \exp(\varphi_b \sigma_{v0b})}{\varphi_a \exp(\varphi_a \sigma_{v0a})}\Big) =$$

$$\approx -\sigma\varphi K\Big(\frac{\varepsilon_{v0a}}{\sigma_a} - \frac{\varepsilon_{v0b}}{\sigma_b}\Big)$$

because the neglected term is of lower order as can be seen from the following. According to eq.(5.2.7) for loading to the creep level, this neglected term is:

$$\ln\Big(\frac{\varphi_a{}^{2\beta_a\alpha_a}}{\varphi_b{}^{2\beta_b\alpha_b}}\Big) = \ln\Big(\frac{\varphi_a \dot{\varepsilon}_a{}^{\alpha_a}}{\varphi_b \dot{\varepsilon}_b{}^{\alpha_b}}\Big) \approx \ln\Big(\frac{\varphi_a}{\varphi_b}\Big)$$

for loading at approximately the same strain rate $\dot{\varepsilon}$ ($\alpha \approx 1$). Because $\sigma\cdot\varphi$ is constant is:

$$\ln\Big(\frac{\varphi_a}{\varphi_b}\Big) = \ln\Big(\frac{\sigma_a\varphi_a}{\sigma_b\varphi_b}\cdot\frac{\sigma_b}{\sigma_a}\Big) = \ln\Big(\frac{\sigma_b}{\sigma_a}\Big) = \ln\Big(\frac{\bar{\varepsilon}K_2}{\sigma_a}\Big) - \ln\Big(\frac{\bar{\varepsilon}K_2}{\sigma_b}\Big) \ll \sigma\varphi K_2\Big(\frac{\varepsilon_{0a}}{\sigma_a} - \frac{\varepsilon_{0b}}{\sigma_b}\Big)$$

and thus neglectable, because $\sigma\varphi \gg 1$. Thus:

$$\ln(t_a) - \ln(t_b) = -\sigma\varphi K\Big(\frac{\varepsilon_{v0a}}{\sigma_a} - \frac{\varepsilon_{v0b}}{\sigma_b}\Big) \qquad (5.4.22)$$

with: $\sigma\varphi = \sigma_a\varphi_a = \sigma_b\varphi_b$. So the shift is mainly dependent on the relative initial plastic strains. These strains arise during the loading to the creep level and because of the faint curved σ-ε- diagram of this loading, a parabolic approximation of the diagram is possible or:

$$\varepsilon = c_1\sigma + c_2\sigma^2$$

and the plastic strain increases quadratic with the stress, showing that the shift of the compliance along the time axis is roughly proportional to the applied stress level σ:

$$\ln(t_a) - \ln(t_b) \approx -\sigma\varphi K c_2(\sigma_a - \sigma_b) = -C(\sigma_a - \sigma_b), \qquad (5.4.23)$$

as also found from testing.

The same applies to eq.(5.4.20) of the second mechanism, that occurs directly for creep without a delay time when loaded to high stress levels and leads to the same relation for the shift. The same can be stated for eq.(5.4.16). Because the shift of the second process is equal to that of the first process, there must be a critical value of the compliance, inde-

pendent on the applied stress, where the second process starts. So it is probable that the first process creates the accumulation of flow units, necessary for the second process. This also applies for wood (even for denser species as for instance Hinoki) and as can be seen in fig. 5.10 by the shift of the lines in proportion to the stress, the compliance increases linearly with the stress level (at a given time, as given in fig. 5.12 for wood). A fit by two lines with positive slopes would have been better in fig. 5.12 and the slope of the line at low stress levels is steeper [6] for dense species and higher moisture contents. However as a first approximation, the line for low stress levels can often be regarded as a horizontal line. This means that for this process ε_v is proportional to σ, and the behaviour is quasi linear. So for loading to ε:

$$\sigma_v = K_1(\varepsilon - \varepsilon_v) = \frac{1}{\varphi} \cdot \ln(2\beta\alpha),$$

or:

$$\varepsilon = \varepsilon_v + \frac{\varepsilon}{K_1\varphi\varepsilon} \cdot \ln(2\beta\alpha) \text{ or: } \varepsilon_v = c\varepsilon, \text{ because } K_1\varphi\varepsilon \text{ is constant.}$$

For higher stress levels (above about 50% of the strength), the increase of ε_v is more than linear dependent of ε [6], what can be explained by eq. (5.4.16) (with $\varepsilon_v(:)\ \varepsilon^2$, as will be discussed later).

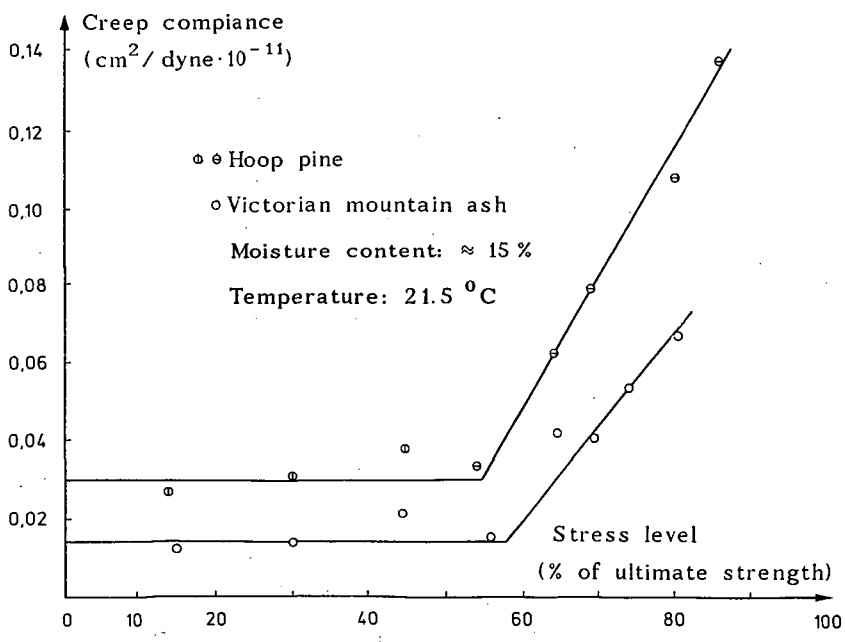

fig. 5.12 Dependence of the creep compliance on the stress level [7]

So wood may behave like holocellulose but the filler properties of the lignin may reduce ε_v for the process at low stresses. It can be shown that $1/\varphi K_2$ has the form: $c_1 + c_2\sigma\omega$ (independent of T) indicating a constant φ when $\omega = 0$. Because c_1 is small, $\sigma\varphi$ is approximately constant for higher values of ω.

This behaviour of the main creep process in wood may be concealed by the occurrence of an other process with constant $\varphi\varepsilon^2$. This mechanism rotates the creep lines (on log-time scale) in proportion with the applied stress, because else the relationship according to fig. 5.12 wouldn't hold. The parameter estimation for creep in [7], clearly shows the tendency of constant $\sigma\varphi$ at low stress levels, while the there estimated changing spring constants at higher stress levels is the indication of the occurrence of the mechanism with constant $\varphi\varepsilon^2$. This will be discussed later.

The constancy of $\sigma\varphi$ can be explained as follows. For compression the number of developing slip planes N is about linear proportional to the stress level σ at lower stress levels. So $\sigma\varphi = \sigma\lambda/N$ is constant. At a level of about 50 to 65% creases are formed, leading to the second mechanism of gross buckling of the cell walls where a constant buckling stress f may be expected so $\sigma\lambda/N = f\lambda_2\lambda_3\lambda$ = constant, or σ/N = constant. Analogous is for crack propagation in tension the real stress f at a sharp crack at any stress level equal to the flow stress and is $f\lambda\lambda_2\lambda_3$ constant or is σ/N constant.

In the analysis above, it is assumed that the temperature is constant. To know the shift of the compliance along the time axis due to temperature, the same stress level has to be used in all tests at different temperatures. Then:

$$\ln(t_a) - \ln(t_b) = E'/kT_a - E'/kT_b$$

where E' is the activation energy. This is only true if $1/\sigma\varphi K_2$ is constant, independent of the temperature (e.g. for creep). If this is not constant, reduced strains are necessary to obtain the right activation energy.

If all Maxwell elements flow, one is determining for the overall rate in the end state and the power equation becomes:

$$\dot{\varepsilon} = A'(\rho_0 + B\varepsilon)\left(\frac{\sigma_a - M\varepsilon}{\sigma_0}\right)^n. \qquad (5.4.24)$$

This equation cannot be integrated. Numerical solutions show that the delay time is due to "dislocation multiplication" similar to yield drop, dependent on the initial flow unit density (see fig. 5.13).

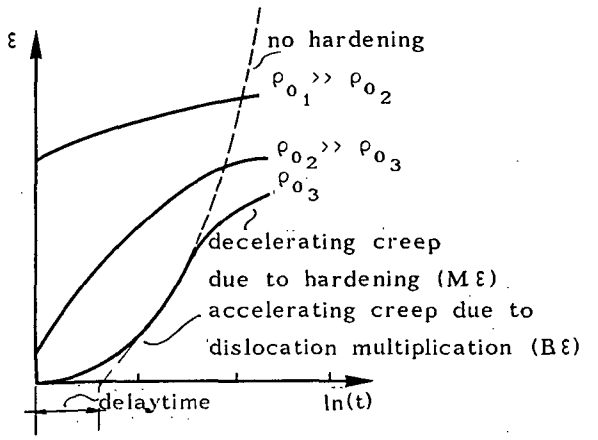

fig. 5.13 Creep dependent on modelparameters

For creep recovery, after long time, the initial conditions are: $\sigma = 0$; $\varepsilon = \varepsilon_\infty$ when $t = 0$, leading for the three-element model to:

$$\varepsilon = \frac{1}{\varphi K_2} \ln\left(\coth\left(-\frac{1}{2}\ln\left(\tanh\left(\frac{\sigma_{v0}\varphi}{2}\right) + \frac{K_1 K_2 A \varphi t}{2(K_1+K_2)}\right)\right)\right) \qquad (5.4.25)$$

analogous to eq.(5.4.2).

5.5 Stress relaxation

The three element model (fig. 5.2) loaded to σ_0 at strain ε_0 at time t_0 gets the stress $\sigma_0 - \sigma_{v0}$ on spring 2. This remains unchanged when by relaxation stress σ_v on spring 1 decreases.
For the Maxwell element is: $\dot{\varepsilon} = 0$, or: $\dot{\sigma}_v = -K_1 \dot{\varepsilon}_v$, or:

$$-\dot{\sigma}_v = K_1 A \sinh(\varphi \sigma_v). \qquad (5.5.1)$$

Integration gives: $\ln(\tanh(\varphi\sigma_v/2)) = -A\varphi K_1 t + C$,
or:

$$\sigma_v = \frac{2}{\varphi}\operatorname{arctanh}\left(\tanh\left(\frac{\varphi\sigma_{v0}}{2}\right)\cdot\exp(-A\varphi K_1 t)\right). \qquad (5.5.2)$$

This equation can be written with: $a = \tanh(\sigma_{v0}\varphi/2)$ and $b = A\varphi K_1$:

$$\sigma_v = \frac{1}{\varphi}\ln\left(\frac{1 + a\cdot\exp(-bt)}{1 - a\cdot\exp(-bt)}\right) = \frac{1}{\varphi}\ln\left(\frac{(\sqrt{a})\cdot\exp(bt/2 - \ln(\sqrt{a})) + (\sqrt{a})\cdot\exp(-bt/2) + \ln(\sqrt{a}))}{(\sqrt{a})\cdot\exp(bt/2 - \ln(\sqrt{a})) - (\sqrt{a})\cdot\exp(-bt/2) + \ln(\sqrt{a}))}\right)$$

or:

$$\sigma_v = -\frac{1}{\varphi}\ln\left(\tanh\left(\frac{bt}{2} - \frac{1}{2}\ln(a)\right)\right), \quad \text{or:}$$

$$\sigma_v = -\frac{1}{\varphi}\ln\left(\tanh\left(\frac{A\varphi K_1 t}{2} - \frac{1}{2}\ln\left(\tanh\left(\frac{\sigma_{v0}\varphi}{2}\right)\right)\right)\right). \qquad (5.5.3)$$

For the early part of the relaxation this is:

$$\sigma_v = -\frac{1}{\varphi}\ln\left(\frac{A\varphi K_1 t}{2} - \frac{1}{2}\ln\left(\tanh\left(\frac{\sigma_{v0}\varphi}{2}\right)\right)\right)$$

or:

$$\sigma_v = -\frac{1}{\varphi}\ln\left(\frac{A\varphi}{2}K_1\right) - \frac{1}{\varphi}\ln\left(t + \frac{2\cdot\operatorname{arccoth}(\varphi\sigma_{v0})}{A\varphi K_1}\right). \qquad (5.5.4)$$

Except for very small times this will have the empirical form:

$$\sigma_v = C_1 - C_2\log(t).$$

The total stress on the specimen is: $\sigma = \sigma_0 - \sigma_{v0} + \sigma_v(t)$, or:

$$\sigma = \sigma_0 - \frac{1}{\varphi}\ln\left(1 + \frac{A\varphi K_1 t}{2\cdot\operatorname{arccoth}(\exp(\varphi\sigma_{v0}))}\right), \qquad (5.5.5)$$

or for not too small values of $\sigma_{v0}\varphi$:

$$\frac{\sigma}{\sigma_0} = 1 - \frac{1}{\sigma_0\varphi}\ln\left(1 + \frac{A}{2}\varphi K_1 t\cdot\exp(\sigma_{v0}\varphi)\right) = 1 - \frac{1}{\sigma_0\varphi}\ln\left(1 + \frac{t}{t'}\right), \qquad (5.5.6)$$

in agreement with our experiments.
For longer times eq.(5.5.6) becomes:

$$\frac{\sigma}{\sigma_0} = 1 - \frac{1}{\sigma_0\varphi}\ln\left(\frac{t}{t'}\right) \text{ with: } t' = \frac{2}{A\varphi K_1\exp(\sigma_{v0}\varphi)} \qquad (5.5.7)$$

and for a horizontal shift of this relaxation line along the ln(t)-axis is:

$$\ln(t_a) - \ln(t_b) = \ln(t'_a) - \ln(t'_b) = \ln\left(\frac{\varphi_b}{\varphi_a}\right) + \frac{\sigma_{v0b}}{\sigma_{0b}} - \frac{\sigma_{v0a}}{\sigma_{0a}}. \qquad (5.5.8)$$

For loading to the same stress level at different speeds is $\varphi_a = \varphi_b$, and the shift is according to eq.(5.2.7):

$$\ln(t_a) - \ln(t_b) = \ln\left(\frac{\dot{\varepsilon}_b\alpha_b}{\dot{\varepsilon}_a\alpha_a}\right), \qquad (5.5.9)$$

where $\dot{\varepsilon}_i$ is the strain-rate for loading to the creep level.
This equation can be compared to the test results of [8] on microspecimens of latewood and earlywood (Spruce and fir). The measured lines, given in fig.5 of [8], can be precisely described by eq.(5.5.6), giving a value of:

$\frac{1}{\varphi\sigma_0}$ = 0,026, for early wood and: 0.032 for late wood. So a mean value of: 0.029 or: $\sigma_0\varphi$ = 34.5,

where t' is dependent on the rate of loading to the creep level, as predicted by the theory. The delay time t' is:

t' = 0.145 sec. for quick loading and is: 4.35 sec. for loading at the slow rate.

So the shift of the line eq.(5.5.7) is:

$$\ln(t_a) - \ln(t_b) = \ln(4.35/0.145) = \ln(30) = 3.4 .$$

According to eq.(5.5.9) the shift, due to the difference of the rates of 0.002 and 0.208 mm/sec. is:

$$\ln(t_a) - \ln(t_b) = \ln(104\alpha_b/\alpha_a), \text{ indicating: } \alpha_b = 0.29\ \alpha_a.$$

$$\frac{\alpha_b}{\alpha_a} = \frac{1 - \exp(-\varphi_b K_1 \varepsilon_{v0b})}{1 - \exp(-\varphi_a K_1 \varepsilon_{v0a})} \approx \frac{\varphi_b K_1 \varepsilon_{v0b}}{1}$$

if ε_{v0b} is very small (fast loading) and ε_{v0a} is sufficient large (slow loading). So: $\varphi_b K_1 \varepsilon_{v0b} \approx 0.29$. With: $\varphi K_1 \varepsilon_0 \approx 0.2\sigma_0\varphi = 0.2 \cdot 34.5 = 6.9$, is:

$$\varphi_b K_1 \varepsilon_{v0b} = \varphi_b K_1 \varepsilon_0 - \varphi\sigma_{v0b} = 6.9 - \varphi\sigma_{v0b} = 0.29, \text{ or: } \varphi\sigma_{v0b} \approx 6.6.$$

$$\ln\left(\frac{t'_a}{t'_b}\right) = 3.4 = \ln\left(\frac{\exp(\varphi\sigma_{v0b})}{\exp(\varphi\sigma_{v0a})}\right) = 6.6 - \varphi\sigma_{v0a}, \text{ giving: } \varphi\sigma_{v0a} \approx 3.2 .$$

The values of $\varphi\sigma_{v0}$ are first estimates because the value of K_1 of: $K_1 = \approx 0.2 \cdot (K_1 + K_2)$ is an estimate. Further, at the fast loading rate, there is a small influence of another very quick relaxing element that is not noticeble at the slow rate (see fig. 5.8). Accounting for this influence would lower the ratio of the strain rates in the analysis above. Nevertheless the data of [8] can be fully explained by the theory and the value of n = $= \sigma_0\varphi = 34$ is comparable with the values of other experiments.

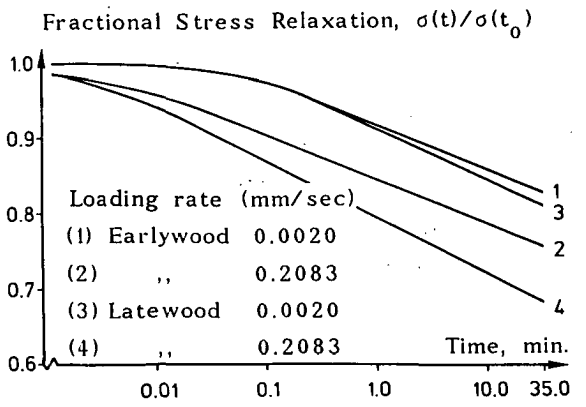

fig. 5.14 Typical curves for relaxation [8]

At relaxation of tropical wood, as measured in [9], there appears to be more plastic deformation increase than for relaxation of the species of [7] (different types of ash, hoop pine and blackbutt).
For paramater estimation in [9], it was assumed that all relaxation processes were finished at the same time (8 hours) independent of the stress level. The consequence of this assumption can be seen by the following equation. Eq. (5.5.7) can be written, with $A = B\varepsilon_{v0}$, for a structural change process:

$$\frac{\sigma}{\sigma_0} = 1 - \frac{\sigma_{v0}}{\sigma_0} - \frac{1}{\sigma\varphi_0}\ln\left(\frac{\varphi K_1 B\varepsilon_{v0}}{2}t\right) = \frac{K_2\varepsilon_0}{\sigma_0} - \frac{1}{\sigma\varphi_0}\ln\left(\frac{t}{t_m}\right) \qquad (5.5.10)$$

Extrapolation of this line to the stress value that is reached at the end of the relaxation: $\sigma = K_2\varepsilon_0$, gives the intersect $t_m = 2/(\varphi\varepsilon_{v0}BK_1)$. So the assumption of equal times of total relaxaton, is equivalent with the assumption that t_m is constant, or $\varphi\varepsilon_{v0}$ is constant (in stead of $\varphi\varepsilon_0$). Because ε_{v0} is proportional to ε_0^2, it is assumed that $\varphi\varepsilon_0^2$ is constant. It can clearly be seen from the parameter estimation of [9] that $K_1\varphi\varepsilon_0$ is constant there and K_1 increases linearly with the strain. Because K_1 has to be constant, it follows that $\varphi(\varepsilon_0)^2$ is constant. This leads to the relaxation line (with $\varepsilon_{v0} = c\varepsilon_0^2$):

$$\frac{\sigma}{\sigma_0} = 1 - \frac{1}{\varphi\sigma_0}\ln\left(\frac{t}{t'}\right) = 1 - \frac{\varepsilon_{v0}}{\varphi\varepsilon_{v0}\sigma_0}\ln\left(\frac{t}{t'}\right) = 1 - \frac{c\varepsilon_0\ln(t/t')}{\varphi\varepsilon_{v0}(K_1 + K_2)} \qquad (5.5.11)$$

and a plot of this equation for t = 8 hours is given in fig. 5.15. It is seen

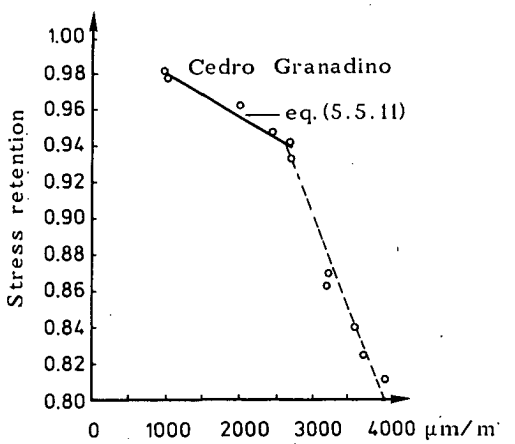

fig. 5.15 Relaxation for compression of tropical wood [9]

that also the second mechanism, above 2600 μm/m, has this dependency

of φ. The constancy of $\varepsilon_{v0}\varphi$, wich only occurs at high stresses for the species of [7], may also appear at low stresses in tropical species. On the other hand, the influence of the creep of the strain gauges is not known and it is possible that the creep of the glue is also measured. The same process lasted 28 hours in [7] (in stead of 8 hours in [9]) by using a very thin glue layer. Because this mechanism is different from those of wood tissues (cell walls), wood pulp (cellulose), and for fracture, and is dominating in dense lignin rich species, it may represent a flow mechanism of the lignin. For high stresses also another mechanism may occur with a constant φ, as measured for Blackbutt in [7], and as found for spruce in this investigation.
It may be supposed that the parabolic loading line, for loading up to the relaxation strain, may be due to a spectre of mechanisms, or at least by two parallel processes. Then the relaxation equations for that case are:

$$\dot{\sigma}_1 + K_1 A_1 \sinh(\varphi_1 \sigma_1) = 0,$$

$$\dot{\sigma}_2 + K_2 A_2 \sinh(\varphi_2 \sigma_2) = 0$$

with: $\sigma = \sigma_1 + \sigma_2$ (or, if there is a parallel spring: $\sigma = \sigma_1 + \sigma_2 + \sigma_3$ where: $\sigma_3 = K_3 \varepsilon$ represents the parallel spring).
The solution of these equations are:

$$\sigma_1 = \sigma_{10} - \frac{1}{\varphi_1} \ln(1 + \frac{t}{t'_1}), \text{ and: } \sigma_2 = \sigma_{20} - \frac{1}{\varphi_2} \ln(1 + \frac{t}{t'_2})$$

or with: $\sigma_0 = \sigma_{10} + \sigma_{20}$ and for longer times:

$$\sigma = \sigma_0 - \frac{1}{\varphi_1} \ln(t) - \frac{1}{\varphi_2} \ln(t) + \frac{1}{\varphi_1} \ln(t'_1) + \frac{1}{\varphi_2} \ln(t'_2) = \sigma_0 - \left(\frac{1}{\varphi_1} + \frac{1}{\varphi_2}\right) \ln(\frac{t}{t'}) \qquad (5.5.12)$$

with:

$$t' = \left(t'_1\right)^{\varphi_2/(\varphi_1+\varphi_2)} \cdot \left(t'_2\right)^{\varphi_1/(\varphi_1+\varphi_2)}. \qquad (5.5.13)$$

If one of these mechanisms is comparable with those of wood tissues and or wood pulp (cellulosis), then for mechanism 1 is: $\varepsilon_0 \varphi_1 = c_1$ is constant or $\sigma_0 \varphi_1$ is approximately constant and for the other is $\varphi_2 \varepsilon_0^2 = c_2$ is constant. Then eq.(5.5.12) becomes:

$$\frac{\sigma}{\sigma_0} = 1 - \frac{1}{\sigma_0 \varphi_1}\left(1 + \frac{c_1 \varepsilon_0}{c_2}\right) \ln(\frac{t}{t'}), \qquad (5.5.14)$$

and this equation doesn't approach the value $\sigma/\sigma_0 = 1$ for ε_0 approaching zero. So this is not probable as can be seen in fig. 5.15.

The influence of temperature on stress relaxation is p.e. given in [10] for wet Hinoki wood. It appears that $\varphi\varepsilon$ is constant and is independent of the temperature below and above the transition temperature (about 50 °C), being smaller above the transition temperature.
For a horizontal shift of the line along the ln(t)-axis due to temperature difference is:

$$\left(\frac{\sigma}{\varepsilon}\right)_a - \left(\frac{\sigma}{\varepsilon}\right)_b = 0$$

leading to the so called Arrhenius equation. This is derived in 6.3, see

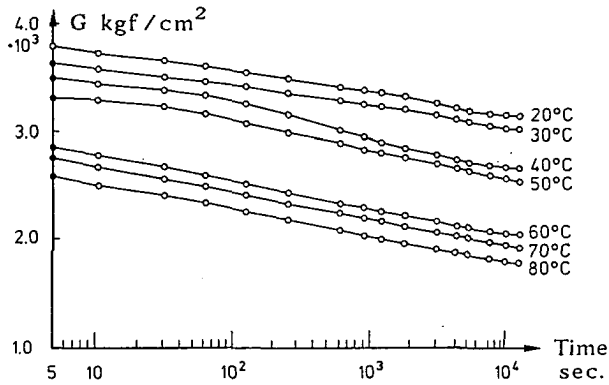

fig. 5.16 Stress relaxation curves for wet Hinoki [10] at various temperatures.

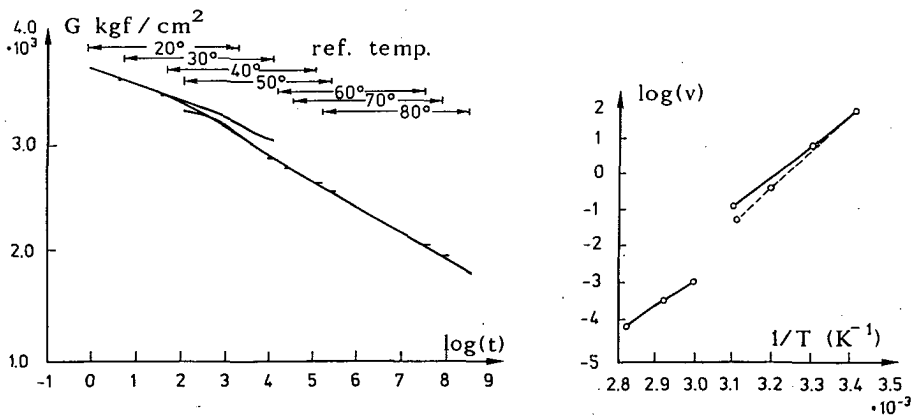

fig. 5.17 Master stress relaxation curves and shift diagram [10]

eq.(6.3.14). So:

$$\ln(v) = \ln(t_a) - \ln(t_b) = \ln\left(\frac{A_b}{A_a}\right) \approx \left(\frac{H}{RT}\right)_b - \left(\frac{H}{RT}\right)_a$$

or:

$$\frac{d(\ln(v))}{d(1/T)} = \frac{H}{R}. \qquad (5.5.16)$$

The shift of the relaxation lines have to be done for both slopes of the lines separately. If this is done on the data of [10] an apparent activation energy H of about 46 kcal/mol is found above and about 28 kcal/mol below transition (as also found for creep in [7]). In the transition region (between 40 ° and 60 °C) also vertical shifts are necessary because of the temperature dependence of $\varphi\varepsilon$ in this region (also possible is a WLF-transition for the small element). So there is a transition to a different mechanism with a smaller value of φ, or with an increased number of activated sites N and a higher activation energy.
For the mechanism with a constant, stress independent value of φ, there is an indication that φ is also independent of the temperature as follows from our investigation.

As mentioned before, the non-linearity of the time dependent behaviour is not strong and there is no well defined point of flow at loading and the loading line can be regarded to be parabolic and the plastic strain ε_{v0} is therefor proportional to ε_0^2. In the following it will be shown that this is a possible approximation.
For loading up to the level of creep or relaxation is:

$$\sigma_v\varphi = \ln\left(\frac{2\dot{\varepsilon}}{\beta\varepsilon_v}\right) \quad \text{or:} \quad \varphi K_1(\varepsilon - \varepsilon_v) = \ln(2\beta/\varepsilon_v). \qquad (5.5.17)$$

Substitution of $\varepsilon_v = c\varepsilon^2$ gives:

$$\varepsilon = c\varepsilon^2 + \frac{\varepsilon}{\varphi K_1\varepsilon}\ln(2\beta/c\varepsilon^2) \quad \text{or:} \quad 1 = c\varepsilon + \frac{1}{\varphi\varepsilon K_1}\ln\left(\frac{2\beta}{c\alpha^2}\cdot\frac{\alpha^2}{\varepsilon^2}\right) \quad \text{or:}$$

$$1 = c\varepsilon + \frac{1}{\varphi\varepsilon K_1}\left(\ln\left(\frac{2\beta}{c\alpha^2}\right) - 2\cdot\ln\left(\frac{\varepsilon}{\alpha}\right)\right). \qquad (5.5.18)$$

α is a constant that is chosen in such way, that $(\varepsilon - \alpha)/\alpha$ is sufficient small with respect to 1. Then:

$$\ln\left(\frac{\varepsilon}{\alpha}\right) = \ln\left(1 + \frac{\varepsilon - \alpha}{\alpha}\right) \approx \frac{\varepsilon - \alpha}{\alpha} = \frac{\varepsilon}{\alpha} - 1. \qquad (5.5.19)$$

Eq.(5.5.18) then becomes:

$$\varphi\varepsilon K_1 = \varphi\varepsilon K_1 c\varepsilon + \ln(2\beta/c\alpha^2) - 2\varepsilon/\alpha + 2.$$

In this equation the terms with ε have to disappear and because $\varphi\varepsilon$ is constant is:

$$\varphi\varepsilon K_1 c\alpha = 2, \text{ and: } \varphi\varepsilon K_1 - 2 = \ln(\beta\varphi\varepsilon K_1/\alpha).$$

So an estimate for c is:

$$c = \frac{2\beta}{(\varphi\varepsilon K_1)^2}\cdot\exp(\varphi\varepsilon K_1 - 2). \qquad (5.5.20)$$

The same can be done when $\varphi\varepsilon^2$ is constant. Eq.(5.5.18) then becomes:

$$\frac{1}{\varepsilon} = c + \frac{1}{K_1\varphi\varepsilon^2}\left(\ln\left(\frac{2\beta}{c\alpha^2}\right) + 2\cdot\ln\left(\frac{\alpha}{\varepsilon}\right)\right)$$

or with eq.(5.5.19):

$$K_1\varphi\varepsilon^2/\varepsilon = cK_1\varphi\varepsilon^2 + \ln(2\beta/c\alpha^2) + 2\alpha/\varepsilon - 2.$$

So:

$$2\alpha = K_1\varphi\varepsilon^2 \quad \text{and:} \quad c = \frac{(K_1\varphi\varepsilon_v)^2}{8\beta}\cdot\exp(2 - K_1\varphi\varepsilon_v). \qquad (5.5.21)$$

As mentioned in 5.4, there is also a possibility of an approximate linear relationship between ε_v and ε (influence of lignin). When α is close to 1, eq.(5.5.17) can be written:

$$\varepsilon_v = \varepsilon\left(1 - \frac{1}{\varepsilon\varphi K_1}\cdot\ln\left(\frac{2\dot{\varepsilon}}{A}\right)\right) = c\varepsilon. \qquad (5.5.22)$$

An example of this relationship is mentioned in 2.3.2, where the number of slip lines increases linearly with the stress level.
When φ is constant, the shift of the creep line (and not the compliance line) or the shift of the relaxation line (and not the line of relative relaxation) has to be regarded to see the dependency of ε_v on ε.

5.6 Conclusions

For many materials there is a dominating mechanism with a constant value of $\varphi\varepsilon_0$ (independent of the temperature and initial strain ε_0 at constant moiture content). Probably this is the case for slip-line formation, local buckling, and crack initiation and propagation, but it also applies for short segments movements of rubbers in the glassy state. Until now it was not recognized that this also applies for wood. Coupled to this mechanism is another mechanism with a lower value of $\varphi\varepsilon$ and a long delay time (flow unit increase) that occurs after some critical visco-elastic

strain (0.4% [6]) of the first mechanism and possibly this first mechanism creates the room, or the flow units, for the second mechanism. The additional creep strain of this second mechanism is irreversible [6]. This mechanism did not occur in cell wall experiments, even not at high stress levels. Because in high loaded wood, the earlywood is higher loaded than in these cell wall experiments and thus flows, this mechanism can probably be related to flow of the earlywood and load transmission from the earlywood to the latewood.

The dependency of this mechanism on the moisture content ω follows from strain rate tests, where it was found that $1/n$ is proportional to ω (or the density of flow units N is proportional to ω). The same was found in creep tests.

Besides these dominating mechanisms, that are related to the cellulose and hemicellulose, there is a small mechanism with a low value of $\sigma\varphi$ ($n = 1$) and a short relaxation time that is only noticeble at very high loading rates.

Of minor importance and mostly neglectable is a primary bond breaking process with $n \approx 63$ and an activation energy of about 50 kcal/mol (controlled crack growth).

With the property of constant $\varphi\varepsilon_0$ (or constant n), it is possible to explain experimental laws as, for instance, the linear dependence of the stiffness on the logarithmic value of the strain rate in a constant strain rate test; the logarithmic law for creep and relaxation; the shift factor along the log- time axis due to stress and temperature; the different power models (of the stress and of the time) as the Forintek model and the Andrade and Clouser creep- equations; the constant of the WLF-equation and the height of the relaxation spectre as shown later.

For clear wood in compression there in no indication of hardening and yield drop, showing the influence of a amorphous polymer (lignin). For wood in tension there is a high yield drop, showing the influence of a crystalline material (cellulose) dominated by a low initial flow unit density ρ_0. There is also no indication of hardening, showing that the change of one model-parameter (λ_1) dominates as also follows from the high value of $\sigma\varphi$.

The viscoelastic and viscous flow strain at loading to the creep or relaxation level, is approximately proportional to the quadrat of the strain: $\varepsilon_v \approx c\varepsilon^2$ for holocellulose (wood structure without lignin) and for flow of the earlywood. For wood at low stresses ε_v is about linear dependent on

ε and the viscoelastic behaviour is quasi linear by the influence of the lignin wherefor $B\varepsilon_v \approx A$ is constant (by the high initial flow unit density and no structural change).

The existence of another mechanism in wood is reported in [7] and [9]. For this structural change mechanism, the relaxation time is independent of the stress level and thus it is not related to the holocellulose. It can be deduced that for this mechanism $\varphi\varepsilon_v$ or $\varphi\varepsilon_0^2$ is constant. So the number of creeping mechanisms N increases with increasing plastic strain ($n = \sigma\lambda/NkT = \sigma(\lambda/\lambda_1)/kTN' = \sigma\varepsilon_v/kTN'$, with $N' = N/\lambda_1$. being the number of flow units per unit volume). Half of the stress was relaxed in about 10 minutes in [9], but the process occurred only at high stress levels and lasted much longer in [7] (halve of the creep in about 3 hours). Possibly there is an influence of creep of the glue of the strain gauges. The thin glue layer of [7] may then explain the much longer relaxation time. However also measured in [7] are mechanisms with constant $\varphi\varepsilon$ at low stress levels and constant φ at high stress levels (with $\varepsilon_v = c\varepsilon$) indicating a right behaviour of the strain gauges. So a better explanation is that this is a mechanism in the lignin. Tropical woods are much denser and contain much more lignin (about twice as much) than the nordic species. Especially the nordic hardwoods have the lessest content of lignin and will not show this mechanism.

The constancy of $\varphi\varepsilon_v$ applies only for constant temperature and moisture content. Probably $1/\varphi\varepsilon_v$ is linear dependent on ω and T. In our investigation an approximate constant φ, independent of the temperature and moisture content, was found for high stress levels (and probably this is due to a dominant influence of diffusion on the creep by the small cycling humidity conditions as discussed in 7.2. In that case, the stress independent part of the activation energy is linear dependent on ω).

5.7 References

[1] Predicting the effect of specific gravity, moisture content, temperature and strain rate on the elastic properties of wood. L.C. Palka, Wood Science and Technology 7, 1973.

[2] For. Prod. Lab. Report No 1767, J.A. Liska, 1950.

[3] Bulletin of A.I.J. no 32, H. Sugiyame 1953.

[4] Deformation kinetics. A.S. Krausz, H.Eyring 1975 John Wiley & Sns.

[5] The creep behaviour of individual pulp fibers under tensile stress, R.L. Hill, Tappi 50, no 8 Aug. 1967.

[6] Creep and strain behaviour of wood, E.G. King, Forest Prod. Journ. Oct. 1957.

[7] Some aspects of the rheological behaviour of wood, R.S.T. Kingston, L.N. Clarke, Austr. Journ. of applied Science 12 no 2, 1961.

[8] On the fractional stress relaxation of coniferous wood tissues, E. Kirbach, L. Bach, R.W. Wellwood, J.W. Wilson, Wood and Fiber 8, no 2, 1976.

[9] Stress relaxation of wood at several levels of strain, H. Echenique Manrique, U.S.N. Office of Naval Research. Techn. Rep., 1967.

[10] The effect of temperature on torsional stress relaxation of wet Hinoki wood, H. Urakami and K. Nakato, Proc. of the 14th meeting of the J.W. Res. Soc. Tokyo, Apr. 1964.

6. OTHER ASPECTS OF THE DERIVED THEORY

6.1 Introduction

The derived general theory must be able to explain the different phenomenological methods and to give a physical meaning to the constants of those methods. This will be discussed here for frequently used models. As shown before, the relations, containing the power of the stress, as the Forintek model and as used in fracture mechanics, can be explained. The same is possible with the relations containing the power of the time, as the Andrade and Clouser equations. It will be shown that the Clouser-type equation is equivalent to the theoretical logarithmic creep behaviour. The derived deformation kinetics model also gives an explanation of the WLF-equation (Williams-Landel–Ferry is WLF) for the shift factor of the creep line at different temperatures along the log-time axis. The theory explaines why this equation also applies for cross-linked polymers at transient creep.
Often, the nonlinear viscoelastic deformation problem is linearized by spliting up the contribution to the rigidity in numerous linear viscoelastic processes giving a relaxation spectrum. It is shown here that a single process may explain the measured, broad, nearly flat spectra of glasses and crystalline polymers, giving a physical meaning to a spectrum. This also has to be so for the spectrum of energy loss at forced vibrations, and the activation volume will have to obey a special relationship.

6.2 Mathematical explanation of the Andrade creep equation or of the power model for creep

The Andrade-type equation for the description of creep is often used for wood and wood-products. The "constants" of this equation depend on the chosen time scale. To explain this equation and this behaviour, a derivation of the constants is given, showing the physical meaning of the "constants" by comparison with the theory of reaction kinetics as given in chapter 4. Andrade divided high temperature creep into three regions: primary or decelerating creep, secondary or steady state creep and tertiary or accelerating creep. For the description of low temperature creep,

that is considered to have only a decelerated stage, Andrade suggested the following equation:

$$\gamma = \gamma_0 + c_1 t^{1/3} + c_2 t \qquad (6.2.1)$$

where γ is the deformation, c_1 , c_2 are constants and t is the time. For the cross-linked polymers in wood c_2 is negligible and eq.(6.2.1) becomes:

$$\gamma = \gamma_0 + c\, t^{1/3}. \qquad (6.2.2)$$

For wood, c is proportional to γ_0 (constant n as will be discussed at the end of 6.2) and eq.(6.2.2) can be expressed in the relative creep δ:

$$\delta = \frac{\gamma - \gamma_0}{\gamma_0} = C\, t^{1/3} \qquad (6.2.3)$$

or more general:

$$\delta = C\, t^{m}. \qquad (6.2.4)$$

This equation is known as the "power-model" or "Clouser" equation. To explain the meaning of this empirical equation it will be compared with the theoretical equation for decelerated creep behaviour as given before in 5.4. From this theory it appears that decelerating creep can be described by:

$$\gamma = c_1 - c_2 \ln(\coth(c_3 + c_4' t)) \qquad (6.2.5)$$

where the constants c_i are known expressions in the molecular parameters. In the early part of the process this reduces to:

$$\gamma = \gamma_0 + c_2 \ln(1 + c_4 t) \qquad (6.2.6)$$

or for not too short times, comparable with the range where eq.(6.2.1) is applicable: $(1 \ll c_4 t)$

$$\delta = B \ln(t/t_1). \qquad (6.2.7)$$

So eq.(6.2.4) has to be compared with this expression. Eq.(6.2.4) can be written like:

$$\delta = A'(t/t_1)^m = A'(t/t_0)^m (t_0/t_1)^m = A'(t_0/t_1)^m (\exp(m \ln(t/t_0))) \qquad (6.2.8)$$

or in Taylor series:

$$\delta = A'(t_0/t_1)^m (1 + m \ln(t/t_0) + \tfrac{1}{2}(m \ln(t/t_0))^2 + \tfrac{1}{6}(m \ln(t/t_0))^3 + \ldots\ldots) =$$

$$\approx A'(t_0/t_1)^m (1 + m \ln(t/t_0) + \psi), \qquad (6.2.9)$$

where t_0 is a scaling time providing that $m \cdot \ln(t/t_0)$ will be smaller than 1 and ψ is the small influence of the higher order terms.
Eq.(6.2.7) can be written:

$$\delta = B \ln(t/t_0) + B \ln(t_0/t_1)$$

and compairing with eq.(6.2.9), the conditions to obtain the same values with both equations are:

$$mA'(t_0/t_1)^m = B \quad \text{and:} \quad A'(t_0/t_1)^m(1 + \psi) = B \ln(t_0/t_1)$$

leading to:

$$1 + \psi = \ln(B/mA') = m \ln(t_0/t_1). \qquad (6.2.10)$$

The value of ψ can be taken at some intermediate time t_b between t_0 and the maximum time of observation t_m.

$$1 + \psi = \exp(m \ln(t_b/t_0)) - m \ln(t_b/t_0) = (t_b/t_0)^m - \ln(t_b/t_0)^m \qquad (6.2.11)$$

or with aid of eq.(6.2.10):

$$\exp(1+\psi) = (t_b/t_1)^m/\ln((t_b/t_1)^m). \qquad (6.2.12)$$

Now is m in eq.(6.2.13) not constant:

$$A'(t/t_1)^m = B \ln(t/t_1). \qquad (6.2.13)$$

If in this equation m is regarded as a function of time then the change of m with time is minimal for B = A' and eq.(6.2.10) becomes:

$$1 = m \exp(1+\psi) \qquad (6.2.14)$$

or with neglectable ψ:

$$1 = m.e \quad \text{or:} \quad m = 1/e = 0.368 \qquad (6.2.15)$$

or better, if $\psi = 0.1$ is chosen for curve fitting, m = 0.334 being the exponent of Andrade.
From eq.(6.2.10) and eq.(6.2.12) it follows that $\psi = 0.1$, $t_0/t_1 = 27$, $t_b/t_1 = 93$ and $t_m/t_1 \approx 195$ can be taken for not to high deviation at t_m. According to eq.(6.2.9), $t_m/t_1 < 540$ to maintain convergence of the series. For larger time scales m will be different. For instance, if $t_b/t_1 = 100000$ to 1000000, than m is about: m = 0.2.

The meaning of the constants of the Andrade equation can now be given. Becase A' = B, A' is equal to the inverse of the initial creep stress times the activation volume parameter:

$$1/A' = \sigma V/RT \qquad (6.2.16)$$

where σ is the creep stress, V the activation volume, R the gas constant and T the absolute temperature. For not to high stress levels A' can be regarded to be constant because V is inverse proportional to σ. As measured in [1], C = 0.02 for m = 0.31 for timber, indicating a value of A' of about A' = 0.03. The value 1/A' has the same meaning as the exponent n (n = 1/A') of the experimental power law of the creep rate $\dot{\varepsilon} = c(\sigma)^n$. The time t_1 is for wood the delay time of the main process where the creep levels off to higher rates. It is a function of the activation parameters and is dependent on the initial flow unit density.
It can be concluded that the Andrade-type equation is equivalent to the theoretical logarithmic creep behaviour and that the constants have a special meaning and can be compared with the theoretical parameters. Because these "constants" are not really constant but functions of many factors it is recommended to use the logarithmic representation instead of the power-model.

6.3 Derivation of the WLF-equation for the time-temperature equivalence above glass-rubber-transition

Like other polymers, wood may show a disconcontinuity in the specific heat that is known as glass transition. Below the glass transition temperature the configuration of the chain backbones are largery immobilized and viscoelastic properties are determined by side group motions. So the flexible chain theory is not applicable and energy storage is not according to an entropy spring (proportional to the temperature). After transition to rubberlike consistency the viscoelastic behaviour is due to cooperative motions of individual chains. This is not appearing in wood because of the cross-linking, and the transition is to a leathery state. The slow transition process having a long relaxation time is explained by a high negative entropy of activation because for a long chain the probability of coordinated segments motions is small. Thus a segment may be supposed to require no bigger hole to move into than the molecules (small activation heats). However a flow segment will frequently be prevented from flowing by the attached segments, thus giving rise to a high negative entropy, or a long relaxation time. Compliance curves etc. measured at different temperatures can be shifted along a logarithmic time or frequency axis (called time-temperature equivalence). The shift factor of the displacement

of the curve along the log-time axis: $\ln(v) = \ln(t_a) - \ln(t_b)$, is given by the so called WLF-equation (Williams- Landel–Ferry is WLF):

$$\ln(v) = -\frac{c_1(T_a - T_b)}{c_2 + T_a - T_b}, \tag{6.3.1}$$

with $c_2 = V/\beta$, where V is the volume fraction of free volume at T_b and β is the difference of the thermal expansion coefficients below and above the transition temperature, representing the increase in free volume above transition.

This equation is explained by the Doolittle viscosity equation or by the free volume model. The disadvantage of this explanation is that the theory predicts flow dependent on the dilatation invariant of the strain tensor, while it is known that flow is dependent on the isovoluminal deviatoric invariant. With a flow criterion there is no principal difference of flow depending on the stress state. Further β is much smaller for cellulose derivatives and for wood than the constant in eq.(6.3.1) and the thermal expansion in grain direction can even be negative. So a better description is necessary and this is possible by the theory of deformation kinetics as will be shown below.

For uncross-linked polymers steady flow viscosity is possible. For that case is $\dot{\varepsilon}_e = 0$ and eq.(5.2.1) becomes the same as eq.(4.3.12):

$$\dot{\varepsilon} = A\cdot\sinh(\varphi\sigma_v) \approx \frac{1}{t_r}\varphi\sigma_v = \frac{1}{t_r}\sigma_v\frac{\lambda}{NkT} \tag{6.3.2}$$

and the relaxation time is:

$$t_r = \frac{\sigma_v}{\dot{\varepsilon}}\cdot\frac{\lambda^2\lambda_2\lambda_3}{\lambda_1\rho kT} = \frac{c\eta}{\rho kT} \tag{6.3.3}$$

where the viscosity: $\eta = \sigma_v/\dot{\varepsilon}$, the concentration: $\rho = N\lambda_2\lambda_3\lambda/\lambda_1$ and c is constant for a constant structure λ_i. So it is seen that the shift $v = t_r/t_0$ for temperatures T and T_0 is:

$$v = \frac{\eta T_0 \rho_0}{\eta_0 T \rho} \tag{6.3.4}$$

in accordance with the Rouse theory and experiments. The relaxation time is also known from eq.(4.3.5):

$$t_r = \varepsilon_0\nu^{-1}\cdot\exp(E/kT) = (c/kT)\cdot\exp(H/kT)\cdot\exp(-S/k) \approx$$
$$\approx (c/kT)\cdot\exp(-S/k)\cdot(1 + H/kT) \approx (c/kT)\cdot\exp(-S/k) = C/kT$$

where c and C are constants. This is in accordance with the Rouse theory

implying that S/k is a large negative value and H/kT is small or $\varepsilon_0 \exp(H/kT)$ is independent of the temperature. Further there may be a spectre of relaxation times where every deformation mode of the strands will have a specific value of S.

For steady flow of entangled polymers at higher stresses is: $\sinh(x) \approx 0.5 \cdot \exp(x)$ and eq.(6.3.2) becomes, with $1/t_r = \nu' \cdot \exp(-E/kT)$:

$$\dot{\varepsilon} = \frac{\nu'}{2} \exp\left(-\frac{E}{kT} + \frac{\sigma\lambda}{NkT}\right) \tag{6.3.5}$$

A horizontal shift along the time axis is performed when ε at temperature T and time t is the same as ε_0 at temperature T_0 and time t_0. So for loading to the same stress σ is:

$$\ln\left(\frac{\dot{\varepsilon}}{\dot{\varepsilon}_0}\right) = \ln\left(\frac{\varepsilon t_0}{\varepsilon_0 t}\right) = \ln\left(\frac{t_0}{t}\right) = \frac{-E}{kT} + \frac{E}{kT_0} + \frac{\sigma\lambda}{kTN} - \frac{\sigma\lambda_0}{kT_0N_0} \tag{6.3.6}$$

Because $E = H - S \cdot T$ with a dominating entropy term $S \cdot T$ and with $\sigma\lambda/kT = \sigma\lambda_0/kT_0$, eq.(6.3.6) becomes:

$$\ln(v) = \ln\left(\frac{t}{t_0}\right) \approx -\frac{\sigma\lambda}{kT}\left(\frac{1}{N} - \frac{1}{N_0}\right). \tag{6.3.7}$$

In this equation: $-H/kT + H/kT_0$ is neglected. To correct for this, a reduced value of ε can be used as can be seen in eq.(6.3.6):

$$-\ln(v') = \ln\left(\frac{\varepsilon t_0}{\varepsilon_0 t}\right) - \ln\left(\exp\left(\frac{-H}{kT} + \frac{H}{kT_0}\right)\right) = \ln\left(\frac{\varepsilon_r t_0}{\varepsilon_0 t}\right) = \ln\left(\frac{t_0}{t}\right)$$

with: $\varepsilon_r = \varepsilon \cdot \exp(H/kT - H/kT_0)$, being a vertical shift of the line on a $\ln(\varepsilon) - \ln(t)$ - plot. According to eq.(6.3.2) this can be associated to a reduction: $\varepsilon_r = \varepsilon \cdot \rho T/\rho_0 T_0$ as often done but only applies for uncross-linked polymers.

With: $n = \sigma\lambda/kTN_0$ and: $N = N_0 + \beta(T - T_0)$, eq.(6.3.7) becomes:

$$\ln(v) = -n\left(\frac{1}{1 + \beta(T - T_0)/N_0} - 1\right) = \frac{n(T - T_0)}{(N_0/\beta) + T - T_0}. \tag{6.3.8}$$

In this WLF-equation is N the concentration of mobile segments and not necessarily the free volume concentration. For most polymers is at transition $N_0 \approx 0.025$. The value of n is around 40 for most polymers and the value of β is in the range of $2 \cdot 10^{-4}$ to $10 \cdot 10^{-4}$. The equation is also used for high polymers where β may be some orders lower and it is seen that β needs not to be identical to the thermal expansion coefficient for creation of free volume.

When the WLF-equation is compared in literature with the theory of deformation kinetics, in order to determine the activation energy, the viscosity $\sigma/\dot{\varepsilon}$ is always taken to be proportional to: exp(E/kT). According to eq. (6.3.5) this implies that $\sigma\lambda/NkT$ is taken constant, independent of temperature. It is seen from this derivation that this is not a right assumption. The WLF-equation is also used for cross-linked polymers at transient creep although a theoretical explanation is lacking. For the derivation of this case the same procedure can be followed as given at eq.(5.4.21), however now with different temperatures T_a and T_b at the same stress σ. According to eq.(5.4.1) and further is for creep:

$$\varphi\sigma_v = \varphi\sigma_{v0} + \ln(1 + \frac{t}{t'}) \approx \varphi\sigma_{v0} + \ln(\frac{t}{t'}) \qquad (6.3.9)$$

for not to short times. So for a shift along the time axis is:

$$\varphi_a(\sigma_{va} - \sigma_{va0}) - \varphi_b(\sigma_{vb} - \sigma_{vb0}) = \ln(t_a/t_b) - \ln(t'_a/t'_b) \qquad (6.3.10)$$

or with eq.(5.2.7):

$$\varphi_a\sigma_{va} - \varphi_b\sigma_{vb} - \ln\left(\frac{\dot{\varepsilon}_a\alpha_a A_b}{\dot{\varepsilon}_b\alpha_b A_a}\right) = \ln(t_a/t_b) - \ln\left(\frac{\varphi_b\dot{\varepsilon}_b\alpha_b}{\varphi_a\dot{\varepsilon}_a\alpha_a}\right) \qquad (6.3.11)$$

giving:

$$\ln(t_a/t_b) = \varphi_a\sigma_{va} - \varphi_b\sigma_{vb} - \ln\left(\frac{\varphi_a\dot{\varepsilon}_a^2\alpha_a^2 A_b}{\varphi_b\dot{\varepsilon}_b^2\alpha_b^2 A_a}\right) \qquad (6.3.12)$$

Now is: $\sigma_{va} = \sigma - K_2\varepsilon_a$ and $\sigma_{vb} = \sigma - K_2\varepsilon_b$ and for a horizontal shift along the time axis is: $\varepsilon_a = \varepsilon_b$, so: $\sigma_{va} = \sigma_{vb} = \sigma_v$ and eq.(6.3.12) becomes, neglecting the last term:

$$\ln(v) = \ln(t_a) - \ln(t_b) \approx \sigma_v(\varphi_a - \varphi_b) \qquad (6.3.13)$$

and this equation is equal to the WLF-equations (6.3.7) and (6.3.8) however based on the stress on the element that performs the transition σ_v in stead of the total stress as is the case for steady flow.
From eq.(6.3.12) it follows that for constant $\varphi = \varphi_a = \varphi_b$ and for a constant rate of loading to the creep level $\varepsilon_a = \varepsilon_b$, the equation is:

$$\ln(t_a/t_b) = -\ln\left(\frac{\varphi_a\dot{\varepsilon}_a^2\alpha_a^2 A_b}{\varphi_b\dot{\varepsilon}_b^2\alpha_b^2 A_a}\right) = 2\cdot\ln(\alpha_b/\alpha_a) + \ln(T_a/T_b) - \frac{E}{kT_a} + \frac{E}{kT_b} \approx -\frac{H}{kT_a} + \frac{H}{kT_b}$$

or:

$$\ln(v) = \ln(t_a) - \ln(t_b) \approx -\frac{H}{kT_a} + \frac{H}{kT_b} \qquad (6.3.14)$$

and this is the Arrhenius equation. It is seen that this is the amount

that is neglected to obtain the WLF-equation. For higher values of the activation enthalpy H it is to be expected that the value of ln(v) lies between the Arrhenius- and WLF-equation.

For wood the temperature ranges of stable behaviour above the transition temperatures is to short to be able to decide whether the Arrhenius equation applies or the WLF-equation for creep. As mentioned in [2], hemicellulose begins to soften at 55, and lignin at 120 °C. However there are structural changes in this region. First the structure of lignin is altered, then transverse shrinkage of wood begins (at 70 °C) and next the lignin starts loosing weight. The transition temperature for amorphous cellulose is at 210 °C. The changes in the region 120 to 210 °C are in succession: hemicellulose begins to decrease and cellulose begins to increase; bound water is freed (140 °C); lignin melts and begins to reharden; rapid weight loss of hemicellulose and then of the wood; Cellulose dehydrates, Above 210 °C, cellulose crystallinity decreases and recovers; cellulose weight loss starts and increases; hemicellulose is completely degradated; wood is carbonized.

Moisture content lowers the transition temperature T_g linearly for polymers: $T'_g = T_g - k\omega$, where ω is the weight fraction diluent, and the time-moisture content superposition is possible. This implies that: $N = N_0 + \beta(T - T_0) + \gamma\omega$, (with $\gamma = \beta k$).

From table 1 of the torsional pendulum tests of [3], giving the relationship between the moisture content of wood and the temperature of the maximum of damping, it can be deduced that:

$$T'_g = T_g - 180\omega \qquad (6.3.15)$$

where T_g is 132 °C or 405 K.

There is an indication that this also applies for the wood components. Because the "powder collapse" tests have a shorter time scale than the dilatometry tests on dry wood, the transition temperatures must be higher than those of the dilatometry method and if the time-moisture content superposition is applicable than the results of the dilatometry method for dry wood must be the same as for moistened wood according to the powder collapse method. The mentioned transition temperatures by the dilatometry method are for dry hemicellulose 55 °C, for dry lignin 120 °C, and for dry cellulose 210 °C [2]. According to the graphs of [4] for the transition temperatures of the powder collapse method, these temperatures indicate a moisture content of 40% of the hemicellulose at a relative air

humidity of about 80%; a moisture content of 6% for lignin at a relative humidity of about 75% and no moisture effect on cellulose powder. So there is a transition to about 75 to 80% relative humidity or to air dry wood and a correlation of the transition with the humidity is also probable for wood components. It has to be remarked that the behaviour of the constituents may be of minor importance in wood. Probably the hemicellulose is bonded to the lignin, and if the lignin is able to prevent moisture uptake by the hemicellulose, than the transition temperature of the copolymer is highly raised. The powder collapse method [4] showed only two, in stead of three, transition points at 140 °C and 218 °C for spruce at 23% moisture content (relative humidity about 95%).

Although the stable temperature ranges for wood are short, making it difficult to decide what type of temperature dependence is acting, the use of tests with different time scales may extend these ranges. The influence of the time scale of the process may be derived as follows.

Because $\varphi_a A_a / \varphi_b A_b$ is a measure of the ratio of the retardation or relaxation times t_{rb}/t_{ra} (see p.e. eq.(5.4.7)) of the processes at temperatures T_a and T_b, eq.(6.3.12) can be written more generally:

$$\ln(v_r) = \ln\left(\frac{t_a}{t_b}\right) = \sigma_v(\varphi_a - \varphi_b) - \ln\left(\frac{t_{ra}}{t_{rb}}\right). \qquad (6.3.16)$$

So this equation gives the shift along the time axis when the time scales of the processes t_{ra} and t_{rb} at T_a and T_b differ. This explains the shifts as given in [5] and fig. 6.3. For instance the frequency at the maximum of damping in a torsional pendulum test corresponds to the relaxation time and the shift of this maximum is given by the equation above. The equation can also be used in the reversed form. If the tests are not done in the same conditions at the different temperatures, then the relaxation times determine the lengths of the processes at different temperatures and the shift is: $\ln(t_{ra}/t_{rb}) = \sigma_v(\varphi_a - \varphi_b) - \ln(t_a/t_b)$, where t_a at T_a and t_b at T_b are the different, not temperature dependent, testing times.

The WLF-equation of fig. 6.3 has the "universal form" being an average of many polymers. According to this equation: $n = \sigma\varphi_0$ on ln-scale (in stead of log-scale): $n = 2.3 \times 17.44 = 40$. As mentioned before in 4.6, the parameter n is equal to the exponent in the power law for damage and is the inverse of the slope of the creep line on the semi- logarithmic plot also in the glass state. So it appears that n is essentially a structure constant and is probably unaffected by moisture and temperature.

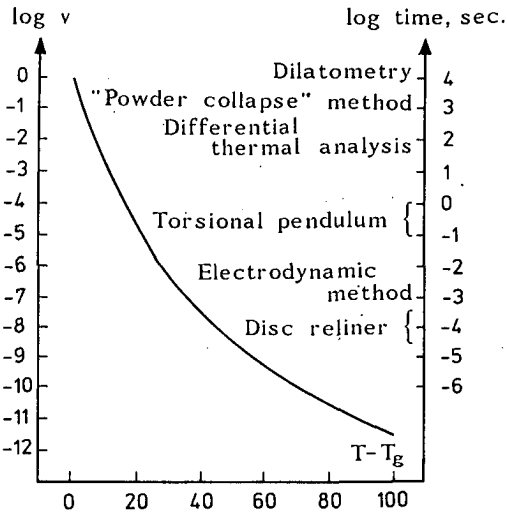

fig. 6.3 Glass transition of lignin [5]

6.4 Relaxation and retardation spectra

The nonlinear viscoelastic deformation problem is often linearized by splitting up the contribution to the rigidity in numerous linear viscoelastic processes. So the contribution: $fd\tau$ is associated with relaxation times in the range τ and $\tau + d\tau$. Mostly a logatithmic time scale is used and the contribution of the range $\ln(\tau)$, $\ln(\tau) + d(\ln(\tau))$ is $H.d(\ln(\tau))$ with $H = f\tau$.
The time dependent rigidity or relaxation modulus is then:

$$G(t) = G_\infty + \int_{-\infty}^{\infty} H\exp(-t/\tau)\cdot d(\ln(\tau)). \qquad (6.4.1)$$

Because this has no physical meaning the equation can be regarded as a mathematical definition of the relaxation spectrum H. For the solution of H, the intensity function $\exp(-t/\tau)$ having values between 0 and 1 for $\tau = 0$ to $\tau = \infty$, can be approximated by a step function from 0 to 1 at $\tau = t$ so:

$$G(t) = G_\infty + \int_{\ln(t)}^{\infty} H d(\ln(\tau)). \qquad (6.4.2)$$

Differentiation of this equation with respect to the limit $\ln(t)$ gives:

$$- \frac{d(G(t))}{d(\ln(t))}\Big|_{t=\tau} \approx H(\tau). \qquad (6.4.2)$$

So the relaxationspectrum at $\tau = t$ is as first approximation the negative slope of the relaxation modulus. This approximation is accurate if H changes slowly with time.

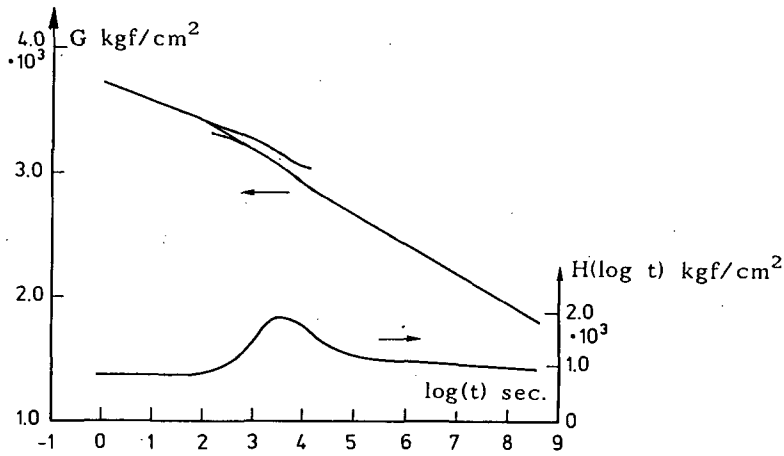

fig. 6.4 Master relaxation curve G(t) and relaxation spectrum [8].

Except for the very beginning and the end of a kinetic process in wood, G(t) has the form:

$$G(t) = G_{\infty} - C\ln(t) \qquad (6.4.4)$$

and H = C (where C is proportional to 1/n) for a wide time range due to a single process. This explains the measured, broad, nearly flat spectra of glasses and crystalline polymers.
As mentioned before a second process is starting in wood and in other highly crystalline polymers after a long time depending on the stress level. At the transition to this second process the change of H is not slow and H can be approximated by:

$$H(\tau) = -\frac{d(G(t))}{d(\ln(t))} + \frac{d^2G(t)}{d(\ln(t))^2}\Big|_{t=2\tau} \qquad (6.4.5)$$

leading to the outline above of the relaxation spectrum for wood in fig. 6.4 that is due to two processes in stead of the assumed infinite number of processes that is regarded to be the basis of the relaxation spectrum of H.

6.5 Spectrum of energy loss at forced vibrations and fatigue behaviour

For a forced vibration on a single Maxwell element by an applied strain: $\varepsilon = a \cdot \sin(2\pi\nu t)$, the stress is: $\sigma = b \cdot \sin(2\pi\nu t + \vartheta)$. With these expressions for σ and ε the absorbed energy is:

$$Z = \int_0^{t_c} \sigma d(\varepsilon) = \pi ab \cdot \sin(\vartheta) \tag{6.5.1}$$

where t_c is the period of the vibration $1/\nu$ and ϑ is the phase angle.
For the three element model at small values of $\varphi\sigma_v$ we have:

$$\sigma = \sigma_v + \sigma_2 = \frac{\dot{\varepsilon}_v}{A\varphi} + K_2\varepsilon \tag{6.5.2}$$

or also:

$$\sigma = K_1(\varepsilon - \varepsilon_v) + K_2\varepsilon. \tag{6.5.3}$$

Elimination of ε_v in the last two equations gives:

$$A\varphi K_1\sigma + \dot{\sigma} = (K_1 + K_2)\dot{\varepsilon} + A\varphi K_1 K_2\varepsilon. \tag{6.5.4}$$

Substitution of the expressions for σ and ε gives:

$$A\varphi K_1 b \cdot \sin(2\pi\nu t + \vartheta) + 2\pi\nu b \cdot \cos(2\pi\nu t + \vartheta) = (K_1 + K_2)2\pi\nu a \cdot \cos(2\pi\nu t) + A\varphi K_1 K_2 a \cdot \sin(2\pi\nu t). \tag{6.5.5}$$

This must be true at any time, so the sum of the terms containing $\cos(2\pi\nu t)$ has to be zero and also the sum of the terms containing $\sin(2\pi\nu t)$. This leads to:

$$b = \left(\frac{2\pi a\nu(K_1 + K_2)}{A\varphi K_1}\right) \cdot \left(\sin(\vartheta) + \frac{2\pi\nu}{A\varphi K_1}\cos(\vartheta)\right)^{-1} \tag{6.5.6}$$

and:

$$\sin(\vartheta) = \frac{2\pi\nu a K_1^2 (A\varphi)^{-1}}{bK_1^2 + 4\pi^2\nu^2 b(A\varphi)^{-2}}. \tag{6.5.7}$$

So from eq.(6.5.1) we find:

$$Z = \frac{2\pi^2\nu a^2 K_1^2 (A\varphi)^{-1}}{K_1^2 + 4\pi^2\nu^2(A\varphi)^{-2}} \tag{6.5.8}$$

The energy of absorption is maximal at the frequency ν_n, where: $\frac{\partial Z}{\partial \nu} = 0$.
So: $\nu_n = K_1 A\varphi / 2\pi$.
For a relaxation time distribution:

$$Z = \pi a^2 \sum_i \frac{K_i \nu/\nu_i}{1 + (\nu/\nu_i)^2}. \tag{6.5.9}$$

Usually this is given for an infinite number of processes as:

$$\int h(\tau)\,\frac{\omega\tau}{1+\omega^2\tau^2}\,d(\tau),$$

where τ is is the relaxation time: $1/\omega_n$ and $\omega = 2\pi\nu$.
The natural frequencies ν_n are far apart and it can be expected that Z between two natural frequencies ν_1 and ν_2 is mainly determined by these two processes:

$$Z = \pi a^2\left(\frac{K_1\nu/\nu_1}{1+(\nu/\nu_1)^2} + \frac{K_2\nu/\nu_2}{1+(\nu/\nu_2)^2}\right). \qquad (6.5.10)$$

For $\nu = \nu_1$:

$$Z_1 = \frac{\pi a^2 K_1}{2}\left(1 + \frac{2K_2\nu_1/K_1\nu_2}{1+(\nu_1/\nu_2)^2}\right) \approx \pi a^2 K_1\left(0.5 + K_2\nu_1/K_1\nu_2\right) \qquad (6.5.11)$$

because $\nu_1 << \nu_2$. In the same way, for $\nu = \nu_2$, $Z = Z_2$:

$$Z_2 \approx \pi a^2 K_2\left(0.5 + K_1\nu_1/K_2\nu_2\right) \qquad (6.5.12)$$

and because the spectrum is flat [6], or Z is about constant, is $Z_1 \approx Z_2$ and the stiffnesses must be equal or: $K_1 \approx K_2$. If for an intermediate value of ν, $\nu = (\nu_1 + \nu_2)/2$, Z is equal to Z_1 and Z_2 then $\nu_1 \approx 0.1\nu_2$. So there will be a range of relaxation times: $t_i = (1/10^i)\cdot t_0$. So: $t_i/t_0 = \exp(E_i/RT - E_0/RT) = (0.1)^i = \exp(-i\cdot\ln(10))$ or:

$$E_i = E_0 - RT\cdot i\cdot\ln(10) = E_0 - 1.35\,i \qquad (6.5.13)$$

and this will show a long range of activation energies in kcal./mol. of for instance: 23 - 22 - 20 - 19 - 18 - 16 - 15 - 14 - 12 - 11 - etc. However measured by other methods are p.e. 23 and 11 kcal./mol. (β - mechanisms). So it is probable that in eq.(6.5.8) in a wide range:

$$\varphi/\nu = \text{constant} = c2\pi/KA = c2\pi t_r/K \qquad (6.5.14)$$

and the flat spectrum is determined by only one process with relaxation time t_r. The analysis shows that ε_v is alternating and thus is reversible. A particular solution of eq.(6.5.4) is:

$$\sigma = C\cdot\exp(-A\varphi K_1 t) = C\cdot\exp(-2\pi\nu t), \qquad (6.5.15)$$

showing that a disturbance disappears within a part of the period. For instance in half the period time is $\sigma = C\cdot\exp(-\pi) = 0.04\cdot C$.
For high loading:

$$\sigma_v = \frac{1}{\varphi}\cdot\ln\left(\frac{2\dot{\varepsilon}_v}{A}\right) = K_1(\varepsilon - \varepsilon_v) \text{ or: } 2\dot{\varepsilon}_v = A\cdot e^{\varphi K_1\varepsilon} - \varphi K_1\varepsilon_v \text{ or:}$$

$$(\varphi K_1 e^{\varphi K_1\varepsilon_v})\cdot d\varepsilon_v = \left(\frac{\varphi K_1 A}{2}\cdot e^{\varphi K_1\varepsilon}\right)\cdot dt.$$

So:

$$e^{\varphi K_1\varepsilon_v} - e^{\varphi K_1\varepsilon_{v0}} = \frac{n}{2}\cdot\int_0^{t_c}\varphi K_1 A\cdot e^{\varphi K_1\varepsilon}\cdot dt = n\cdot C_1$$

where t_c is the time of high stressing within the period and n is the number of cycles. So:

$$\varphi K_1\varepsilon_v = \varphi K_1\varepsilon_{v0} + \ln\left(1 + C_1\cdot n\cdot e^{-\varphi K_1\varepsilon_{v0}}\right). \tag{6.5.16}$$

For higher values of n: $\ln\left(1 + C\cdot n\cdot e^{-\varphi K_1\varepsilon_{v0}}\right) \approx \ln\left(C\cdot n\cdot e^{-\varphi K_1\varepsilon_{v0}}\right) =$
$= \ln(n/n_0)$ and eq.(6.5.16) becomes:

$$\varphi K_1\varepsilon_v = \varphi K_1\varepsilon_{v0} + \ln(n/n_0). \tag{6.5.17}$$

Outside the high stress region the stress and ε_v resume quickly, according to eq.(6.5.15), the low stress values (as described by eq.(6.5.1) to (6.5.8)), but ε_v has increased according to eq.(6.5.17). At high frequencies this increase is small and ε_v is mainly determined by $\sin(\vartheta)$ of the low stress region. If now the stress and strain in the high stress region are approached by a half sinus form with the same area as the real stress and strain curves, then the top-values of these σ and ε are almost the same and close to the real maximum values. The top-value of the sinus approach of the almost constant ε_v will be $\pi/2$. so the relation between the top-values is:

$$\bar{\sigma} - K_2\bar{\varepsilon} = \bar{\sigma}_v = K_1(\bar{\varepsilon} - \varepsilon_v(\pi/2)) \text{ or: } \bar{\sigma} = (K_1 + K_2)\bar{\varepsilon} - K_1\bar{\varepsilon}_{v0} - \frac{\pi}{2\varphi}\ln\left(\frac{n}{n_0}\right)$$

or:

$$\frac{\sigma}{\sigma_0} = 1 - \frac{1}{\varphi\sigma_0(2/3)}\ln(n/n_0). \tag{6.5.18}$$

For low frequencies, $\sin(\vartheta)$ is small and the increase of ε_v is curvilinear and now the top values of the sinus approach of ε,σ, and ε_v have a comparable factor with respect to their maximum values and the relation between these top values becomes:

$$\frac{\sigma}{\sigma_0} = 1 - \frac{1}{\varphi\sigma_0}\ln(n/n_0). \tag{6.5.19}$$

Although these equations give the stress relaxation for a constant strain amplitude, the result is the same for a constant stress amplitude and

with a maximum strain condition $\varepsilon_v = \varepsilon_{vm}$, the equations give the number of cycles until fracture.

Eq.(6.5.18) applies for wood at frequencies above about one Hz (up to 10^4 Hz). For cases where peak-stresses play a role, as at knots, in particle board and at finger joints, it can be deduced from the regression lines, given in [7], that the empirical fatigue equation is:

$$\frac{\sigma}{\sigma_0} = 1.14 - 0.103 \cdot \log(n) \qquad (6.5.20)$$

Eq.(6.5.19) applies for wood below about 0.1 Hz. Depending on the frequency, fracture may occur in a few cycles. However, this equation can be written in the total time to failure t:

$$\frac{\sigma}{\sigma_0} = 1 - \frac{1}{\varphi\sigma_0}\ln(\nu t/\nu t_0) = 1 - \frac{1}{\varphi\sigma_0}\cdot\ln(t/t_0) \qquad (6.5.21)$$

and this equation is identical to the long duration strength of a specimen loaded by a constant load, equal to the top value of the fatigue loading. The equation of this long duration strength is:

$$\frac{\sigma}{\sigma_0} = 1.17 - 0.070 \cdot \log(t), \qquad (6.5.22)$$

showing that the slope of the high frequency line is indeed about a factor 1.5 steeper. Or more precise: 0.103/.070 = 1.47. If there is a stress level where below there is no fatigue or no failure for long term loading, then the maximum strain condition predicts that this level will be a factor 1.47 lower for high frequency loading. Beause the stress level for no damage at long term loading is supposed to be 0.5, the fatigue level is about 0.5/1.47 = 0.35. This is in agreement with the expectation from tests on rotorblades (NASA).

For very low frequencies (lower than about 10^{-6} Hz), recovery may occur at the period of unloading and only the sum of the loading times have to be taken for t in eq.(6.5.22). So it is seen that at least half of the "permanent" strain at higher stress levels is recoverable.

For a small initial flow unit density: $A = B\varepsilon_v$, the analysis is comparable as done before and as done for static loading.

$$\sigma_v = \frac{1}{\varphi}\cdot\ln\left(\frac{2\dot{\varepsilon}_v}{B\varepsilon_v}\right) = K_1(\varepsilon - \varepsilon_v) \text{ or: } 2\dot{\varepsilon}_v = B\varepsilon_v \cdot e^{\varphi K_1 \varepsilon} - \varphi K_1 \varepsilon_v \text{ or:}$$

$$(e^{\varphi K_1 \varepsilon_v})\cdot d\ln(\varphi K_1 \varepsilon_v) = \left(\frac{B}{2}\cdot e^{\varphi K_1 \varepsilon}\right)\cdot dt.$$

So:

$$E_i(\varphi K_1 \varepsilon_v) - E_i(\varphi K_1 \varepsilon_{v0}) = \frac{n}{2} \cdot \int_0^{t_c} B \cdot e^{\varphi K_1 \varepsilon} \cdot dt = n \cdot C_1$$

or:

$$\varphi K_1 \varepsilon_v = E_i^{-1}(n \cdot C_1 + 0.577 + \ln(\varphi K_1 \varepsilon_{v0})) \qquad (6.5.23)$$

and there is a delay time for fatigue. The fatigue line starts with a small slope and bends down at higher values of n to a straight line on log(n)-scale. Because for higher values of ε_v and n, this equation becomes:

$$\exp(\varphi K_1 \varepsilon_v) = \varphi K_1 \varepsilon_v \cdot (n \cdot C_1 + 0.577 + \ln(\varphi K_1 \varepsilon_{v0}))$$

or:

$$\varphi K_1 \varepsilon_v = \ln(\varphi K_1 \varepsilon_v) + \ln\left(C_1 \cdot (n - n_1) \cdot e^{-\varphi K_1 \varepsilon_{v0}}\right) + \varphi K_1 \varepsilon_{v0} \quad \text{or:}$$

$$\varphi K_1 \varepsilon_v = \varphi K_1 \varepsilon_{v0} + \ln\left(\frac{n - n_1}{n_0}\right), \qquad (6.5.24)$$

the same fatigue equations occur as given before, however in a shifted position on the log(n)-axis.

A delay time is not to be expected for particle board, because of the high concentration of holes. Knots in timber act however as flow units with a low density, as can be seen by the yield drop in a constant strain rate test, and timber will show a delay time for fatigue.

6.6 References

[1] Rheology, Theory and Applications. T. Ree, H. Eyring 1958 New York.

[2] Influence of Heat on Creep of Dry D.-Fir. E.L. Schaffer For. Prod. Lab. Madison, Wisconsin.

[3] Studies on Dynamic Torsional Viscoelasticity of Wood, H. Becker, D. Noack, Wood Science and Technology Vol. 2 (1968) p. 213-230.

[4] Softening of fibre components in hot pressing of fibre mats, N. Takamura, Journ. Japan Wood Res. Soc. 14 (4) p. 75-79 (1968).

[5] R.J. Hoyle, M.C. Griffith, R.Y. Itany, 1985, Wood and Fiber Science, July 1985 V.17.

[6] Rheology and the study of wood, R.E. Pentoney, R.W. Davies, For. Prod. Journ. May 1962, p. 248.

[7] J.P. McNatt, Wood Science 11, 1979, 1.

[8] The effect of temperature on torsional stress relaxation of wet Hinoki wood, H. Urakami, K. Nakato, Proc. of the 14 th meeting of the J.W. Res. Soc. Tokyo, Apr. 1964.

.IE MECHANO-SORPTIVE EFFECT

of moisture content at low stresses

oisture content or moisture gradient, moisture acts as lubri-
ng the relaxation time of wood. At changing moisture content,
.our of adjacent layers can be very different because one layer
ink and the other may elongate, causing high internal stresses.
.e description of the mechano-sorptive effect the strain rate is split-
.nto a part that acts by the constant part of the moisture content: $\dot{\varepsilon}_v$
.id an additional part $\dot{\varepsilon}_m$ that acts due to the changing part of the moisture content. For relaxation of the three-element model $\dot{\varepsilon} = 0$ and for the Maxwell element:

$$\dot{\varepsilon} = \dot{\varepsilon}_e + \dot{\varepsilon}_v + \dot{\varepsilon}_m = 0. \tag{7.1}$$

At changing moisture content conditions there is a rapid reaction of water with the hydrogen bonds. So a low activation energy and volume can be expected and the equation for relaxation may be approximated to:

$$\dot{\sigma}_1 + K_1 A \sinh(\varphi\sigma_1) + K_1\dot{\varepsilon}_m \approx \dot{\sigma}_1 + K_1 A'\omega\varphi\sigma_1 + K_1\dot{\varepsilon}_m = 0. \tag{7.2}$$

$\dot{\varepsilon}_m$ is proportional to ω, when ω is changing and proportional to the loading σ_1. So at low stresses is: $\dot{\varepsilon}_m = c\sigma_1 K_1 \varphi A'\omega$ and the equation becomes:

$$\dot{\sigma}_1 + \alpha K_1 A'\omega\varphi\sigma_1 = 0, \quad \text{with } \alpha = 1 + c \tag{7.3}$$

and it is assumed that there is no swelling or that the strain rate is directed in such a way that it follows the free swelling rate in order to get true relaxation. For creep the same equation applies with K_1 replaced by K ($1/K = 1/K_1 + 1/K_2$). The solution of eq.(7.3) is:

$$\ln\left(\frac{\sigma}{\sigma_0}\right) = -K_1\alpha A\varphi t = -K_1\alpha A'\omega\varphi t \tag{7.4}$$

where ω is the suddenly applied difference in moisture concentration. This equation is based on the bond breaking process and can also be obtained by the starting rate equation of bond breaking:

$$\dot{\rho} = -k\rho\omega \tag{7.5}$$

where ρ is the concentration of mobile bonds, having as solution:

$$\ln\left(\frac{\rho}{\rho_0}\right) = -k\omega t \tag{7.6}$$

and it is seen that this result is identical to eq.(7.4). So the stress supported by the reactive bonds is proportional to the number of bonds and the ratio ρ/ρ_0 can be determined from the stress relaxation test (or from a creep tests).

These equations apply for very thin specimens. For thicker specimens the moisture has to diffuse into the specimen. From Fick's second law the concentration rate for a long, round specimen is:

$$\frac{d\omega}{dt} = D\left(\frac{\partial^2\omega}{\partial r^2} + \frac{1}{r}\frac{\partial\omega}{\partial r}\right). \tag{7.7}$$

The solution of this equation is [1]:

$$\frac{\omega}{\omega_0} = 1 - \frac{4}{d}\sum_{n=1}^{\infty}\frac{J_0(\psi_n r)}{\psi_n J_1(\psi_n d)}\exp\left(-\frac{4D\psi_n^2}{d^2}t\right), \tag{7.8}$$

where ω_0 is the concentration surrounding the specimen, D is the diffusion coefficient, ψ_n is the n-th root of the zero-order Bessel function, d the diameter of the specimen and J_n is the Bessel function of the order n. Because the stress relaxation in tension or compression depends on the mean stress in the specimen, only the mean concentration is of importance. So the average concentration is:

$$\bar{\omega} = \frac{4}{d^2\pi}\int_0^{d/2} 2\pi\omega r\,d(r) = \omega_0\left[1 - \sum_{n=1}^{\infty}\frac{4}{\psi_n^2}\exp\left(-\frac{4D\psi_n^2}{d^2}t\right)\right]. \tag{7.9}$$

Substituting $\bar{\omega}$ in eq.(7.3) or eq.(7.5) will give the measured stress- or bond decay. Because only the first term of the summation is of importance and the other terms may be neglected:

$$\ln\left(\frac{\rho}{\rho_0}\right) = -k\omega_0\left[t + \frac{d^2}{D\psi_1^4}\left\{\exp\left(-\frac{4D\psi_1^2}{d^2}t\right) + c_1\right\}\right], \tag{7.10}$$

or for the stress with $c_1 = -1$ as boundary condition:

$$\ln\left(\frac{\sigma}{\sigma_0}\right) = -K_1A'\varphi\omega_0\left[t + \frac{d^2}{D\psi_1^4}\left\{\exp\left(-\frac{4D\psi_1^2}{d^2}t\right) - 1\right\}\right]\alpha, \tag{7.11}$$

where $\psi_1 = 2.405$ is the first root of the Bessel function.

For long times the exponential function is approximately zero so this line becomes:

$$\ln\left(\frac{\sigma}{\sigma_0}\right) = -K_1A'\varphi\omega_0\left[t - \frac{d^2}{D\psi_1^4}\right]\alpha. \tag{7.12}$$

The intercept of this line with the time axis is thus: $d^2/D\psi_1^4$ showing the time lag due to diffusion. This equation applies exactly for p.e. human hair [1], where there is no swelling or shrinking during wetting and drying. At moistening the stress quickly dropped to about 1/3 of the applied value. At drying the stress totaly restores to the initial level before wetting in the relaxation tests. So this work is due to the chemical energy of bond reformation and there is no need to search for any other source of energy as is done for wood, where the slight restoring of the stress at moistening is attributed to the heat of diffusion.

Tests with alkali hydroxide solutions on cotton, that has a comparable structure as wood, showed an instantaneous relaxation as rapidly as the solution could be added. After that, a slower process occured of convertion of the crystalline regions into an amorphous structure. The instantaneous stress reduction indicates a very fast reaction where equilibrium is directly reached according to the reaction:

$$\omega + \rho \underset{k_b}{\overset{k_f}{\rightleftharpoons}} (\rho_0 - \rho)$$

or:

$$-\dot{\rho} = \rho\omega k_f - k_b(\rho_0 - \rho) = 0 \qquad (7.13)$$

or:

$$\omega = \frac{k_b}{k_f}\cdot\frac{\rho_0 - \rho}{\rho} = \frac{k_b}{k_f}\cdot\frac{\Delta\rho/\rho_0}{1 - \Delta\rho/\rho_0} \qquad (7.14)$$

where $\Delta\rho/\rho_0 = (\rho_0 - \rho)/\rho_0$. So $\Delta\rho/\rho_0$ is about proportional to ω ($\Delta\rho/\rho_0 << 1$), but this relation bends off to a limiting value at high values of ω according to the measurements [1] and eq.(7.14). The limiting value for alkali hydroxides at high concentration seems to approach unity according to eq.(7.14), indicating that the structure of cotton may be completely accessible for alkali reagents. This reaction with both the amorphous and crystalline regions followed also from X-ray diffraction experiments. Because $\Delta\rho$ is not noticeble dependent on the temperature, the enthalpy will be small.

For strong acids $\Delta\rho/\rho_0$ approaches a limitting value well below 1, being of the same order as the quantity of disordered regions as follows from X-ray measurements. So $(\Delta\rho/\rho_0)_{lim}$ can be expected to be a direct measure of the accessibility of the amorphous regions. The linear increasing value of $(\Delta\rho/\rho_0)_{lim}$ with the temperature increase shows the equilibrium between ordered and disordered regions. The equilibrium constant K is:

$$K = (k_f \omega_m / k_b) = \frac{(\Delta\rho/\rho_0)_{lim}}{1 - (\Delta\rho/\rho_0)_{lim}} \qquad (7.15)$$

and the energy of cellulose conversion is: $E_f - E_b = - RT \cdot \ln(K)$, what was found to be 4 kcal/mol. The same can be expected for wood. Because acids effect only the amorphous regions and because the limiting value of the instantaneous reduction is far below 1, there is no cross section totally disordered and the ordered region is the continuous phase.

The nature of the reagents and the rapidlity of the reactions indicate an attack of secondary bonds, so probably the hydrogen bonds between the cellulose chains. After removal of the reagents, some types of bonds are inable to move back against the force to assume their original positions, but combine with new neighbours in a relaxed position.

The influence of water on the hydrogen bonds is comparable with the influence of acids because only the amorphous regions are effected and $\Delta\rho_0/\rho$ will be proportional to ω. Although there is an immediate reaction with water, there is no instantaneous stress drop in a relaxation test because the water has to diffuse into the structure and the rate of diffusion determines the reaction rate with the hydrogen bonds. There is thus an equilibrium and any change of moisture content gives a reaction close to the equilibrium at the rate of the moisture supply. For the reaction near equilibrium (after longer times for wood), eq.(7.13) becomes:

$$- \dot{\rho} = \rho\omega k_f - k_b(\rho_0 - \rho) = \rho k_f(\omega - \omega_0), \qquad (7.16)$$

where: $\omega_0 = k_b(\rho_0 - \rho)/(k_f \rho)$ is the equilibrium moisture content (where $\dot{\rho} = 0$).

Eq.(7.9), for a moisture increase from zero to ω_0, is, for the first expanded term, with a rounding off to account for the other terms, to be approximated to:

$$\bar{\omega} = \omega_s(1 - \exp(- at)), \qquad (7.17)$$

where $a = 4D\psi_1^2/d^2 = 23D/d^2$, and ω_s is the maximal amount of adsorbed water.

For a loaded test specimen with a moisture content ω_0 that is placed in a dry environment causing a moisture content of $\omega_0 - \omega_s$ after long time, eq.(7.17) modifies to:

$$\bar{\omega} = \omega_0 - \omega_s + \omega_s \exp(- at) \qquad (7.18)$$

and the solution of eq.(7.5), that applies in the first stage, becomes:

$$\ln(\rho/\rho_0) = -k(\omega_0 - \omega_s)t + \frac{k}{a}\omega_s\left(\exp(-at) - 1\right) \tag{7.19}$$

or with eq.(7.18):

$$\ln(\rho/\rho_0) = \ln(\rho'/\rho'_0) - \frac{k}{a}(\omega_0 - \omega) \tag{7.20}$$

where: $\ln(\rho'/\rho'_0) = -k(\omega_0 - \omega_s)t$ is the relaxation (or creep) at the constant equilibrium moisture content $\omega_0 - \omega_s$. The same solution is obtained from eq.(7.3) and the equations can be read by replacing ρ by σ and with $k = K_1 A'\varphi\alpha$ for relaxation and $k = KA'\varphi\alpha$ for creep. So eq.(7.20) for desorption becomes:

$$\ln(\sigma/\sigma_0) = \ln(\sigma'/\sigma'_0) - \frac{k}{a}(\omega_0 - \omega). \tag{7.21}$$

It is seen that: $\ln\left(\frac{\sigma'}{\sigma'_0}\cdot\frac{\sigma_0}{\sigma}\right) = c(\omega_0 - \omega)$ is a straight line, that is the same as given in [2] and fig. 7.1. Here: $\omega_0 - \omega$ the amount of desorbed water.

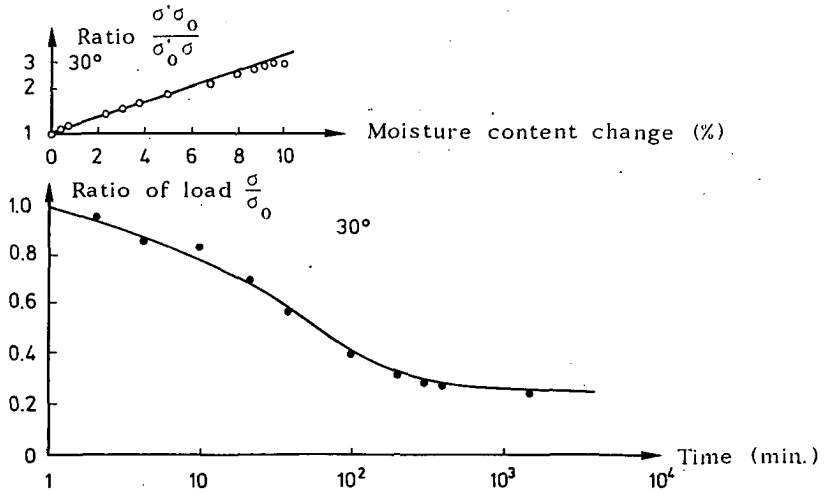

fig. 7.1 Comparison of the theoretical equation (7.21) with measurements of [2]

For adsorption, when a loaded test specimen with a moisture content ω_0 is placed in a wet environment causing a moisture content of ω_1 after long time, eq.(7.17) modifies to:

$$\bar{\omega} = \omega_1 - (\omega_1 - \omega_0)\cdot\exp(-at) \tag{7.22}$$

and the solution of eq.(7.5) is:

$$\ln(\rho/\rho_0) = - k\omega_1 t - \frac{k}{a}(\omega_1 - \omega_0)\cdot\left(\exp(- at) - 1\right) \tag{7.23}$$

or:

$$\ln(\rho/\rho_0) = - k\omega_1 t + \frac{k}{a}(\omega - \omega_0) \tag{7.24}$$

or:

$$\ln(\rho/\rho_0) = \ln(\rho'/\rho'_0) + \frac{k}{a}(\omega - \omega_0) \tag{7.25}$$

where: $\ln(\rho'/\rho'_0) = - k\omega_1 t$, is the relaxation at constant maximum moisture content ω_1. This equation is identical to eq.(7.20) if the adsorbed amount: $\omega - \omega_0$ can be regarded as a negative desorption. Eq.(7.20) shows that there is an increase of deformation on drying and eq.(7.31) shows a restoring of the bond structure on rewetting. So there is at least one dominating element with an opposed behaviour to other materials.
For the derivation of this effect a three element model was used consisting of a Maxwell element (i. e. a spring with a dashpot) and a parallel spring. The possible nearly total unloading in a relaxation test by a high moisture change as shown in fig. 7.1 (for a low change), demonstrates that both springs have dashpots. There may be another very weak parallel spring if there is hardening, but this can be neglected as a first approximation and the behaviour can be described by two parallel Maxwell elements. The small deviation of the measurements from the straight line eq.(7.21) in fig. 7.1 at very low moisture changes shows that there is a second process besides the dominating process. The deviation at higher moisture changes shows the departure from the linear approach eq.(7.3). This will also be so for high stresses.

7.2 Influence of high stresses and moisture changes

Interesting for mechanosorptive effects is creep loading at sufficient high stresses where sinh(x) can be approached by (exp(x))/2. The strain rate equations for the two nonlinear Maxwell elements 1 and 2 are then:

$$\dot{\varepsilon} = \frac{\dot{\sigma}_1}{K_1} + A'_1 \frac{\omega}{2}\exp(\varphi_1\sigma_1) + \dot{\varepsilon}_m \tag{7.26}$$

$$\dot{\varepsilon} = \frac{\dot{\sigma}_2}{K_2} + A'_2 \frac{\omega}{2}\exp(\varphi_2\sigma_2) - \dot{\varepsilon}_m \tag{7.27}$$

where the material is devided in two types of layers, one with mechanosorptive slip ε_m at desorption and recovery at adsorption, and one with the more common reversed behaviour.

Elimination of $\dot{\varepsilon}$ from eq.(7.26) and eq.(7.27) gives:

$$\frac{\dot{\sigma}_1}{K} + A'_1 \cdot \frac{\omega}{2} \cdot \exp(\varphi_1 \sigma_1) - A'_2 \cdot \frac{\omega}{2} \cdot \exp(\varphi_2 \sigma_2) + 2\dot{\varepsilon}_m = 0 \qquad (7.28)$$

where $1/K = 1/K_1 + 1/K_2$ and $2\dot{\varepsilon}_m$ is the relative strain rate of the layers $\dot{\varepsilon}_r$. Because the process is a matter of side bonds breaking it can be assumed that the sites of the parts are the same as for the compound layer for the mechano- sorptive effect, or: $\varphi_1 = \varphi_2 = \varphi$, and eq.(7.28) becomes ($\sigma_2 = \sigma - \sigma_1$):

$$\frac{\dot{\sigma}_1}{K} + \frac{\omega}{2} e^{\varphi\sigma/2} C\left(e^{\varphi\sigma_1 - \varphi\sigma/2 + \ln(\beta)} - e^{-\varphi\sigma_1 + \varphi\sigma/2 - \ln(\beta)} \right) + 2\dot{\varepsilon}_m = 0$$

where $C = \sqrt{A'_1 A'_2}$, and $\beta = \sqrt{A'_1 / A'_2}$. So:

$$\frac{\dot{\sigma}_1}{K} + e^{\varphi\sigma/2}\, \omega \sqrt{A'_1 A'_2} \cdot \sinh\left(\varphi\sigma_1 - \varphi\sigma/2 + \ln\left(\sqrt{A'_1 / A'_2}\right)\right) + 2\dot{\varepsilon}_m = 0. \qquad (7.29)$$

The mechanosorptive rate of bondbreaking has the form: $\dot{\varepsilon}_m = A\sinh(\varphi\sigma) \approx A\varphi\sigma$ for small stresses as used before. For high stresses is: $\dot{\varepsilon}_m \approx \frac{A}{2}\exp(\varphi\sigma)$. This rate is zero for constant moisture content and is proportional to the rate of change of the moisture content.
So $2\dot{\varepsilon}_m$ can be given in the form:

$$2\dot{\varepsilon}_m \approx \frac{\dot{\omega}}{a} \sqrt{A'_1 A'_2} \cdot \frac{1}{2} \exp\left(\frac{\varphi\sigma}{2} + c\right) \approx \frac{\dot{\omega}}{a} \sqrt{A'_1 A'_2} \cdot \exp\left(\frac{\varphi\sigma}{2}\right) \sinh(c). \qquad (7.30)$$

With: $\omega = \omega_0 + (\omega_e - \omega_0) \cdot (1 - e^{-at})$ is: $\omega = \omega_e - \frac{\dot{\omega}}{a}$, and eq.(7.29) can be splited in a creep equation for the part of constant moisture content ω_e:

$$\frac{\dot{\sigma}_1}{K} + e^{\varphi\sigma/2} \cdot \omega_e \sqrt{A'_1 A'_2} \cdot \sinh\left(\varphi\sigma_1 - \varphi\sigma/2 + \ln\left(\sqrt{A'_1 / A'_2}\right)\right) = 0, \qquad (7.31)$$

and in a mechanosorptive change:

$$\frac{\dot{\sigma}_1}{K} - e^{\varphi\sigma/2} \frac{\dot{\omega}}{a} \sqrt{A'_1 A'_2} \cdot \sinh\left(\varphi\sigma_1 - \varphi\sigma/2 + \ln\left(\sqrt{A'_1 / A'_2}\right)\right) + 2\dot{\varepsilon}_m = 0. \qquad (7.32)$$

Substitution of eq.(7.30) in eq.(7.32) shows that a particular solution of eq.(7.32) is:

$$\varphi_1 \sigma_1 = \frac{\sigma\varphi}{2} - \frac{1}{2} \ln\left(A'_1 / A'_2\right) + c. \qquad (7.33)$$

The general part of this equation is:

$$\frac{\dot{\sigma}_1}{K} - e^{\varphi\sigma/2} \frac{\dot{\omega}}{a} \sqrt{A'_1 A'_2} \cdot \sinh\left(\varphi\sigma_1 - \varphi\sigma/2 + \ln\left(\sqrt{A'_1 / A'_2}\right)\right) = 0$$

and the integration of this equation has the form:

$$\int \frac{d(x)}{\sinh(x)} = + \frac{C}{a}\int \dot{\omega} d(t), \qquad \text{or with: } \frac{\dot{\omega}}{a} = -(\omega_0 - \omega_e)(e^{-at}):$$

$$\ln(\tanh(x/2)) = C\left(\frac{\omega_0 - \omega_e}{a} e^{-at}\right) + C_1$$

or in terms of eq.(7.32) this becomes:

$$\ln\left(\tanh\left(\frac{\varphi\sigma_1}{2} - \frac{\varphi\sigma}{4} + \frac{1}{4}\ln(A'_1/A'_2)\right)\right) = C_1 - \varphi K e^{\sigma\varphi/2}\sqrt{A'_1 A'_2}\left(\frac{\omega_e - \omega_0}{a} e^{-at}\right). \tag{7.34}$$

Calling $p = \varphi K e^{\sigma\varphi/2}\sqrt{A'_1 A'_2}\cdot(\omega_0 - \omega_e)\frac{e^{-at}}{a} = \varphi K e^{\sigma\varphi/2}\sqrt{A'_1 A'_2}\cdot(\omega - \omega_e)$,

eq.(7.34) becomes:

$$\frac{\varphi\sigma_1}{2} - \frac{\varphi\sigma}{4} + \frac{1}{4}\ln(A'_1/A'_2) = \operatorname{arctanh}(\exp(p + C_1)) \tag{7.35}$$

and the total solution is:

$$\frac{\varphi\sigma_1}{2} - \frac{\varphi\sigma}{4} + \frac{1}{4}\ln(A'_1/A'_2) = \operatorname{arctanh}(\exp(p + C_1)) + \frac{c}{2}. \tag{7.36}$$

The value of C_1 follows from the initial value $\sigma_1 = \sigma_{10}$. For this case is:

$$\ln\left(\tanh\left(\frac{\varphi\sigma_{10}}{2} - \frac{\varphi\sigma}{4} + \frac{1}{4}\ln(A'_1/A'_2) - \frac{c}{2}\right)\right) - p_0 = C_1. \tag{7.37}$$

Substitution of eq.(7.37) in eq.(7.36) gives:

$$\frac{\varphi\sigma_1}{2} - \frac{\varphi\sigma}{4} + \frac{1}{4}\ln(A'_1/A'_2) - \frac{c}{2} =$$

$$= \operatorname{arctanh}\left(\tanh\left(\frac{\varphi\sigma_{10} - \varphi\sigma_{20} + \ln(A'_1/A'_2) - 2c}{4}\right)\cdot e^{\varphi K\sqrt{A'_1 A'_2}\cdot e^{\varphi\sigma/2}(\omega - \omega_0)/a}\right). \tag{7.38}$$

Calling: $q = \frac{\varphi\sigma_1}{2} - \frac{\varphi\sigma}{4} + \frac{1}{4}\ln(A'_1/A'_2) - \frac{c}{2}$, then this equation becomes:

$$q = \operatorname{arctanh}(\tanh(q_0)\cdot e^{\varphi K\sqrt{A'_1 A'_2}\cdot e^{\varphi\sigma/2}(\omega - \omega_0)/a}).$$

For small values of q_0 this becomes: $q = q_0 \cdot e^{\varphi K\sqrt{A'_1 A'_2}\cdot e^{\varphi\sigma/2}(\omega - \omega_0)/a}$

or:

$$\varphi\sigma_1 = \varphi\sigma_{10} + \frac{1}{2}\left(\varphi\sigma_{20} - \varphi\sigma_{10} - \ln(A'_1/A'_2) + 2c\right)\cdot\left(1 + \right.$$

$$\left. - e^{\varphi K\sqrt{A'_1 A'_2}\cdot e^{\varphi\sigma/2}(\omega - \omega_0)/a}\right). \tag{7.39}$$

For high values of q is $\tanh(q) \approx 1$, and:

$$q \approx \operatorname{arctanh}\left(e^{\varphi K\sqrt{A'_1 A'_2}\cdot e^{\varphi\sigma/2}(\omega - \omega_0)/a}\right),$$

and because: $\operatorname{arctanh}(e^x) = 0.5\cdot\ln\left(\frac{1+e^x}{1-e^x}\right) = 0.5\cdot\ln(\coth(-x/2))$ is:

$$\frac{\varphi\sigma_1}{2} - \frac{\varphi\sigma}{4} + \frac{1}{4}\ln(A'_1/A'_2) - \frac{c}{2} = -\frac{1}{2}\ln\left(\tanh\left(\varphi K\sqrt{A'_1A'_2}\cdot e^{\varphi\sigma/2}(\omega_0 - \omega)/2a\right)\right). \tag{7.40}$$

For not to high moisture changes this becomes:

$$\frac{\varphi\sigma_1}{2} - \frac{\varphi\sigma}{4} + \frac{1}{4}\ln(A'_1/A'_2) - \frac{c}{2} = -\frac{1}{2}\ln\left(\varphi K\sqrt{A'_1A'_2}\cdot e^{\varphi\sigma/2}(\omega_0 - \omega)/2a\right) \tag{7.41}$$

and for high values of: $\varphi K\sqrt{A'_1A'_2}\cdot e^{\varphi\sigma/2}(\omega_0 - \omega)/2a$, eq.(7.40) turns to:

$$\frac{\varphi\sigma_1}{2} - \frac{\varphi\sigma}{4} + \frac{1}{4}\ln(A'_1/A'_2) - \frac{c}{2} \approx 0. \tag{7.42}$$

This is also the limit of eq.(7.39) for high moisture changes at small stresses q_0.

According to eq.(7.30) is:

$$\frac{c}{2} + \frac{\sigma\varphi}{4} = \frac{1}{2}\ln\left(\frac{4\dot{\varepsilon}_m{}^a}{\dot{\omega}\sqrt{A'_1A'_2}}\right) \tag{7.43}$$

and the maximal mechanosorptive stress σ_1 of eq.(7.42) is:

$$\varphi\sigma_1 = \ln\left(\frac{4\dot{\varepsilon}_m{}^a}{\dot{\omega}A'_1}\right). \tag{7.44}$$

For high moisture changes (p.e. ω_0 maximal and $\omega_e \approx 0$) this is ($\dot{\varepsilon}_r = 2\dot{\varepsilon}_m$)

$\varphi\sigma_1 = \ln\left(\frac{4|\dot{\varepsilon}_m|}{A_1}\right)$ and this is at the level of the flow stress:

$\varphi\sigma_1 = \ln\left(\frac{2\dot{\varepsilon}_r}{A_1}\right)$ of element I (see for instance eq.(5.2.16)).

So flow of the elements limits the maximal possible mechano-sorptive stress.

An other aspect of eq.(7.44) is that: A_1/a is proportional to: $\exp(-E_1/kT + E_d/kT)$ and the activation energy of the process is the difference of the activation energy for creep and for diffusion, explaining a low retardation time or an high rate of the process.

7.3 Simplification of the model

In order to avoid complex calculations for creep at high moisture cycling and at higher stresses it is sufficient to neglect the logarithmic creep and to use the property of the non-linear Maxwell elements of an approxi-

mate elastic-full plastic behaviour. This model can be compared with the model of [3] that consists of two parallel strings each consisting of a Maxwell element and a Voigt element in series. This is totally equivalent to a model with four parallel Maxwell elements and these four parallel Maxwell elements can be replaced by two parallel Maxwell elements with non-linear dashpots, because those dashpots contain one more parameter than the linear dashpots. So it is seen that each of the two strings can be replaced by a spring attached to a non-linear dashpot as was assumed for the derivation of the sorption equations. The loading of the two parallel strings in a creep test in the model of [3] was done by a running block that moved the total load between the strings by means of a hygroscopic element. This block may however be removed because this sorption effect is given by eq.(7.20) or (7.39) and the behaviour of the hygroscopic material is exactly the same as can be seen in eq.(7.19) where the part: $(k\omega_s/a)(1 - \exp(- at)$ is identical to the time function of that element. The swelling and shrinkage is proportional to the adsorbed amount of water and has also this form: $\omega = \omega_s \cdot (1 - \exp(- at))$. In the model of [3] it is also assumed that the viscoelastic constants change according to this function, however eq.(7.19) and eq.(7.31) show immidiate creep at the equilibrium moisture content of the end state and also this changing constants function may be removed. In [3] it is assumed that there are two diffusion processes, one slow process of sorption, eliminating the differential shrinking with $a = 23D/d^2 = 0.06$, and one quick process with $a = 0.5$ effecting the load bearing bonds. In most tests the change of moisture content is slow and the result has to be regarded as a succession of end states due to these two processes. The influence of the slow process can be eliminated by subtracting the strains of the dummy from the strains of the loaded specimen at moisture cycling.

In the following scheme the influence of moisture cycling is given where the two elastic- plastic elements consist of: II, the layers with a dominating slip at desorption and I, layers with a pronounced slip at adsorption.

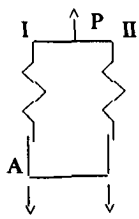

initial loading of element I and II: $P = P_1 + P_2$

The mechano-sorptive forces can be divided in a part that eliminates the differential shrinking and a part that interacts with the loading as done in [3]. In an unloaded dummy only the first part is working.
For an initial wet unloaded specimen, the first drying cycle will give the following forces:

I	II	
$P_{m2}\uparrow$	$\downarrow P_{m2}$	slip due to desorption in II.
$P_{m1}\downarrow$	$\uparrow P_{m1}$	recovery of slip in I.
$P_s\downarrow$	$\uparrow P_s$	force due to differential shrinking of I.

The differential shrinking: δ_{sh} will cause the shrinking force: P_s
The strain: δ of element I will be the same of element II. So:

$$\left.\begin{array}{ll} \text{I:} & \delta = -\delta_{sh} + P_s/K_1 - \delta_\alpha \\ \text{II:} & \delta = -P_s/K_2 - \delta_\alpha \end{array}\right\} \rightarrow P_s\left(\frac{1}{K_1} + \frac{1}{K_2}\right) = \delta_{sh}$$

where δ_α is the free shrinking of the specimen.
In II there will be a slip: δ_{m1} at drying in the direction of the compressive force P_s and the mechano-sorptive force P_{m2} will be against this force. In I there will be recovery of extentional slip: $-\delta_{m1}$ and a force P_{m1} in the direction of the tensile force P_s. So:

$$\left.\begin{array}{ll} \text{I:} & \delta = -\delta_{sh} + P_s/K_1 - \delta_\alpha + P_{m1}/K_1 - P_{m2}/K_1 - \delta_{m1} \\ \text{II:} & \delta = -P_s/K_2 - \delta_\alpha - P_{m1}/K_2 + P_{m2} - \delta_{m2} \end{array}\right\} \therefore (P_{m2} - P_{m1})\left(\frac{1}{K_1} + \frac{1}{K_2}\right) = \delta_{m2} - \delta_{m1}.$$

It is possible that the mechano-sorptive forces eliminate the shrinking forces if drying is slow enough for interaction. Then: $P_s + P_{m1} - P_{m2} = 0$

$$\left.\begin{array}{ll} \text{I:} & \delta = -\delta_{sh} - \delta_{m1} - \delta_\alpha \\ \text{II:} & \delta = -\delta_{m2} - \delta_\alpha \end{array}\right\} \rightarrow \delta_{m1} = \delta_{m2} - \delta_{sh}$$

and δ_{m1} is limited by the amount: δ_{sh}.
For a loaded specimen the mechano-sorptive force can be divided in the part that occurs in the dummy and the part that interacts with the external forces. In the following the corrected strains, by subtraction of the dummy values, will be regarded. This will be compared with the measured values of [4] for compression that has the strongest mechano-sorptive mechanism with plastic deformations. The following scheme is for drying at compression.

I	II	
$P_1 \downarrow$	$\downarrow P_2$	initial values
$P_m \downarrow$	$\uparrow P_m$	sortive bond breaking causing slip: $-\delta_{m2}$ in II, and a resultant flow δ_f in element II. $P_m = P_{m1} + P_{m2}$.
$P'_1 \downarrow$	$\downarrow P'_2$	Total forces: $P'_1 = P_{u1}$, the flow stress of elementI and: $P'_2 = P - P_{u1}$. So: $P_m = P_{u1} - P_1$.

The initial deformation by the external loading: $P = P_1 + P_2$ is:

$$\delta_0 = P_1/K_1 = P_2/K_2 = \frac{P}{K_1 + K_2}$$

As can be seen in fig. 7.2, P_m will cause a deformation of: $4\delta_0$. So:

$$\text{I: } -4\delta_0 = -\frac{P_{u1} - P_1}{K_1} - \delta_f$$

$$\text{II: } -4\delta_0 = \frac{P_{u1} - P_1}{K_2} - \delta_{m2}$$

The loading level is about 40 %. So $P_{u1}/K_1 = P_{u2}/K_2 = P_u/(K_1 + K_2) \approx$ $\approx 2.5\delta_0$. So:

$$\text{I: } -2.5\delta_0 + \delta_0 - \delta_f = -4\delta_0 \quad \rightarrow \quad \delta_f = 2.5\delta_0 \qquad (7.45)$$

$$\text{II: } (K_1/K_2)(2.5\delta_0 - \delta_0) - \delta_{m2} = -4\delta_0 \rightarrow \quad \delta_{m2} = 4\delta_0 + 1.5\delta_0(K_1/K_2) \qquad (7.46)$$

On rewetting the specimen, after the first drying cycle, P_m changes of sign and the forces will be:

I	II	
$P_{u1} \downarrow$	$\downarrow P - P_{u1}$	initial values
$P_m \uparrow$	$\downarrow P_m$	elastic forces by slip and flow
$P'_1 \uparrow$	$\downarrow P'_2$	Total forces: $P'_1 = P_m - P_{u1}$ (= P_{u1} for low loading giving flow back of I). $P'_2 = P - P_{u1} + P_m$ (= P_{u2} for high loading giving flow of II).

For low loading, element I may flow back and the strain at the end of the cycles show little or no change as mentioned in [4] for compression at the loading level of 24%. For higher loadings P'_2 may reach P_{u2}. Then there is an increase in flow and slip in each cycle and the maximum deformation will not tend to a limiting value but increases until fracture. This is also known from measurements for instance in [5] for bending. Fig. 7.3 suggest that P'_2 may just have reached P_{u2} and the increase of deformation after each cycle is determined by the creep part for constant ω_e. It may be assumed that there is one limit for flow forwards and back-

wards and also P'_1 just reaches P_{u1}. Then:

$P'_1 = P_{u1}$ and: $P = P_{u2} - P_{u1}$ and because: $P \approx 0.4P_u = 0.4(P_{u1} + P_{u2})$, is:

$1.4P_{u1} = 0.6P_{u2}$, or: $P_{u1} = 0.3P_u$ and $P_{u2} = 0.7P_u$,

and because the stiffness is proportional to the potential energy of the bonds it is to be expected that:

$$K_1 = 0.3K_t \text{ and } K_2 = 0.7K_t \qquad (7.47)$$

where $K_t = K_1 + K_2$.

According to eq.(7.46) is: $\delta_{m2} = 4\delta_0 + 1.5\delta_0(K_1/k_2) = \delta_0(4 + 1.5 \cdot 0.3/0.7) \approx$

$\approx 4.7\delta_0$.

The recovery of slip at rewetting is about $2.5\delta_0$ drifting to $2.7\delta_0$ (see fig. 7.2). Taking $2.6\delta_0$, the strains are with $P_m = 2P_{u1}$ or with $P_m/K_1 =$

$= 2P_{u1}/K_1 = 5\delta_0$:

$$\text{I: } \frac{P_m}{K_1} - \delta_{m1} \approx 2.6\delta_0 = 5\delta_0 - \delta_{m1} \rightarrow \delta_{m1} \approx 2.4\delta_0 \qquad (7.48)$$

$$\text{II: } -\frac{P_m}{K_2} + \delta_{m2} \approx 2.6\delta_0 = -\frac{K_1}{K_2}5\delta_0 + \delta_{m2} = \frac{0.3}{0.7} \cdot 5\delta_0 + \delta_{m2} \rightarrow$$

$$\delta_{m2} \approx 4{,}7\delta_0. \qquad (7.49)$$

It is seen that δ_{m2} is the same for drying as for rewetting. The difference $\delta_{m2} - \delta_{m1} \approx 2.3\delta_0$ is equal to the part δ_{m2} for the dummy that is used with opposed sign to eliminate the differential shrinking. So δ_{sh} is smaller than or equal to $2.3\delta_0$.

An analogous scheme for an initial dry specimen on first wetting is given below.

I	II	
$P_1 \downarrow$	$\downarrow P_2$	initial values.
$P_m \uparrow$	$\downarrow P_m$	elastic forces by internal slip and flow.
$P'_1 \uparrow$	$\downarrow P'_2$	Total forces: $P'_2 = P_{u2}$ causing flow of element II. $P'_1 = P_{u2} - P$. The change of the force is: $P_m = P_{u2} - P_2$.

The measured change of strain is $1.5\delta_0$ and if δ_m is the resultant slip and flow, this strain is:

$$\text{II: } 1.5\delta_0 = -\frac{P_{u2} - P_2}{K_2} + \delta_{m2}$$

$$\text{I: } 1.5\delta_0 = \frac{P_{u2} - P_2}{K_1} - \delta_{m1}.$$

This leads to:

II: $(-2.5 + 1)\delta_0 + \delta_{m2} = 1.5\delta_0 \quad \rightarrow \quad \delta_{m2} = 3\delta_0$ (7.50)

I: $(K_2/K_1)\cdot(2.5 - 1)\delta_0 - \delta_{m1} = 1.5\delta_0 \quad \rightarrow \quad \delta_{m1} = 2\delta_0$ (7.51)

These values of δ_m show that there is flow in both elements as also can be expected from the foregoing for this case of loading to the flow limit. So also P'_1 reaches P_{u1}. As a control, the equations are then:

$$\text{II:} \quad 1.5\delta_0 = -\frac{P_{u1} + P_1}{K_2} + \delta_{m2}$$

$$\text{I:} \quad 1.5\delta_0 = \frac{P_{u1} + P_1}{K_1} - \delta_{m1}$$

or: $1.5\delta_0 = \delta_0(2.5 + 1)\delta_0(0.3/0,7) + \delta_{m2} \rightarrow \delta_{m2} = 3\delta_0$ (7.52)

$1.5\delta_0 = 3.5\delta_0 - \delta_{m1} \quad \rightarrow \delta_{m1} = 2\delta_0$ (7.53)

as to be expected.

For redrying the specimen, after the first wetting cycle, the forces will be:

I	II	
$P - P_{u2} \downarrow$	$\downarrow P_{u2}$	initial values.
$P_m \downarrow$	$\uparrow P_m$	elastic forces by internal slip and flow.
$P'_1 \downarrow$	$\downarrow P'_2$	Total forces: $P'_1 = P_{u1}$ and becausee: $P'_1 = P - P_{u2} = -P_{u1}$, is $P_m = 2P_{u1} = 1.5P$.

The measured change of strain is $2,7\delta_0$, so with $K_1 = 0,3K_t$ and $K_2 = 0.7\ K_t$ the strains are:

$$\text{I:} \quad -\frac{P_m}{K_1} + \delta_{m1} = -\frac{1.5}{0.3}\delta_0 + \delta_{m1} = -2,7\delta_0 \quad \rightarrow \quad \delta_{m1} = 2.3\delta_0 \qquad (7.54)$$

$$\text{II:} \quad \frac{P_m}{K_2} - \delta_{m2} = \frac{1.5}{0.7}\delta_0 - \delta_{m2} = -2.7\delta_0 \quad \rightarrow \quad \delta_{m2} = 4.8\delta_0. \qquad (7.55)$$

The difference $\delta_{m2} - \delta_{m1} \approx 2.5\delta_0$ is equal to δ_{m2} of the dummy. Because the change of the strain of the dummy is also about $2.5\delta_0$ is P_{m1} of the dummy about zero and also δ_{m1} and δ_α will be zero. So the free swelling and shrinking δ_α can be neglected and de differential shrinking or swelling will be about: $\delta_{sh} \approx 2.5\delta_0$ in this case.

For tension the change of the strains is small and it is unlikely that flow occurs. The change of the strains can be analized with eq.(7.39) or eq. (7.42). A first attempt shows that it has to be assumed that the shrinking stresses are not eliminated by the mechano- sorptive mechanism. For bending the situation is complex because every layer has another plastic and elastic deformation and the tests, and a first analysis, show that

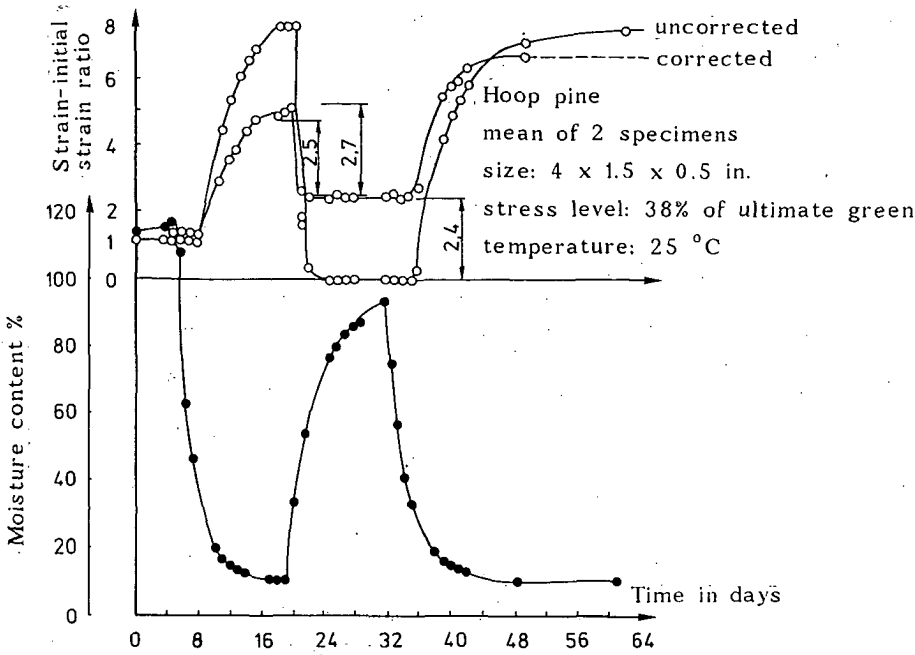

fig. 7.2 Strain ratio-time and moisture content-time curves for initially green compression specimens at moisture cycling [4].

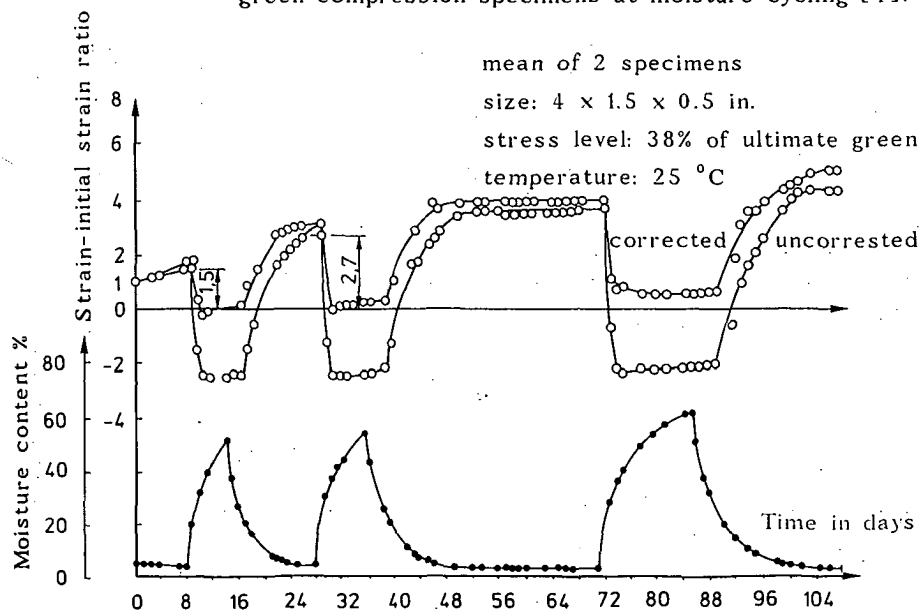

fig. 7.3 Strain ratio-time and moisture content-time curves at moisture cycling for compression, initially at 4% moisture content [4].

the leverarm between compression and tension will be strongly reduced by the different behaviour of the compression zone and the tension zone on moisture cycling.
It can be concluded that it is for the first time possible to describe the mechano-sorptive effect. The model predicts that for large dimensions of the test specimens, when $a = 23D/d^2$ is sufficient small there will be only a small force exchange between the layers and the sorption effect is of no importance.
Other publications on the subjects of chapter 6 and 7 can be found in [6] to [11].

7.4 References

[1] Deformation kinetics, A.S. Krausz, H. Eyring 1975 John Wiley & Sns.
[2] Plastic properties of wood in relation to the non-equilibrium states of moisture content, T. Takemura, Mem. Coll. Agric., Kyoto Univ., No 88, 31 (1966).
[3] Modeling and simulation of viscoelastic behaviour of wood under moisture change, J. Mukudai, S. Yata, Wood Science and Techn. Vol. 20 (1986) p.335-348.
[4] The effect of moisture content changes on the deformation of wood under stress, L.D. Armstrong, R.S.T. Kingston, Wood Science 1979, p. 301-306.
[5] Moisture content changes and creep of wood, R.F.S. Hearmon, J.M. Paton, For. Prod. Journ. Aug. 1984. p. 357-358.
[6] Derivation of the mechano-sorptive effect by the kinetic approach, T.A.C.M. van der Put, Comportement Mechanique du bois, coll. scientific rheologie du bois, Bordeaux juin 1988.
[7] Explanation of the mechano-sorptive effect, T.A.C.M. van der Put, Proc. IUFRO, S 5.02 conf. 1988.
[8] Basis of the Clouser-type power equations for creep,
[9] Derivation of the WLF-equation for glass transition,
[10] Retardation spectra,
[11] Explanation of phenomenological laws by the theory of deformation kinetics,
[8] to [11] by: T.A.C.M. van der Put, Proc. IUFRO, Turku, Finland.

8. EXPERIMENTAL RESEARCH

8.1 Scope of the experimental program

The aim of the testing was to verify the model and to get a first estimate of the order of the parameters and the dependence on temperature and moisture content. Because of the very small viscoelastic deformations, at constant rate tests, a precise determination has to wait until very accurate testing machines are available. The loading machine showed an oscillating behaviour, probably due to disturbances of the electricity network, that has an influence on the scatter of the data, especially at low loading. There was, however no noticeble drift of the machine. Because of the goal to measure the mean overall behaviour, this was accepted and for that reason, also no corrections of the data were made for temperature differences around the mean temperature and dummy movements due to moisture differences. Because data are available for perfect constant humidity conditions, it was decided to use periodical relative air humidity conditions.

The theoretical derivation of the model leads to a parallel system of Maxwell elements with the general strain rate equation (of element *i*):

$$\dot{\varepsilon} = \frac{\dot{\sigma}_i}{K_i} + (A_i + B_i\varepsilon_i)\sinh\left(\sigma_i\varphi_i(1 - C_i\varepsilon_i)\right) \qquad (5.1.1)$$

where σ_i is the stress on the Maxwell element i, ε_i is the strain of the nonlinear dashpot and K_i is the spring stiffness. A_i, B_i, C_i and φ_i are constants.

The process, that is determining at the start of the creep test, showes no delay time and thus $B_i \cdot \varepsilon_i$ is neglectable in comparison with A_i in eq.(5.1.1) and also $C_i\varepsilon_i$ will have a neglectable influence on the first creep stage. Because the relaxation times of the different processes are far apart from each others, only one process has to be regarded. So the first estimate of the parameters can be based on:

$$0 = \frac{\dot{\sigma}_1}{K_1} + A_1\sinh(\sigma_1\varphi_1) \qquad (8.1)$$

for a relaxation test, and:

$$0 = \frac{\dot{\sigma}_1}{K} + A_1\sinh(\sigma_1\varphi_1), \qquad (8.2)$$

with $K = K_1 \cdot K_2 / (K_1 + K_2)$, for the creep test.
The solution of eq.(8.2) for the early part of the total creep process is:

$$\frac{\varepsilon}{\varepsilon_0} = 1 + \frac{1}{\varphi K_2 \varepsilon_0} \ln\left(1 + \frac{K_1 K_2 A \varphi t}{2(K_1 + K_2)} \exp(\sigma_{v0} \varphi)\right). \qquad (8.3)$$

This equation has the form:

$$Y = 1 + C \cdot \ln(1 + t/T) \qquad (8.4)$$

Where t = time in seconds and T is a "delay" time in seconds.
The estimation of the parameters C and T was done with a regression procedure with a computer.

8.2 Test program

It was planned to do creep and relaxation tests. However the parameters of both types of tests appeared to differ not much. So only relaxation tests were done in tension to show the conformity with the creep tests. For comparison creep tests were done in compression, tension and shear, along the grain and perpendicular to the grain. According to table 8.1, 5x2x3 specimens are tested in creep mostly at 2 temperatures depen-

Table 8.1 Overview of test-numbers

test-type	humidity	load-type	temperat.	spec.nr.
1 compr. ∥	1 45%	1 relax.	1 -25 deg.	1 to 3
2 compr. ⊥	2 85%	2 creep	2 + 5	
3 tens. ∥			3 +25	
4 tens. ⊥			4 +50	
5 shear			5 +70	

example: test-code 32241 is: tension ∥; wet; creep test; 50 °C; specimen nr. 1.

ding on the moisture content. Two series of test specimens were used, cut close behind each other from one board. One series was conditioned at about 45% relative air humidity, and the other at 85%.
The tests were done on Spruce and the dimensions of the specimens are given below.

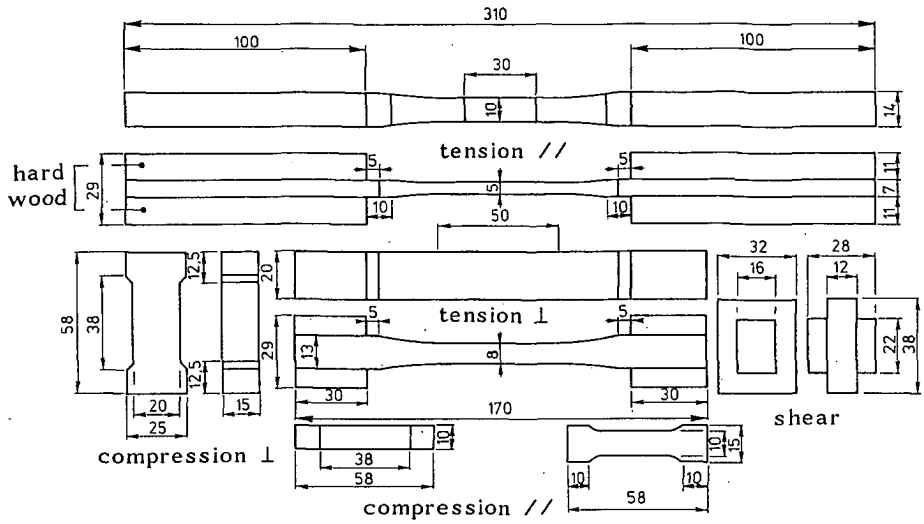

Fig. 8.1 Dimensions of the test-specimens

The loading sequence of the tests (see fig. 8.2) was:
The specimen is loaded at a constant strain rate to a stress level of about 70% of the short term strength, followed by a creep test during about 1 to 3 hours, depending on the deformation. Then the load is decreased to the level of zero creep, what is found by a searching procedure, and maintained at this level during approximately 1 hour. At this level the "dashpot" of the 3-element model is unloaded and creep may not occur. Then, after unloading the recovery is measured. The times of each sequence depends on the amount of creep. With this loading cycle it is in principle possible to determine the constants of a three element model. To maintain the different temperatures and moisture contents, climate boxes were used around the test-specimens. Before the loading, the three specimens of each test-type, were conditioned in the climate boxes until the movement of the specimen due to the moisture exchange was small. Then the test was done on one specimen, while the other two served as dummy to detect weight differences due to change of moisture content. If the temperature was raised, higher relative humidity was some-

times necessary to stop the movement of the dummy due to water exchange. The weight and the dimensions of the test-specimen was controled, just before and after the test. To study the influence of moisture content, mainly tests were done above 0 °C.

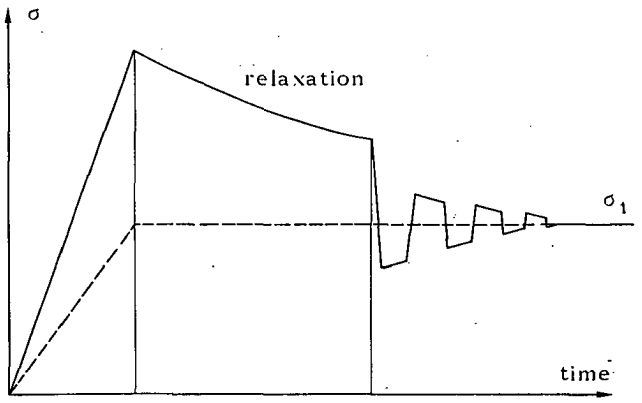

fig. 8.2 Sceme of the searching procedure for zero relaxation

The measurements were taken with a data logger and stored on files. An example of loading sequences of a relaxation test is given in fig. 8.3.

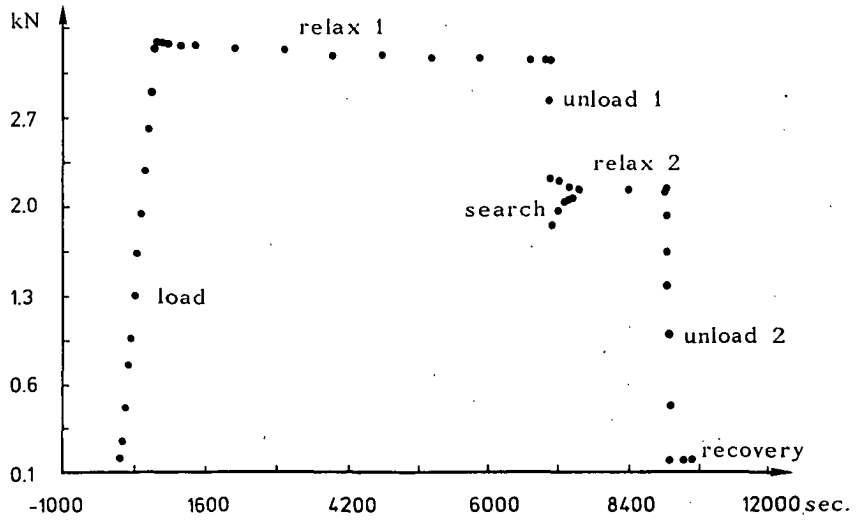

8.3 Loading sequences of the relaxation test

An example of the regression for relaxation and for creep in tension along the grain, done on the same specimen, is given in fig. 8.4

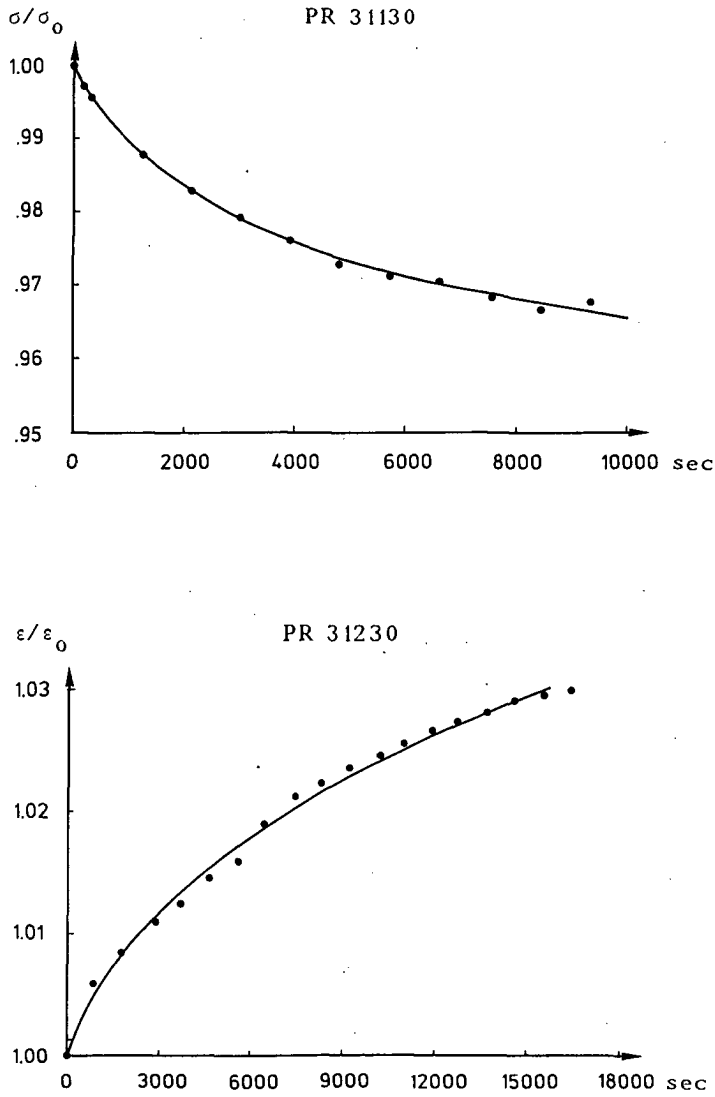

fig. 8.4 Regression of relaxation and creep on one specimen

An example of creep in shear is given in fig. 8.5, together with a plot on logarithmic time scale. Probably there is a start of a second process at the end.

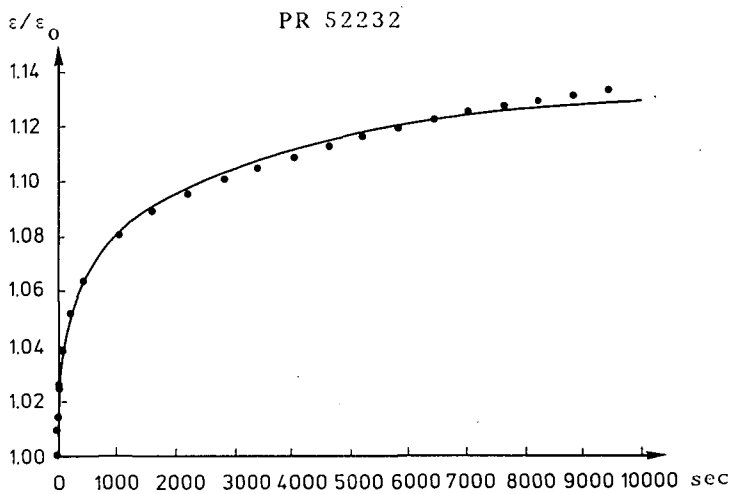

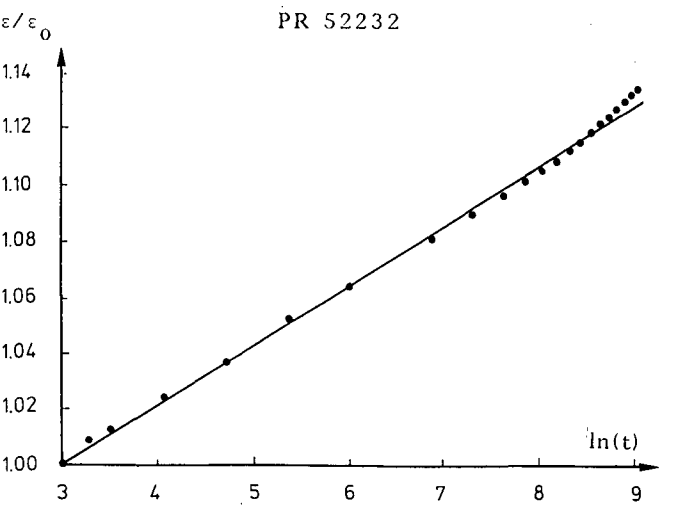

fig. 8.5 Creep test in shear

8.3 Results of the parameter estimation

In general, the stress-strain loading line was only faintly curved and nearly straight, indicating a constant value of C for loading and a gradual increase of viscoelastic strain. The first unloading to the level of zero creep, showed a perfectly straight line, so no recovery of viscoelastic strain. The second unloading line was curved and and showed recovery. Because of the small viscoelastic effects and the scatter, curve fitting of the loading and unloading tests is inaccurate. When these lines are approximated by linear lines, the general tendency is that the mean stiffness of the first unloading line is the highest, and the mean stiffness of the loading line is mostly the lowest. In fig. 8.6 and 8.7, the loading and unloading lines are given of a compression test, where the differences of the stiffnesses are pronounced.

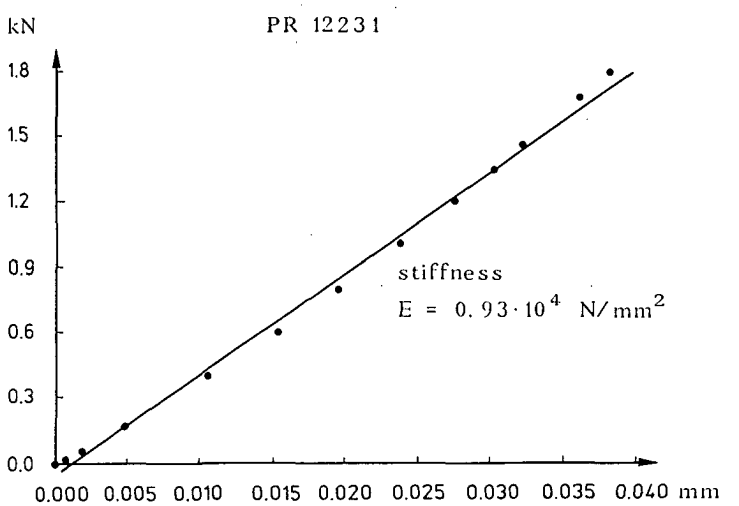

fig. 8.6 First loading of a compression test

The estimation of the compound parameters of the relaxation tests and creep tests, according to eq.(8.4), are given in [1] to [5].
For some tests the level of zero creep or relaxation was maintained for long times in order to control the constancy of the parallel "spring constant". In one test in tension (series 3), for instance, this level remained constant during the test time of 20 hours, despite the changing relative humidity (+and - 15% around equilibrium level).

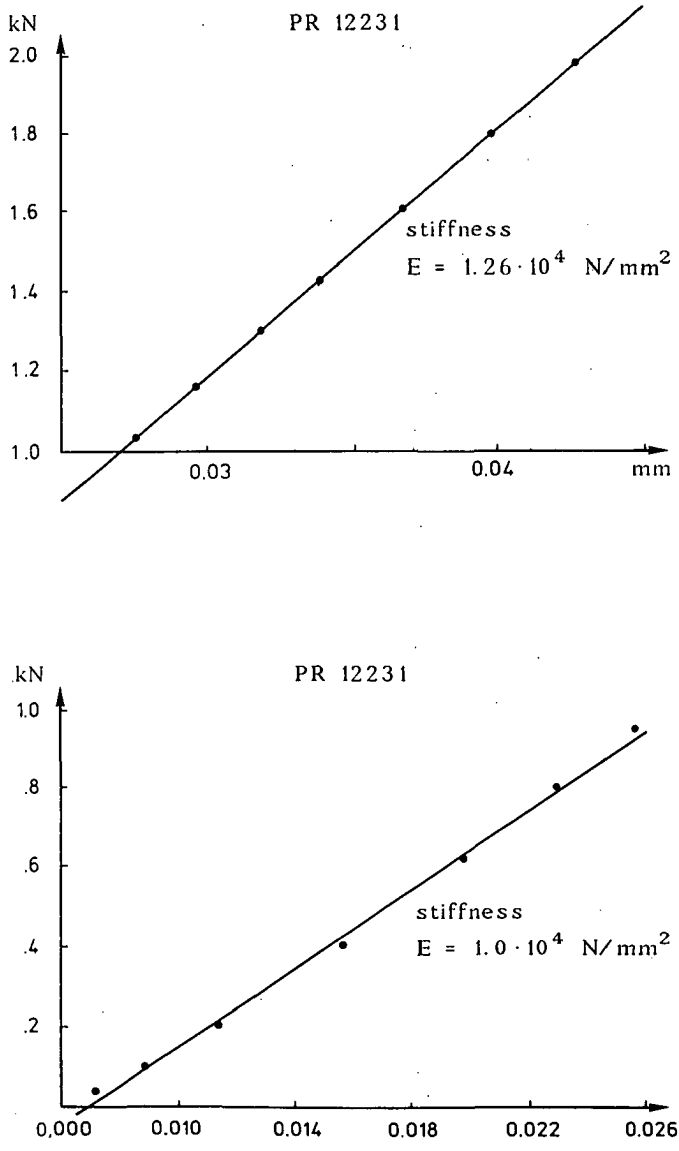

fig. 8.7 First and second unloading sequences of a compression test

8.3.1 Model-parameters for shear

An overview of the parameters C and T of eq.(8.4) for shear is given in table 8.2. The parameter T of the creep equation, that is a measure of the delay time, is the result of a multiplication of a very large value by a very small value and determination of these parameters, containing the relaxation time, will be very inaccurate. A better determination of the relaxation time, by increasing the creep time, appeared to be not pos-

Table 8.2 Results of the shear tests along the grain

Test nr.	Force kN	R.H.	Temp. deg.C	C		T	
				mean	95%confid.	mean	95%confid.
52231	1.6	.64	29	.015	.014/.017	20	12/27
2	1.6	.74	31	.021	.020/.023	22	16/29
3	1.6	.87	30	.027	.025/.030	19	9/28
52251	.8	.88	51	.050	.047/.054	125	97/153
2	.8	.85	50	.028	.024/.032	79	41/117
3	.8	.88	49	.039	.036/.042	47	32/61
51231	2.0	.58	27	.013	.011/.014	12	5/19
2	2.0	.63	28	.016	.015/.017	13	10/15
3	2.0	.45	27	.021	.020/.023	21	13/28
51251	1.0	.27	74	.14	.13/.15	249	204/293
2	1.0	.29	74	.10	.10/.11	292	228/355
3	1.0	.28	75	.064	.06/.07	131	102/160

sible because of the start of a second mechanism after longer times. The value of T can be highly dependent on the initial flow unit density or initial plastic strain and the variation shows that this is a random property for wood. A long delay time indicates a low initial flow unit density and the process reflects probably a structural change with an increase of flow unit density. The automatic control of the air humidity could show rather great oscillation around the mean value, depending on the temperature and the humidity. To maintain a sufficient low humidity cycle, hand steering appeared to be necessary.

The value T/C is:

$$\frac{T}{C} = \frac{2}{KA}K_2 \cdot \exp(-\sigma_{v0}\varphi) = \frac{K_2}{K\alpha\dot{\varepsilon}} = \frac{1}{c\alpha} \qquad (8.5)$$

where α is given below eq.(5.2.7) and c is a constant for loading to the creep level at constant strain rate ($3 \cdot 10^{-5}$ sec^{-1}). It appears that the mean value of T/C is about 1.0 10^{-3} for series 52231/3 and 51231/3 and about 2.2 10^{-3} for series 52251/3 and 51251/3, in accordance with the two times slower rate that was chosen for these series. So α is not dependent on the moisture content and temperature and the main influence on the variability of T is due to to the variability of C. The parameter C is the slope of the strain-log(time) plot. Every specimen has another value of C as can be seen in the series, where the stress and the climatic conditions are the same in the tests but the values are outer each confidence intervals. This indicates different structures and loading histories of the fibres during lifetime in the tree and in the drying process. The value of C ranges from 0.013 to 0.04 for resp. high and low stresses for not too high oscillations of air humidity. For higher R.H.-oscillations and high temperatures there appeared to occur a transition of φ giving a much higher value of C. This was controlled in series 51251/3 where the specimens were conditioned at 50% R.H. and tested at 28% R.H. causing a decrease in moisture content during the test. So moisture movement is the major influence on φ and the model has to be adapted for this phenomenon.

For the series with small cycling humidity conditions the product of the force with C appeared to be constant. The mean values of the series 52231/3, 52251/3 and 51231/3 are 0.03. This shows that C is stress dependent or that φ is constant, independent on temperature and moisture content.

8.3.2 Model-parameters for tension in tangential direction

An overview of the parameters C and T of eq.(8.4) for this case is given in table 8.3. The parameters are comparable with those of the shear tests when relative humidity fluctuations are kept small (see 41231/3). Test nr. 42231 showed some shrinkage although there was some increase in moisture content of the specimen during the test. Specimen 42232 showed some permanent lengthening, although the moisture content decreased and specimen 42233 showed almost complete recovery at a con-

stant moisture content. Parameter C of 42232 and 42233 was however the same.

To investigate the behaviour of the determining mechanism for changing humidity, higher humidity cycles (+10% to -10%) were used in the other series 4223/5. The mean values of C in the series 4125 (0.34) and 4224 (0.31), suggest not much influence of moisture content and temperature. The lower value of series 4223 is probably due to smaller relative humidity changes. It appears that also for this mechanism C decreases on the increase of stress. The product of the force times C (about 0.055) has also not much variation. So it is possible that φ is approximate constant independent of the stress. The deviations occur near the transition temperatures i.e. about 50 °C for wet wood, and about 70 °C for dryer wood. The mean values of T/C of the series show no tendency and can probably regarded to be constant independent on temperature and moisture content. The great variability shows a major influence of the structure and previous history.

8.3.3 Model-parameters for compression in radial direction

An overview of the parameters C and T of eq.(8.4) for compression perpendicular to the grain is given in table 8.4. Also for this case is C in the range of 0.016 to 0.034 for high stresses at low humidity cycles. For larger cycles is the mean value of C of the series about constant C = 0.16 except near the transition temperature (series 22241/2). So there is not much influence of moisture content and temperature. Test nr. 22243 showed some swelling but hardly any increase in moisture content (less than 0.2%). All other specimens showed shrinkage at moisture content decreases between 0 and 1%.

Except near the transition temperature (22241/3), the mean value of T/C can likewise be regarded as a constant with respect to temperature, humidity and stress.

The tendency of constant C and T/C, (at sufficiently low temperatures below the transition temperatures) at high cycling humidity is thus the same for shear, tension perpendicular to the grain and compression perpendicullar to the grain. This mechanism could appear in these cases because of the short grain length in the specimens. In the case of tension and compression along the grain, the period of the cycles is too short to

Table 8.3 Results of the tension tests perpendicular to the grain

Test nr.	Force kN	R H	Temp. deg.C	C		T	
				mean	95%confid.	mean	95%confid.
41231	.40	.46	26	.013	.011/.015	10	3/18
1	first	creep	range	.018	.016/.020	26	17/35
2		shrinkage					
3	.40	.47	27	.009	.005/.013	15	-17/48
3	first	creep	range	.015	.006/.19	28	-10/66
41251	.19	.46	68	.33	.26/.40	821	475/1168
2	.20	.43	69	.43	.21/.65	600	-14/1215
3	.20	.46	68	.26	.18/.34	122	4/241
42231	dominating shrinkage			(small negative creep)			
2	.30	.80	24	.15	.10/.20	209	31/386
3	.28	.75	26	.15	.06/.25	572	-127/1269
42241 high	.20	.99	49	.36	.21/.50	112	47/177
1 low	.15	.97	48	.26	.20/.32	358	212/503
2/3 warped, full plastic behaviour in constant strain rate test							

Table 8.4 Results of the compression tests perpendicular to the grain

Test nr.	Force kN	R H	Temp. deg.C	C		T	
				mean	95%confid.	mean	95%confid.
21231	.67	.47	34	.016	.008/.024	1	-3/5
1	first	creep	range	.034	.015/.054	10	-7/28
2	.66	.44	33	.064	.054/.074	60	29/91
3	.66	.51	33	.26	.25/.28	49	42/56
21251	.30	.48	63	.12	-.01/.26	821	475/1168
2	.30	.49	62	.23	.20/.26	230	152/308
3	.30	.51	62	.15	.11/.19	282	93/472
22231	.51	.77	24	.16	.12/.21	307	96/518
2	.50	.78	26	.13	.09/.16	469	197/741
3	.51	.75	25	.20	.16/.24	299	144/457
22241	.25	.85	48	.14	.07/.21	51	-37/140
2	.25	.82	48	.56	.50/.62	569	437/701
3	swelling dominates creep						

change the overall moisture content in the specimen.

8.3.4 Model-parameters for compression in grain direction

An overview of the parameters C and T of eq.(8.4) for compression along the grain is given in table 8.5.

Table 8.5 Results of the compression tests in grain direction

Test nr.	Force kN	R.H.	Temp. deg.C	C		T	
				mean	95%confid.	mean	95%confid.
11231	2.49	.47	26	(.01)		(300)	
2	swelling in stead of creep						
3	shrinkage, no creep			(.01)			
11251	1.25	.33	70	.058	.04/.08	175	15/335
2	1.26	.37	69	.032	-.01/.07	300	-632/1232
3	1.32	.32	72	.018	-.05/.04	22	-100/1443
12231	1.93	.77	29	.027	.02/.04	558	94/1021
2	shrinkage, no creep						
3	swelling, no creep						
12241	1.0	.84	48	.041	.03/.05	89	7/172
2	1.0	.83	48	.054	-.14/.25	1212	-5113/7537
3	1.0	.83	47	.056	.03/.08	571	100/1042

The strain data showed a great variability, especially at high loading, because the strain in the outer layers of the specimen tends to follow humidity and temperature changes in an irregular way. Because of the intermitted scans of the strain, the curve through these scans is not reliable for high cycling. Probably, this is due to an influence of the mechano-sorptive effect, causing also shrinking and swelling effects. Because of this, only the more reliable data are given in the table. The values of C are in the range of 0,01 to 0.05 for resp. high and low stresses as found for the other loading types given before. Also the tendency of an approximate constant value of the product: C times the stress, is clear. The value of T/C is very irregular because the regression procedure tends to

straighten the curve through the irregular measurements.

8.3.5 Model-parameters for tension in grain direction

An overview of the parameters C and T of eq.(8.4) for tension along the grain is given in table 8.6.

Table 8.6 Results of the tension tests in grain direction

Test nr.	strain x 10^{-3}	RH	Temp. deg.C	C		T	
				mean	95%confid.	mean	95%confid.
relaxation tests:							
31130	2.44	63	20	.013	.012/.015	771	- 553/989
31111	3.04	41	- 8	.019	.015/.023	48	390/1107
31121	3.62	44	- 2	.011	.010/.013	78	83/273
31131	3.68	47	22	.011	.009/.012	93	84/303
31112	2.95	48	- 10	.0085	.008/.009	70	50/90
31122	Specimen is broken at first loading						
31123	3.78	46	7	.014	.012/.016	96	- 573/1220
31133	3.00	50	27	.016	.016/.017	31	25/36
creep tests:							
Stress: N/mm^2							
31233	52.3	47	27	.013	.009/.016	379	10/748
temperature correction				.020	.015/.026	1698	761/2636
31230	62.8	66	19	.016	.014/.018	1864	1407/2320
temperature correction				.017	.014/.019	3102	2267/3937

Because of the similarity of the constants so far and the independency of the parameters of the moisture content, only tests at one moisture content were done for tension and to verify the independency on temperature at low temperatures, measurements were taken at lower values of the temperature.

The tests were done in relaxation, and for comparison some tests in creep were done on the same specimens as well (specimen 31130 is the

same as specimen 31230, and specimen 31133 is the same as 31233). For specimen 0, first the relaxation test was done and for specimen 3, first the creep test. After each type of test, there was a recovery period. The strain of the creep test of specimen 3, was waved by the following of the humidity and temperature cycles, and temperature correction of the data had a strong influence. The influence of this correction on the relaxation tests was neglectable.

The ratio of the parameters C for creep and for relaxation of these tests:

$$\varphi\sigma_0/\varphi\varepsilon_0 K_2 \approx (K_1 + K_2)/K_2 = 0.016/0.013 \text{ to } 0.020/0.016 = \\ = 1.23 \text{ to } 1.25,$$

suggests a ratio of spring stiffnesses in the model of $K_1/K_2 = 0.24$, or: $K_1/(K_1 + K_2) \approx 0.2$, as used before.

The value of the parameter C is in the range of 0.01 to 0.02 for high stresses as is also found for the other loading cases. The mean values of the series show no influence of temperature on C. It is striking that different mechanisms may act in a specimen at the same situation. For instance tests 31121 and 31131 show the same value of C and T at different temperatures. However, 31111 shows that on first loading of this specimen nr. 1, there is another mechanism acting, giving a quite different value of C and of T. The same occurs by the mechano-sorptive effect and probably there is some influence.

8.4 Conclusions

- Because data are available for perfectly constant moisture conditions and because changes in moisture content may have a great influence on the parameters of the overall process, the tests were done by cycling relative air humidity conditions, as will be encountered in practice, to see this influence on the different processes.
- The creep behaviour is well described by the kinetic theory, showing one dominating process in the first hours. As theoretically derived, the term $B_i\varepsilon_i$ in eq.(5.1.1) will behave as $B_i\bar{\varepsilon}_i$, ($\bar{\varepsilon}_i$ is the mean value of ε_i) in a creep process and any change of $A_i + B_i\varepsilon_i$ is not detectable; thus this term can be regarded as a constant. $B_i\varepsilon_i$ is only determinable at flow for the strength determining process (when all parallel elements flow) in the ultimate stage when $\dot{\sigma}_i/K_i$ in eq.(5.1.1) is zero. The same applies for the term $C_i\varepsilon_i$ wich will only be noticeable as hardening term at flow

in the ultimate stage. For creep processes, the change of σ_i with ε_i dominates far above the change of $C_i\varepsilon_i$ and it will not be possible to measure this change and the term will mathematically behave like a constant: $C_i\bar{\varepsilon}_i$ (or can be neglected).

So it is seen that for creep processes eq.(8.2) applies and although A_1 and φ_1 in this equation act mathematically as constants, they can be expected to be random because of the random values of the initial plastic or viscoelastic strains ε_i, depending on the loading and temperature history during the lifetime and the drying process. Further it is possible that eq.(8.2) represents the mean behaviour of all processes with comparable retardation times. In order to distinguish for instance, between the processes of diffusion and creep, it is necessary to have some orders difference in relaxation times of these processes. This is possible by using thin specimens. However, as shown before, the mechano-sorptive effect is quite different then.

- It appears that the three-element model holds and that the parallel spring is constant during the testing time. The retardation time for creep of the Maxwell-element is very long with respect to the testing time of three hours, and the behaviour can be described by the logarithmic law:

$$\frac{\varepsilon}{\varepsilon_0} = 1 + C\cdot\ln(1 + t/T) \approx 1 + C\cdot\ln(t/T) \tag{8.6}$$

representing the theoretical equation for the early part of the total creep with the approximation for longer times after the start of the creep. The breakdown of this logarithmic law [6] is predicted by the theory. This law only applies in the first creep stage (and $t \gg T$). The same equation holds for relaxation:

$$\frac{\sigma}{\sigma_0} = 1 - C'\cdot\ln(1 + t/T) \approx 1 - C'\cdot\ln(t/T) \tag{8.7}$$

Because $C \approx C'$, and $T \approx T'$ and $C\cdot\ln(t/T) \ll 1$, the product of eq.(8.6) and eq.(8.7) is:

$$\frac{\sigma.\varepsilon}{\sigma_0\varepsilon_0} \approx 1. \tag{8.8}$$

This is not a prove of linearity of the viscoelastic behaviour as assumed in [6], but an indication that the spring constant: $K_1 \ll K_2$ in the three element model.

- The values of the parameters are comparable, independent of the type

of loading and loading direction.

- Oscillating relative air humidity at a relative high frequency appeared to have influence on the parameter C for the short grains of the specimens for shear and tension and compression perpendicular to the grain.
- The parameter T of the creep equation, wich is a measure of the delay time, is the result of a multiplication of a very large value by a very small value and determination of these values, containing the retardation time, will be very inaccurate. A better determination of the retardation time, by increasing the creep time, appeared to be not possible because of the start of a second mechanism after longer times. The value of T can be highly dependent on the initial dislocation density or initial plastic strain and the variation shows that this is a random property for wood. A long delay time indicates a low initial flow unit density and the process reflects probably a structural change with an increase of flow unit density.

It appears that the mean value of T/C is about constant, but has a higher value near the transition temperatures. So α is not dependent on the moisture content of the wood and can be dependent on temperature in the neighbourhood of the transition regions and the main influence on the variability of T is due to to the variability of C.

- The parameter C is the slope of the strain-log(time) plot. Every specimen has another value of C. This indicates differences in structure and loading history of the fibres during lifetime in the tree and at drying.

At low cycling humidity conditions, the value of C is about 0.02 to 0.04 for resp. high and low stresses and the product of the force (stress) with C appeared to be approximately constant. This shows that C is stress dependent or that φ is constant, independent on temperature, stress and moisture content. This constancy is probably due to the dominating influence of the mechno-sorptive mechanism on the creep as discussed below eq.(7.20). The ratio of the parameters C for creep and for relaxation suggest a ratio of spring stiffnesses in the model of approximately 0.24. This means that the lowest spring constant is 1/5 of the total stiffness according to the model of fig. 2.3 of not fully bonded cellulose chains.

For higher R.H.-oscillations and high temperatures there appeared to occur a transition of φ giving a much higher value of C (at constant T/C, containing not the value φ). So moisture movement is the major influence on φ and any model has to account for this phenomenon. The mean values of this high C (C = 0.16) suggest not much influence of moisture content and temperature. Near the transition temperatures, i.e. about

50 °C for wet wood, and about 70 °C for dryer wood, is C twice this value. The mean values of T/C of the series show no tendency and can probably regarded to be constant independent on temperature and moisture content. The great variability shows a major influence of the differences of the structure and the previous history.
The tendency of constant C and T/C, (at suficient low temperatures below the transition temperatures) for the mechanism for high cycling humidity is probably due to mechano-sorptive flow and is thus the same for shear, tension perpendicular to the grain and compression perpendicullar to the grain. This mechanism could appear in these cases because of the short grain length in the specimens. For tension and compression along the grain, the period of the cycles is to short to cause high moisture exchange.

8.5 References

[1] Put, ir. T.A.C.M. van der
Shear test along the grain. Parameter determination of a non- linear rheological model based on deformation kinetics. Report 4-86-5 June 1986.

[2] Put, ir. T.A.C.M. van der
Tension tests in tangential direction of Spruce. Parameter determination of a deformation kinetics model. Report 4-86-6 June 1986.

[3] Put, ir. T.A.C.M. van der
Compression tests in radial direction in Spruce. Parameter estimation of a nonlinear rheological model based on reaction kinetics of bond breaking. Report 4-86-7 June 1986.

[4] Put, ir. T.A.C.M. van der
Compression tests in grain direction in Spruce. Parameter estimation of a nonlinear rheological model based on reaction kinetics of bond breaking. Report 4-86-8 June 1986.

[5] Put, ir. T.A.C.M. van der
Reaction kinetics of bond exchange of deformation and damage processes in wood. Proc. IUFRO-Conference Firenze Italy, Sept. 1986.

[6] P.U.A Grossmann, R.S.T. Kingston
Some aspects of the rheological behaviour of wood III, Tests of linearity. Aust. J. Appl. Sci. 14, 305-317. October 1963.

9 CONCLUSIONS

9.1 General conclusions

- An extension has been given to the theory of molecular deformation kinetics by the development of a general rheologic model that is solely based on the reaction equations of the bondbreaking processes.
By expressing the concentration of flow units of this equation in the dimensions of the flow units, the expressions for the strain rate, fracture, hardening and delay time are directly derived. Because of the small changes, the reaction is of first order or quasi first order.
- By series expansion of the potential energy curve the generalized flow theory is derived, showing that the assumptions that where made for this theory are consequences of the series expansion. This provides a general rheological model that must be general applicable for the description of time dependent behaviour of materials and of fracture processes.
- Several processes are acting in wood at loading. For the main damage process the stress independent part of the activation enthalpy and entropy is constant, independent of the temperature and the moisture content. For this process also σV is constant, independent of temperature, moisture content, where σ is the short term strength. The activation volume V is linear dependent on the temperature and moisture content and thus V is inverse proportional to short term strength. The work term n of this process is about 30 to 40, depending on the scaling strength ($n = \sigma V/kT = \sigma\lambda/NkT \approx K_2\varphi\varepsilon_0$). The activation enthalpy is about 36 kcal/mol. Probably this is the result of a primary and a side bond rupture process. Creep tests in wood show a quick process (by high internal peak stresses) with an activation enthalpy of about 50 kcal/mol (primary C-O-bond rupture) and a side bond rupture process with an activation energy of about 21 kcal/mol. The primary bond breaking process (with $n \approx 60$) dominates at controlled crack growth tests.
- The features of the main creep process are different. The work term n or $\varphi\varepsilon_0$ is constant independent of the temperature and initial strain ε_0 at constant moisture content (as also applies for short segments movements of rubbers in the glassy state). The enthalpy is about 24 kcal/mol and n is about 36 for dry wood. The flow unit density N is proportional to the moisture content (or is constant for $\omega = 0$). Coupled to this me-

chanism is another mechanism with a lower value of $\varphi\varepsilon_0$ and a long delay time (flow unit multiplication) that occurs after some critical visco-elastic strain of the first mechanism and possibly this first mechanism creates the flow units for the second mechanism. The additional creep strain of this second mechanism is irreversible. This mechanism did not occur in cell wall experiments, even not at high stress levels. Because in high loaded wood, the earlywood is higher loaded than in these cell wall experiments and thus flows, this mechanism can probably be related to flow of the earlywood and load transmission from the earlywood to the latewood.

Besides these dominating mechanisms, that are related to the cellulose and hemicellulose, there is a small mechanism with a low value of $\sigma\varphi$ (n = 1) and a short relaxation time that is only noticeble at very high loading rates.

For dense species with a high lignin content, a flow unit multiplication mechanism dominates with a stress independent relaxation time. It can be deduced that for this mechanism $\varphi\varepsilon_v$ or $\varphi\varepsilon^2$ is constant. So the density of the flow units is proportional to the plastic strain. The constancy of $\varphi\varepsilon_v$ applies only for constant temperature and moisture content. Probably $1/\varphi\varepsilon_v$ is linear dependent on ω and T. This process causes rotation of the relaxation lines at short times in proportion of the strain. When this process is finished ($t = t_m$), it can be seen from eq.(5.5.10), that the relaxation lines for longer times ($t > t_m$), are shifted vertically according to: $\sigma_1/\sigma_2 = \varepsilon_{01}/\varepsilon_{02}$. So besides horizontal shifts, also vertical shifts can be necessary at some stress levels for the construction of a master creep curve for long loading times.

Also possible is a mechanism with constant φ and a creep model has to contain all of these processes as parallel acting mechanisms.

- For clear wood in compression there in no indication of hardening and yield drop, showing the influence of a amorphous polymer (lignin). For wood in tension there is a high yield drop, showing the influence of a crystalline material (cellulose) dominated by a low initial flow units density ρ_0. There is also no indication of hardening, showing that the change of one model-parameter (λ_1) dominates as also follows from the high value of $\sigma\varphi$.
- A kinetic explanation of the WLF-equation (Williams-Landel–Ferry is WLF) for the temperature dependence of creep above glass- rubber transition is derived, showing that the change of the concentration of mobile

segments and not necessarilly the change of the free volume concentration is the cause of the transition. The theory is extended for cross-linked polymers at transient creep for the element that performs the transition. It follows from the theory that for the special case of constant concentration of flow units the temperature dependence is according to the Arrhenius equation. For higher values of the activation enthalpy, if not the entropy alone is dominating, the theory predicts a shift factor between the Arrhenius- and WLF-equation. The WLF- equation is further extended for the influence of the time scale of the process.

- It is shown that a single process may explain the measured, broad, nearly flat spectra of glasses and crystalline polymers and the relaxation spectrum for wood can be explained by two processes in stead of the assumed infinite number of linear processes. This also has to be so for the spectrum of energy loss at forced vibrations and the activation volume will show a special relationship. Also the fatigue behaviour can be explained by one dominating mechanism in a wide frequency range, and the behaviour at long term loading and at fatigue loading is coupled by the same mechanism. So it will be possible to use fatigue tests in order to predict the long term strength.
- The model is able to explain the existing creep and damage models and phenomenological laws of creep and fracture. It explains for instance the yield drop and the logarithmic strain rate law of the modulus of elasticity in the constant strain rate test; the logarithmice time law of the strength in the constant loading rate test; the logarithmic time law of the creep and the bend off of the creep line at long times (delay time of the structural change process) and the shift of this line along the time axis depending on the stress level and depending on the temperature.
- The different power models (of the stress and of the time) are derived giving the physical meaning of the exponents and constants and the change of these "constants" in certain circumstances. The Gerhards model for instance is an expression of forward activation only and this will be right for high loading in the end state. The theory explains the Forintek model of the strength and the Andrade and Clouser equations and provides a better description of the governing phenomena than these models.

9.2 Results of the experimental research

- The activation-parameters are different for every piece of wood, indicating an unique structure of every test-specimen. The average values are comparable for tension, compression and shear, along the grain and perpendicular to the grain. There are two main processes. One with a high concentration of flow units and one with a low concentration causing a delay time (depending on the stress level as predicted by theory), indicating a structural change process. The long "relaxation time" of the first process cannot be measured accurately because of the start of the second process (even if this starts after a long time at a low stress level), so a constant average value can be taken in all circumstances for practice. The activation volume parameter $\varphi = V/kT$ has the tendency to be constant (between transition regions, at a high stress level and with small humidity cycling), independent of temperature, moisture content and stress. $1/\varphi$ is probably proportional to the dry strength σ_{ui} in the concerning loading direction. So the value $\sigma_{ui}\varphi$ is constant independent of the loading direction. The constancy of φ is probably due to the dominating influence of the mechno-sorptive mechanism on the creep as discussed below eq.(7.20), or $\alpha \approx c \gg 1$ in eq.(7.3). High humidity cycling shows an additional bond breaking process that may cause plastic flow (with $\sigma V/kT$ constant). The resultant behaviour was comparable with other processes, according to the sinh-law of the strain rate and this result was used to explain the mechano-sorptive effect in chapter 7.
- The ratio of the spring constants of the 3-element model is about 1:4. As discussed below fig. 2.3, this indicates that the process in the amorphous region is determined by not fully side-bonded cellulose and hemicellulose chains.

SUMMARY

Structure and mechanical properties of wood

Timber can be defined as a cellular polymeric fibre composite with slender microfibrils as fibres in a cementing matrix of relatively unoriented (amorphous) short-chained or branched polymers (lignin and hemicellulose).
The cell wall is also a laminated composite because of the layered structure of the wall with different kinds of layers. The structure of the layers varies from amorphous cross-linked polymers without microfibrils to closely packed parallel layers containing spiral microfibrils with various pitches to the longitudinal axis. The microfibrils consist of parallel cellulosic molecules having regions of high crystallinity with intermediate low-crystalline zones.
There are different types of disturbances of the structure that may cause stress concentrations and transient processes as for instance knots, defects, ray-crossings, tracheid ends, pits, interlayer imperfections, voids, second order pores and previous cracks in weak layers.
Because of the heterogenous structure, the structural deviations, the deviations of the alignment, and stress states, many processes will occur and random values of the activation parameters of the kinetic model can be expected.
It can further be expected that stress redistribution causes mainly shear with compression in the matrix, increasing the tensile stress in the fibres. The measured negative contraction for creep in tension is an indication of this mechanism.
The polymers in wood determining the time dependent behaviour are densely cross-linked filled amorphous polymers and highly crystalline and oriented polymers.
At room temperature the amorphous parts in wood are probably in the glassy state, and only the so called β-mechanism appears (the α-mechanism represents the glass-leather transition due to mobility of the backbones of the polymers). The β- or secondary mechanism is due to local readjustment of side groups in glassy amorphous polymers or in the amorphous strands of crystalline polymers. The temperature dependence of this mechanism follows the Arrhenius equation and the activation energy lies between 20 and 30 kcal/mole. The stress reduction in relaxation is

smaller than by the α-mechanism and will be a factor 0.5 to 0.8. The same as for the α-mechanism is the behaviour nonlinear for high stresses and these properties are explained here by the kinetic model.
Above the transition temperature of the amorphous regions, there is a, in comparison with other cross-linked and crystalline polymers, relative slow relaxation or creep due to a very high cross-linking of these regions. The creep is recoverable and increase of stress shortens the retardation time. The creep rate on logarithmic time scale is more than linear dependent on the stress at higher stresses. The temperature dependence of the viscoelastic properties follows the WLF- or the Arrhenius equation. The Arrhenius form applies for cellulose because the crystallinity doesn't change much and there are no vertical shifts (due to change of the pseudo equilibrium modulus) of the creep lines along the log- time-axis. The creep can be described by the Andrade-equation or is a straight line on a log-time-plot. This mechanism is also attributed to the mobility of the short strands in the amorphous regions, probably due to co-operative motions of groups of strands coupled through linkage points. The thermal and mechanical history is very critical for the behaviour as for glasses and also traces of diluent have an influence.
The time dependent behaviour of wood is non-linear and can be explained by the kinetic theory. The behaviour is only quasi linear at suficient small ranges of stress, time, temperature and moisture content. Distinctions between viscoelastic and viscous behaviour cannot be made because "irrecoverable" flow is only quasi irrecoverable due to the nonlinear behaviour providing a immobile behaviour for the low internal stresses after unloading. Real irrecoverable behaviour may occur due to structural changes (damage processes).
Absorption of water by wood causes swelling up to a moisture content of about 28%. Swelling of the secondary wall is much greater than swelling of the middle lamella. It is to be expected that the high restraints for swelling and shrinkage will cause "flow" in the gel-like matrix. This flow is directed if a specimen is maintained under stress during a change in moisture content. The moisture movement through the wood involves breaking of stressed hydrogen bonds and reformation of these bonds in a shifted position by swelling and shrinking ofadjacent layers, causing the large creep deformation at desorption. At absorption there is a partial recovery of this deformation by the reversed behaviour.
An explanation can been given of the strength behaviour of cellulose chains

depending on the logarithmic value of the degree of polymerization. The influence is simular to a dislocation propagation process and this will be covered by the kinetic model.
The explanation, of the short periodic processes of loading and unloading in the amorphous regions at a creep test, as a result of the ability of the lignin network to act as an energy sink and to control the energy set up of the stressing is not probable. A better explanation of this time dependent behaviour of the amorphous regions in the fibrils is given as a dynamic crystallization process.

Extension of the theory of molecular deformation kinetics

A general rheological model is developed and the mathematical derivation of the model is solely based on the reaction equation of bondbreaking and reformation. Because of the small changes, the reaction is of the first order or quasi first order and the activation enthalpy, entropy and external work can be regarded to be linear dependent on temperature, moisture content and stress. If the concentration of flow units in this equation is expressed in the dimensional parameters of the flow units, the reaction equation is transformed to the strain rate equation of time dependent deformation, containing a delay time parameter and a hardening term. For larger changes of the dimensional parameters of the flow units the equations explain the existing damage models and phenomenological laws of fracture.
In the original theory, the plastic strain rate is rather arbitrarily taken to be proportinal to the rate of change of the flow unit concentration and the form of the parameters in the rate equation that determine e.g. the hardening and the delay time, are arbitrary phenomelogic expressions of the strain. By expressing the rate equations in the dimensions of the flow units, the expressions for the strain rate, fracture, hardening and delay time are directly derived.
It is possible to expand the total potential energy curve into (Fourier-) series leading to parallel acting systems of symmetrical consecutive barriers. Because a system of the same symmetrical consecutive barriers act as one symmetrical barrier, the process is equivalent to a parallel system of simple, processes. The derivation leads to the generalized flow theory proving the basis assumptions that the flow unit spectrum exists

(as expanded terms) and may be approximated by a limited number of elements with distinct average relaxation times and that the deformation rate of all units is the same.

By comparison with the model, the different power models (of the stress and of the time) are derived giving the physical meaning of the exponents and constants. It can be shown that the Andrade-type equation is equivalent to the theoretical logarithmic creep behaviour. The inverse of one of the parameters of the Andrade or Clouser equations is equal to the work parameter of the activation energy ($\sigma V/RT$) and has same meaning as the exponent n ($n = \sigma V/RT$) of the experimental power law equation for the creep rate and the exponent of the Forintek damage model. Further is $1/n$ the slope of the normalized logarithmic creep and relaxation lines and of the logarithmic time to failure law of the creep strength or long duration strength. The value of n is p.e. in the Clouser equation $n \approx 33$. In the Forintek model is $n = 34$. As slope of the logarithmic creep-to-failure law $n = 38$ is found, if the line is scaled to the $\sim$ 1 sec. strength, but $n = 34$ when scaled to the 5 min. strength. The value of n following from the universal form of the WLF-equation as applied for the glass transition of lignin is: $n = 2.3 \times x\ 17.44 = 40$, equivalent to a scaling to a very short duration strength. So it appears here that n is essentially a structure constant and is as such probably unaffected by moisture content and temperature.

For wood the logarithmic law of the creep-to-failure strength is one line for different wood species, moisture contents, stress states (bending, shear, compression etc.) and types of loading, indicating that n has to be constant, independent on moisture content and also that the activation enthalpy and entropy are approximately independent on the moisture content. The activation volume is however strongly dependent of the moisture content (and thus the inverse of the strength has the same dependence). Based on this form of the activation energy, the experimental creep-to-failure tests at different temperatures and moisture contents could be explained as well as the straight line of the strength on log-time scale for dry wood as the curved line for saturated wood. Saturated wood shows an enthalpy of about 36 kcal/mole above a transition temperature of - 8 °C and about 30 kcal/mole below this transition temperature. Dry wood doesn't show this transition. It has to be emphazised that these values are tentatively following from a curve fitting with the least number of parameters. Systematic measurements may show the influence of the

here neglected terms.
The value of n is probably the result of two main processes. Values of $n \approx 62$ are given in literature for controlled crack growth tests, to $n \approx 65$ in constant strain rate tests, and $n \approx 30$ in constant load tests to failure as apparent value of the first overall process. In other experiments also values of n = 25 to 39 are mentioned. Analysing the creep values at not too high stress, the existence of two parallel barriers was clearly demonstrated. The quick process had a high internal stress (forward activation) and an activation energy of approximately 50 kcal/mole. The slower process was approximately symmetrical and had an activation energy of about 21 kcal/mole. The quick process, that was determining in the first stage of the loading may probably be associated with the first determining crack propagation process with $n \approx 62$ and the second process may be associated with the slower process with $n \approx 30$. The activation energy of this slow process is comparable with other values mentioned in literature where from creep tests at different temperatures for bending: H'= 22 kcal/mole to 24.4 kcal/mole, depending on the temperature range, have been found. From normal-to-grain relaxation tests 23 kcal/mole was reported for wet beechwood. This energy is often regarded to be the energy of cooperative hydrogen bond breaking. The activation energy of 50 kcal/mole is probably high enough for C-O-bond or C-C-bond rupture.

Compliance curves etc. measured at different temperatures can be shifted along a logarithmic time or frequency axis (called time-temperature equivalence). The shift factor of this displacement of the curve along the log-time axis is given by the so called WLF-equation in the glass transition region of the amorphous components of wood. An explanation by the kinetic model of the WLF-equation is shown to be possible. It appears that the change of the concentration of mobile segments and not necessarilly the change of the free volume concentration is the cause of the transition. The theory is extended for cross-linked polymers at transient creep for the element that performs the transition. It follows from the theory that for the special case of constant concentration of flow units the temperature dependence is according to the Arrhenius equation. For higher values of the activation enthalpy, if not the entropy alone is dominating, the theory predicts a shift factor between the Arrhenius- and WLF-equation. The WLF- equation is further extended for the influence of the time scale of the process.

The nonlinear viscoelastic deformation problem is often linearized by splitting up the contribution to the rigidity in numerous linear viscoelastic processes giving a relaxation spectrum. It is shown here that a single process may explain the measured, broad, nearly flat spectra of glasses and crystalline polymers and that the spectrum for wood can be given by two processes in stead of the assumed infinite number of linear processes that is regarded to be the basis of the relaxation spectrum. The same is possible for the spectrum of energy loss at forced vibrations and for fatigue behaviour.

Solutions of the model equations are given for transient processes for different loading histories to show that the model can explain the phenomenological laws as e.g. the linear dependence of the stiffness on the logarithmic value of the strain rate in a constant strain rate test; the logarithmic law for creep and relaxation and the necessary breakdown of the law for longer times; the shift factor along the log-time axis due to stress and temperature and the influence on this factor of the transition to the second mechanism. At the usual test conditions there is an influence of two processes, one with a high initial flow unit density and one with a very low initial dislocation density. Real hardening can be neglected. The model is able to explain the mechano-sorptive effect as is shown by the derivation of the basis equations. The derivation trows a new light on the mechanism, being a separated bondbreaking and reformation process due to sorption and not an interaction of creep and moisture change or an interaction of loading on the overall shrinkage. The model predicts that for large dimensions of the test specimens, this effect is of minor importance.

Experimental research

The aim of the testing, reported here, was to verify the model for higher stress levels and to get a first estimate of the order of the parameters and the dependence on temperature, moisture content and loading direction. Because data are available for perfect constant humidity conditions, it was decided to use oscilating relative air humidity conditions as may occur in practise. Quick and low relative humidity cycling may be expected to behave like constant moisture content conditions. However the behaviour

of the wood polymers is very sensitive for traces of diluent, the previous history and moisture changes and this will cause a different behaviour in comparison to perfect constant moisture conditions. Tests with quick larger moisture cycling around a mean value where also done for a first impression on this behaviour that effects mainly the outer layers. At low cycling humidity conditions, and high stress level the value of $1/n$ is about 0.02 to 0.04 for resp. high and low stresses and not $n = \sigma\varphi$ is constant but φ is approximately constant, independent on temperature, stress and moisture content. This constancy is probably due to the dominating influence of the mechno-sorptive mechanism on the creep (that shows a constant value of φ). For higher R.H.- oscillations and high temperatures there appeared to occur a transition of φ giving a much higher value of $1/\varphi$. The value $\sigma\varphi$ is constant for this mechanism, probably due to flow. The mean value of this high $1/\sigma\varphi$ ($1/\sigma\varphi = 0.16$) does not suggest much influence of moisture content and temperature.

VERVORMINGS- EN SCHADE-PROCESSEN IN HOUT
SAMENVATTING

Structuur en mechanische eigenschappen van hout

Hout kan gedefinieerd worden als een cellulair polymeer. Dit polymeer is een vezelkomposiet dat bestaat uit dunne microfibrillen als vezels in een matrix van een amorf vertakt en verknoopt polymeer (lignine en hemicellulose). Het materiaal is ook een gelaagde composiet omdat de celwand is opgebouwd uit een groot aantal verschillende lagen. De samenstelling van deze lagen varieert van een laag met een amorf polymeer zonder microfibrillen en een laag met random gerichte microfibrillen, tot lagen met dicht opeengepakte, georienteerde microfibrillen, met per laag een andere hellingshoek.
De microfibrillen bestaan uit evenwijdige cellulosemoleculen die periodiek kristallijne gebieden vormen met tussenliggende amorfe gebieden.
Er zijn verschillende soorten verstoringen van de regelmatige structuur die spanningsconcentraties en spanningsherverdelende processen kunnen veroorzaken. Voorbeelden hiervan zijn kwasten, groeistoringen, harszakken, scheurtjes, doorsnijding van houtstralen, tracheid beeindigingen, hof-

stippels, imperfecties tussen de lagen, holle ruimten en microporien.
De heterogene structuur van de celwand zal verschillende spanningstoestanden veroorzaken in de verschillende lagen en verschillende kruipsnelheden waardoor spanningsherverdeling optreedt. Zo zullen, bij trekbelasting, de trekspanningen snel uit de lignine kruipen en geschiedt de spanningsoverdracht tussen de vezels d.m.v. druk met afschuiving in de matrix (als in gescheurd beton om de wapeningsstaven). De gemeten negatieve contractie bij trekbelasting is een aanwijzing voor het optreden van dit mechanisme. Door deze heterogene structuur en vele verstoringen op elk niveau en de vele daaruit volgende transiente processen zullen de activeringsparameters van het hier ontwikkelde kinetisch model een random karakter vertonen.
Het tijdseffect in hout wordt bepaald door sterk georienteerde kristallijne polymeren en door sterk verknoopte en opgevulde amorfe polymeren. Op kamertemperatuur zijn de bepalende amorfe gebieden in het hout waarschijnlijk in de glastoestand en treedt alleen het z.g. β-mechanisme op bij belasten (Het α-mechanisme treedt op in het gebied van de glas-leer overgang doordat de bewegingsmogelijkheid van de ketens vergroot wordt door de volumetoename t.g.v. temperatuursverhoging). Het β- of secundaire mechanisme wordt veroorzaakt door locale verplaatsingen van de zijgroepen of locale segmentbewegingen in de amorfe gebieden. De temperatuursafhankelijkheid van dit mechanisme volgt de Arrheniusvergelijking en de activeringsenergie ligt tussen de 20 en 30 kcal/mol. De spanningsafname door relaxatie is kleiner dan bij het α-mechanisme en bedraagt een factor van 0,5 à 0,8. Boven de glasovergangstemperatuur is er een, in vergelijking met andere polymeren, geringe relaxatie of kruip t.g.v. de sterke verknoping en orientatie van de polymeren. Net als bij het β-mechanisme is de kruip reversible en niet-lineair en heeft de spanning invloed op de relaxatietijd i.o.m. het hier afgeleide kinetische model.
De temperatuursafhankelijkheid van de viscoelastische eigenschappen boven de glasovergangstemperatuur volgt de WLF- of Arrhenius vergelijking. De Arrhenius betrekking geldt voor cellulose omdat de kristalliniteit weinig verandert en alleen locale segmentbewegingen mogelijk zijn.
De kruip in dit gebied kan (als voor het β-mechanisme) beschreven worden met de Andrade-vergelijking of door een rechte lijn als functie van de logarithme van de tijd. Dit mechanisme wordt toegeschreven aan de mobiliteit van de korte segmenten in de amorfe gebieden die waarschijnlijk gecoordineerd verplaatsen tussen de knooppunten. Zoals ook geldt voor

de glastoestand heeft de thermische en mechanische voorgeschiedenis een grote invloed op het gedrag en heeft ook de aanwezigheid van vocht een sterke invloed. Het tijdsafhankelijk gedrag van hout is niet-lineair, wat verklaard kan worden met het hier ontwikkelde kinetische model. Het gedrag is quasi lineair bij voldoende lage spanningen, korte belastingstijden, en voldoende lage temperaturen en vochtgehalten. Onderscheid tussen visco-elastisch en visco-plastisch gedrag is er niet volgens dit model omdat de blijvende vervormingen quasi blijvend zijn door het niet-lineaire gedrag. Hierdoor verloopt de terugvering zeer langzaam bij de lage inwendige spanningen na ontlasten. Werkelijk blijvende vervorming kan optreden door structurele veranderingen (schadeprocessen).
Absorptie van water veroorzaakt zwelling van het hout tot een vochtgehalte van ca. 28%. De zwelling van de secundaire celwand is veel groter dan die van de middenlamel. Het is te verwachten dat dit verschil leidt tot vloeispanningen in de gel-achtige matrix. Dit vloeien kan georienteerd worden wanneer het proefstuk belast wordt gedurende de vochtwisseling. De vochtbeweging door het hout veroorzaakt het verbreken van belaste verbindingen en het vormen van nieuwe bindingen in een onbelaste toestand. Bovendien zijn er lagen die verlengen onder vochttoename. Hierdoor ontstaan grote vervormingen bij desorptie. Bij adsorptie treedt een partieel herstel op van deze vervormingen door de tegengestelde bewegingen waarbij terugvloeien kan optreden afhankelijk van het belastingsniveau.
De sterkte van bestraald hout, afhankelijk van de logarithme van de polymerizatiegraad van de cellulose ketens kan verklaard worden. Het gedrag is te vergelijken met een schadeproces zoals dit door het kinetisch model beschreven wordt.
De verklaring van de korte periodieke processen van belasting en ontlasting van de amorfe gebieden gedurende een kruipproef, door te veronderstellen dat de lignine kan werken als een energie-opslagplaats die de energietoevoer regelt bij het belasten, is onwaarschijlijk. Een betere verklaring van dit tijdsafhankelijke effect van de amorfe gebieden in de fibrillen is te geven door dit verschijnsel te beschouwen als een proces van dynamische kristallisatie.

Uitbreiding van de theorie van de moleculaire vervormingskinetiek

Een algemeen rheologisch model is hier ontwikkeld, uitsluitend gebaseerd

op de chemische reactievergelijking van het verbreken en opnieuw vormen van de bindingen. Omdat er kleine concentratieveranderingen kunnen optreden is de reactie van de eerste orde of een quasi eerste orde proces. Door de symmetrie van het proces en de kleine structurele veranderingen kan de activeringsenergie lineair afhankelijk beschouwd worden van de spanning en temperatuur en van het vochtgehalte.
Als de concentratie van mobiele segmenten uitgedrukt wordt in aantal en afmetingen van de segmenten, ontstaat uit de reactievergelijking de vergelijking van de plastische reksnelheid. Als de veranderingen van deze afmetingsparameters niet verwaarloosbaar zijn en in rekening gebracht worden, ontstaat uit de reactievergelijking het algemene geval van de bekende fenomenologische schadevergelijkingen.
In de oorspronkelijke theorie werd de plastische reksnelheid nogal willekeurig evenredig gesteld met de concentratieterm van de reactievergelijking en de parameters van de reactievergelijking die b.v. de versteviging en wachttijd voor kruip bepalen, werden als fenomenologische uitdrukkingen ingevoerd. Door het invoeren van de afmetingen van de mobiele segmenten worden de vergelijkingen voor de reksnelheid, versteviging en wachttijd direct afgeleid.
Het is mogelijk de potentiele energie kromme te ontbinden in een fourierreeks. Hierdoor ontstaat een parallel systeem van rijen van dezelfde symmetrische energiebarrières achter elkaar. Aan te tonen is, dat zo'n rij equivalent is aan een symmetrische barrière en het hele systeem equivalent is aan een parallel systeem van eenvoudige (symmetrische) processen. De afleiding leidt tot de gegeneraliseerde vloeitheorie en levert de theoretische basis voor de uitgangspunten van deze theorie. Zo blijkt een energiespectrum te bestaan van afzonderlijke verdelingen om uiteenliggende relaxatietijden heen in de vorm van de ontbondenen van de reeks zodat binnen de tijdschaal van een proef een beperkt aantal processen met verschillende gemiddelde relaxatietijden een rol spelen. Verder volgt uit de afleiding dat de reksnelheid van deze processen gelijk moet zijn zodat dit niet langer een hypothese voor deze theorie is.
Met behulp van dit model zijn de verschillende experimentele kruip- en schade- vergelijkingen, die als machtsfuncties van de spanning of de tijd gegeven zijn, af te leiden en is een fysische betekenis te geven aan de constanten en machten. Het is daarmee mogelijk het Forintek model voor de sterkte en de Andrade en Clouser vergelijkingen voor kruip te verklaren. Deze kruipvergelijkingen blijken equivalent te zijn met het theore-

tische, lineair met de logarithme van de tijd, toenemende deel van het kruipverloop. De inverse van een van de parameters vande Andrade of Clouser vergelijkingen is gelijk aan de arbeidsparameter van de activeringsenergie ($\sigma V/RT$) en is ook gelijk aan de machtsexponent n ($n = \sigma V/RT$) van de experimentele machtsfunctie van de kruipsnelheid en van het canadese (Forintek) schademodel. Verder is $1/n$ de helling van de genormaliseerde logarithmische kruip- en relaxatie- lijnen en van de logarithmische duursterkte lijn. De waarde van n is in de Clouservergelijking $n \approx 33$. In het Forintek model is $n = 34$, indien de sterkte betrokken wordt op de duursterkte van 5 minuten. Dit komt overeen met de waarde die volgt uit de helling van de logarithmische duursterkte lijn. Indien deze lijn wordt betrokken op de duursterkte van ca 1 sec. dan wordt de inverse van de helling $n = 38$ in overeenstemming met de metingen. De waarde van n volgens de universele WLF-vergelijking is $n = 2{,}3 \times 17{,}44 = 40$, wat overeenkomt met een schaling naar een duursterkte beneden de 1 sec. Het blijkt dus dat n een struktuurconstante is en als zodanig waarschijnlijk onafhankelijk is van het vochtgehalte en de temperatuur.

Voor hout is de genormeerde duursterkte, als functie van de logarithme van de levensduur, een lijn, onafhankelijk van de houtsoort (dichtheid), vochtgehalte, spanningstoestand (buiging, afschuiving, druk etc.) en belastingswijze. Dit betekent dat de term van de uitwendige arbeid van de activeringsenergie constant is. Verder zijn ook de enthalpie en entropie constant voor deze schadeprocessen. Het activeringsvolume is echter sterk lineair afhankelijk van het vochtgehalte (en dus heeft de inverse van de sterkte dezelfde afhankelijkheid). Uitgaande van een constante enthalpie en verwaarloosbare entropie, is het mogelijk de verschillende duursterkten te verklaren afhankelijk van de temperatuur en het vochtgehalte. Het blijkt dat er, o.i.v. vocht, een transitie is bij $-8\ ^{\circ}$ C en dat de enthalpie ca 40 kcal/mol is boven deze temperatuur en ca 30 kcal/mol beneden deze temperatuur. Droog hout vertoond deze transitie niet. Deze waarden volgen uit een parameterbepaling met zo min mogelijk parameters. De invloed van de hier eventueel verwaarloosde parameters kan alleen bepaald worden door systematische metingen gebaseerd op het hier ontwikkelde model. De waarde van n bijvoorbeeld kan het gevolg zijn van twee hoofdprocessen. Waarden van $n \approx 62$ zijn in de literatuur te vinden voor scheurgroeiproeven en $n \approx 65$ voor de constante reksnelheids proef. Voor de sterkte volgens de constante belastingssnelheidsproef wordt $n \approx 30$ genoemd, maar ook waarden van $n = 25$ tot 39 zijn te vinden, wat mede

samenhangt met de keuze van de referentiesterkte. Uit de analyse van de kruipvervormingen bij een relatief lage belasting, blijken er duidelijk twee paralelle processen op te treden. Het snelle proces was hoog belast (d.w.z. alleen voorwaartse activering was merkbaar en het proces verliep snel ondanks de hoge activeringsenergie) en had een activeringsenergie van 50 kcal/mol. Het langzame proces liet een bij benadering symmetrische barrière zien en had een activeringsenergie van 21 kcal/mol. Het snelle proces kan geassocieerd worden met een initiele scheurvoortplanting waarvoor $n \approx 62$ is, en voor het tweede proces kan $n \approx 30$ zijn. De activeringsenergie voor dit langzamere proces is vergelijkbaar met de waarden die in de literatuur genoemd worden van 22 tot 24 kcal/mol voor buiging, afhankelijk van de temperatuur. Uit relaxatieproeven op nat beukenhout, loodrecht op de vezelrichting belast, volgde een waarde van 23 kcal/mol. Deze energie wordt vaak beschouwd als de energie voor een cooperatief proces, waarbij meerdere waterstofbindingen gezamelijk moeten breken. De activeringsenergie van 50 kcal/mol is waarschijnlijk hoog genoeg voor het verbreken van de primaire C-O- of C-C bindingen.

Lijnen, die het verloop van de kruip, of de compliantie etc. met de logarithme van de tijd geven bij verschillende temperaturen, kunnen langs de logarithmische as of frequentie-as verschoven worden tot een basis kromme die de voorspelling geeft van het gedrag bij een temperatuur na zeer lange tijd (equivalentie van tijd en temperatuuur). De verschuivingsfactor van deze verplaatsing van de de kromme langs de tijdsas wordt gegeven door de z.g. WLF-vergelijking in het gebied van de glas-rubber overgang van de amorfe gebieden. Het blijkt mogelijk de WLF-vergelijking te verklaren met het hier gegeven kinetische model. Hieruit volgt dat bij dit proces de enthalpie niet verandert maar bepaald wordt door een entropieverandering. Verder blijkt dat niet noodzakelijk de verandering van het vrije volume op zich nodig is voor deze transitie, maar wel de toename van de concentratie van mobiele segmenten. De theorie verklaart ook waarom deze vergelijking tevens voor verknoopte polymeren kan gelden en verder dat, voor een constante concentratie van mobiele segmenten, de verschuivingsfactor volgens de Arrhenius vergelijking geldt. De WLF-vergelijking is verder ontwikkeld zodat de invloed van de tijdschaal van het proces in rekening gebracht kan worden.
Het niet-lineaire viscoelastisch gedrag wordt gewoonlijk benaderd als een som van de bijdragen van een zeer groot aantal lineaire viscoelastische

processen, die te samen een spectrum van relaxatietijden vormen. Aangetoond kan worden dat een enkel niet-lineair proces het gemeten, brede, bijna vlakke spectrum, voor materialen in de glastoestand en kristallijne polymeren, kan verklaren. Het relaxatiespectrum van hout kan verklaard worden uit de invloed van twee processen i.p.v. het aangenomen oneindig aantal lineaire processen dat als uitgangspunt dient van het relaxatiespectrum. Met deze verklaring heeft het relaxatiespectrum een fysische betekenis gekregen. Hetzelfde is mogelijk voor het spectrum van gedwongen trillingen en voor vermoeiing.
Oplossingen van de differentiaalvergelijkingen van het model worden hier gegeven voor spanningsherverdelende processen bij verschillende belastingswijzen om aan te tonen dat het model de fenomenologische wetten kan verklaren. Voorbeelden hiervan zijn de lineaire afhankelijkheid van de stijfheid van de logarithmische waarde van de reksnelheid in een constante reksnelheidsproef; het logarithmisch verloop van kruip en relaxatie en de noodzakelijke afwijking van dit verband na lange tijd; de verschuivingsfactor langs de logarithmische tijdas o.i.v. spanning en temperatuur en de invloed op deze factor door de overgang naar een tweede mechanisme. Onder de gebruikelijke proefcondities is er een invloed van twee processen, een met een hoge initiele concentratie van vloei-elementen en een met een zeer lage initiele concentratie (wat de lange vertragingstijd van dit proces verklaard). Echte versteviging bij locale vloei van hout kan verwaarloosd worden.
Het hier gegeven model kan het mechano-sorptieve effect verklaren. Het blijkt dat dit een afzonderlijk mechanisme is en geen interactie van kruip en vochtverandering of interactie van de belasting op de krimp. De theorie voorspelt dat dit effect gering is voor proefstukken met grotere afmetingen.

Experimenteel onderzoek

De hier gegeven beproeving had tot doel het model te verifieren bij hogere spanningsniveau's en een eerste indruk te krijgen van de grootte van de parameters afhankelijk van het vochtgehalte, de temperatuur en de belastingsrichting. Omdat er al veel gegevens zijn voor zuiver constante vochtcondities, is beproefd bij periodiek wisselende relatieve luchtvochtigheden wat ook in de praktijk zou kunnen optreden. Verwacht kan worden

dat bij geringe en snelle wisselingen, het gedrag vergelijkbaar is met dat onder constante vochtcondities. Echter het gedrag van houtpolymeren is zeer gevoelig voor vocht en de bevochtiginsgeschiedenis zodat een afwijkend gedrag waarschijnlijk is. Proeven met snelle grote vochtwisselingen zijn ook uitgevoerd om een eerste indruk te krijgen van deze invloed die zich zal beperken tot de buitenste lagen van het proefstuk.

Bij vochtwisselingen met een geringe amplitude en een hoog spanningsniveau lag de waarde van $1/n$ ($n = \sigma V/kT = \sigma\varphi$) tussen ca 0,02 en 0,04 voor resp. hoge en lage spanningen en niet $n = \sigma\varphi$ is constant, maar φ is bij benadering constant, onafhankelijk van de temperatuur, het vochtgehalte en spanning. $1/\varphi$ is waarschijnlijk evenredig met de sterkte in droge toestand σ_{ui} van de betreffende belastingsrichting zodat $\sigma_{ui}\varphi$ constant is onafhankelijk van de belastingsrichting.

De trek- en druk- proefstukken die loodrecht op de vezelrichting belast werden, hadden een kleine afmeting in vezelrichting. Hierdoor kon het vocht ver in de doorsnede indringen via de kopse zijvlakken tijdens de vochtwisselingen. Voor deze proefstukken bleek, bij hogere vochtwisselingen en temperaturen, een transitie mogelijk naar een veel hogere waarde van $1/n \approx 0{,}16$, onafhankelijk van het gemiddelde vochtgehalte en de temperatuur. Grotere vervormingstoename is blijkbaar afhankelijk van de gemiddelde vochtwisseling in de hele doorsnede, waarbij φ constant kan worden aangenomen. Dit is daarom het uitgangspunt geweest voor de afleiding van het mechano-sorptieve effect.

NOTATIONS

A = reaction rate constant times the constant "concentration" of flow units ε_{v0}. $A = \varepsilon_{v0} \cdot C = \varepsilon_{v0} \cdot \nu \cdot \exp(-E/kT) \approx$ (for cellulose: $\varepsilon_{v0} \approx 1$) $\approx \approx \nu \cdot \exp(-E/kT)$.

a = $23D/d^2$; D is the diffusion coefficient; d is diameter of the specimen

$B\varepsilon_v$ = the same as A, however with changing ε_v.

C_p = the heat capacity at constant pressure

C = reaction rate constant

$= (\varkappa kT/h)\exp(-E/kT) = (\varkappa kT_m/h)\exp((-E/kT) - \ln(T_m/T) =$

$= \nu \cdot \exp((-E/kT) - \ln(1 + (T_m - T)/T)) \approx \nu \cdot \exp(-E/kT - kT_m/kT + 1) =$

$= \nu \cdot e \cdot \exp((-E - kT_m)/kT) \approx \nu \cdot \exp(-E/kT)$ because: $kT_m - kT \ll E$.

E = the activation energy

f = local real stress on the flow unit in the direction of the movement

G = Gibb's free energy

H = enthalpy (H is also used as height of the relaxation spectre)

h = Planck's constant = $4.135 * 10^{-15}$ eVsec

k = Boltzmann's Constant = $8.616 * 10^{-5}$ eVK

K = local rigidity

N = the number of flow units per unit area.

n = exponent of the power law, or work term of the activation energy: $n = f \cdot \lambda \cdot \lambda_2 \cdot \lambda_3 / kT = \sigma_v \cdot \lambda / (NkT) = \sigma_v \cdot \varphi$

P = pressure

Q = heat of the system

R = gas constant = $N_m k$ = 1.987 cal $K^{-1} mol^{-1}$, where $N_m = 6.02 \cdot 10^{23}$ is Avogadro's number.

S = entropy

T = the absolute temperature

t = time; t_r = (apparant) relaxation time

U = internal energy

V = volume

W = work done by the system

α see β (α and β are also localy used as constants)

$\beta = \dot{\varepsilon}/A$ or $\dot{\varepsilon}/B$; $\beta\alpha \approx (\dot{\varepsilon}/A) \cdot (1 - \exp(-\varphi \varepsilon_v K_1))$ or $\approx \dot{\varepsilon}/(B\varepsilon_v)$

ε = strain; ε_v = viscoelastic, or viscous strain; ε_{v0} is the initial value.

$\varphi = \lambda/(NkT)$ (see n)

γ = deformation

η = viscosity = $\sigma_v/\dot{\varepsilon}$

$\varkappa$ = transmission coefficient or the ratio of activated complexes going into the product state and don't return to the reactant state. $\varkappa \approx 1$

λ = jump of the flow segment at activation

$\lambda_2 \cdot \lambda_3$ = area of the flow unit; $\lambda \cdot \lambda_2 \cdot \lambda_3$ = activation volume;

λ_1 = length of the flow segment or distance of points of flow

ν = frequency or also: $\nu = kT_m/h$ is the Debye frequency (about 10^{-13})

ρ = concentration of flow units = $N \cdot \lambda \cdot \lambda_2 \cdot \lambda_3 / \lambda_1$

σ = mean stress; σ_v = part of the mean stress on the flow units:

$\sigma_v = N \cdot f \cdot \lambda_2 \cdot \lambda_3$

ω = moisture content

μ = the chemical potential

Stellingen bij het proefschrift van T.A.C.M. van der Put

1 De stabiliteitsberekening in de Eurocode 5 voor uitkippen van liggers is onvoldoende en niet algemeen geldig. Deze dient vervangen te worden door eenvoudig afleidbare algemene betrekkingen.

2 Op grond van het volume-effect van de sterkte van hout kan verwacht worden dat vingerlassen alleen een reductie van de sterkte veroorzaken in relatief kleine proefstukken. De richtlijnen dienen hieraan aangepast te worden.

3 De experimentele betrekkingen voor de sterkte van nagelverbindingen volgens de Eurocode en de Duitse norm zijn af te leiden uit het bezwijkmechanisme van de nagels. Algemenere betrekkingen zijn daarom mogelijk en dienen in de richtlijnen ingevoerd te worden.

4 De lineaire afhankelijkheid van de stijfheid van een stiftdeuvelverbinding met de diameter is af te leiden en dient in de richtlijn opgenomen te worden.

5 De relatief hoge stuiksterkte van spaanplaat is verklaarbaar en daarmee het gedrag van de spaanplaat-hout-verbinding.

6 De sterkte van hout en andere orthotrope of anisotrope materialen kan beschreven worden met een tensorpolynoom. Dit levert een consistent algemeen breukcriterium dat in de richtlijn ingevoerd dient te worden.

7 Statisch onbepaald construeren volgens de C.E.B.-methode (methode Baker) is eenvoudiger mogelijk in hout dan in staal en beton.

8 De temperatuurscheuren in de Rotterdamse metrokolommen leveren geen gevaar op voor de constructie. Herstel van deze scheuren kan gevaarlijk zijn.

9 De experimentele betrekkingen voor de trillingsvoortplanting in de grond van Barkan en Major zijn beperkt geldig, afhankelijk van het meetgebied. Deze betrekkingen dienen vervangen te worden door exacte betrekkingen die hiervoor zijn af te leiden.

10 In verband met de veiligheid is het uit sterkteoverweging nodig een stijfheidseis op te nemen om "wind-flutter" van de daarvoor gevoelige constructies te voorkomen. Deze eis is eenvoudig te formuleren.

11 Aangetoond kan worden dat de ondergrens van de druksterkte van beton bepaald wordt door scheurvoortplanting. Het mechanisme van trekbreuk van de drukzone van elementen zonder dwarskrachtwapening is daarmee te verklaren. Het schoormechanisme, dat de sterkte van oplegblokken, korte consoles en de schuifsterkte van balken nabij de oplegging bepaalt, is ook te verklaren m.b.v. de evenwichtsmethode.
Beide mechanismen bepalen het z.g. "dal van Kani" voor de dwarskrachtsterkte van beton en de berekeningsmethode dient hiermee in overeenstemming gebracht te worden om veilig en economisch te kunnen construeren.

12 De evenwichtsmethode voor de berekening van betonwanden wordt niet consequent toegepast en dient vervangen te worden door een betere methode. Dit geldt ook voor de berekening van liggers van gewapend beton. Deze berekening dient i.v.m. de veiligheid gebaseerd te zijn op de bepaling van de critieke scheurhelling in het lijf en de vermindering van de rotatiecapaciteit door het dwarskrachtaandeel van de drukzone.

13 In de discussie over de mens als zingevende existentie wordt door R.C. Kwant,* tegengesteld aan het Marxisme, het primaat van het "wijzen" boven het "aangrijpen" (arbeid) toegekend voor het ontstaan van zin. Het zou beter in overeenstemming zijn met het interiorisatie-idee van zijn filosofie (existentiele fenomenologie) uit te gaan van de ambiguiteit van het wijzend grijpen en grijpend wijzen.

14 In tegenstelling tot de heersende opvatting zijn er aanwijzingingen dat het pelogtoonsysteem van de javaanse gamalan ouder is dan het slendro-systeem.

* Fenomenologie van de Taal, Prof. Dr. R.C. Kwant, Het Spectrum, Utrecht 1963.